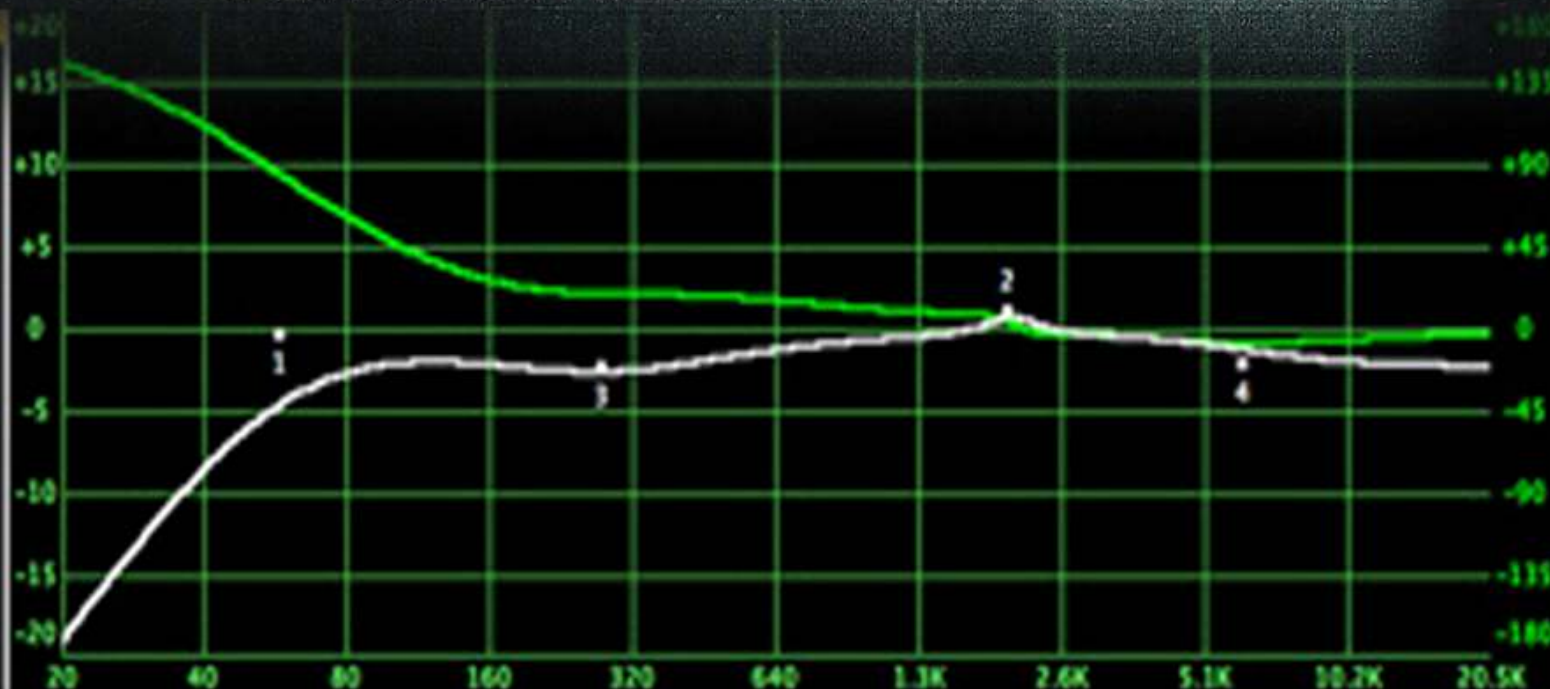


Signal Processing: An International Journal (SPIJ)

ISSN : 1985-2339

VOLUME 4, ISSUE 2

PUBLICATION FREQUENCY: 6 ISSUES PER YEAR



Signal Processing: An International Journal (SPIJ)

Volume 4, Issue 2, 2010

Edited By
Computer Science Journals
www.cscjournals.org

Editor in Chief Dr. Saif alZahir

Signal Processing: An International Journal (SPIJ)

Book: 2010 Volume 4 Issue 2

Publishing Date: 31-05-2010

Proceedings

ISSN (Online): 1985-2339

This work is subjected to copyright. All rights are reserved whether the whole or part of the material is concerned, specifically the rights of translation, reprinting, re-use of illustrations, recitation, broadcasting, reproduction on microfilms or in any other way, and storage in data banks. Duplication of this publication of parts thereof is permitted only under the provision of the copyright law 1965, in its current version, and permission of use must always be obtained from CSC Publishers. Violations are liable to prosecution under the copyright law.

SPIJ Journal is a part of CSC Publishers

<http://www.cscjournals.org>

© SPIJ Journal

Published in Malaysia

Typesetting: Camera-ready by author, data conversion by CSC Publishing Services – CSC Journals, Malaysia

CSC Publishers

Editorial Preface

This is second issue of volume four of the Signal Processing: An International Journal (SPIJ). SPIJ is an International refereed journal for publication of current research in signal processing technologies. SPIJ publishes research papers dealing primarily with the technological aspects of signal processing (analogue and digital) in new and emerging technologies. Publications of SPIJ are beneficial for researchers, academics, scholars, advanced students, practitioners, and those seeking an update on current experience, state of the art research theories and future prospects in relation to computer science in general but specific to computer security studies. Some important topics covers by SPIJ are Signal Filtering, Signal Processing Systems, Signal Processing Technology and Signal Theory etc.

This journal publishes new dissertations and state of the art research to target its readership that not only includes researchers, industrialists and scientist but also advanced students and practitioners. The aim of SPIJ is to publish research which is not only technically proficient, but contains innovation or information for our international readers. In order to position SPIJ as one of the top International journal in signal processing, a group of highly valuable and senior International scholars are serving its Editorial Board who ensures that each issue must publish qualitative research articles from International research communities relevant to signal processing fields.

SPIJ editors understand that how much it is important for authors and researchers to have their work published with a minimum delay after submission of their papers. They also strongly believe that the direct communication between the editors and authors are important for the welfare, quality and wellbeing of the Journal and its readers. Therefore, all activities from paper submission to paper publication are controlled through electronic systems that include electronic submission, editorial panel and review system that ensures rapid decision with least delays in the publication processes.

To build its international reputation, we are disseminating the publication information through Google Books, Google Scholar, Directory of Open Access Journals (DOAJ), Open J Gate, ScientificCommons, Docstoc and many more. Our International Editors are working on establishing ISI listing and a good impact factor for SPIJ. We would like to remind you that the success of our journal depends directly on the number of quality articles submitted for review. Accordingly, we would like to request your participation by submitting quality manuscripts for review and encouraging your colleagues to submit quality manuscripts for review. One of the great benefits we can provide to our prospective authors is the mentoring nature of our review process. SPIJ provides authors with high quality, helpful reviews that are shaped to assist authors in improving their manuscripts.

Editorial Board Members

Signal Processing: An International Journal (SPIJ)

Editorial Board

Editor-in-Chief (EiC)

Dr. Saif alZahir
University of N. British Columbia (Canada)

Associate Editors (AEiCs)

Professor. Raj Senani
Netaji Subhas Institute of Technology (India)

Professor. Herb Kunze
University of Guelph (Canada)

Professor. Wilmar Hernandez
Universidad Politecnica de Madrid (Spain)

Editorial Board Members (EBMs)

Dr. Thomas Yang
Embry-Riddle Aeronautical University (United States of America)

Dr. Jan Jurjens
University Dortmund (Germany)

Dr. Teng Li Lynn
The Chinese University of Hong Kong (Hong Kong)

Dr. Jyoti Singhai
Maulana Azad National institute of Technology (India)

Table of Contents

Volume 4, Issue 2, May 2010.

Pages

- 68 - 74 A Text-Independent Speaker Identification System based on The Zak Transform
Abdulnasir Hossen, Said Al-Rawahy
- 75 - 84 Wavelet Packet based Multicarrier Modulation for Cognitive UWB Systems
Haleh Hosseini, Norsheila Fisal, Sharifah K. Syed-Yusof
- 85 - 96 DSP Based Implementation of Scrambler for 56kbps Modem
Davinder Pal Sharma , Jasvir Singh
- 98 - 113 Time domain analysis and synthesis using Pth norm filter design
M.Y.Gokhale, Daljeet Kaur Khanduja
- 114 - 122 Computing Maximum Entropy Densities: A Hybrid Approach
Badong Chen, Jinchun Hu, Yu Zhu
- 123 - 137 Symbol Based Modulation Classification using Combination of Fuzzy Clustering and Hierarchical Clustering
Negar ahmadi, Reza Berangi

A Text-Independent Speaker Identification System Based on the Zak Transform

Abdulnasir Hossen

*Department of Electrical and Computer Engineering
College of Engineering
Sultan Qaboos University
P.O. Box 33, PC 123, Al-Khoud, Muscat, Oman*

abhossen@squ.edu.om

Said Al-Rawahi

*Department of Electrical and Computer Engineering
College of Engineering
Sultan Qaboos University
P.O. Box 33, PC 123, Al-Khoud, Muscat, Oman*

s_raw@yahoo.com

•

Abstract

A novel text-independent speaker identification system based on the Zak transform is implemented. The data used in this paper are drawn from the ELSDSR database. The efficiency of identification approaches 91.3% using a single test file and 100% using two test files. The method shows comparable efficiency results with the well known MFCC method with an advantage of being faster in both modeling and identification.

Keywords: Speaker identification, Zak transform, Feature extraction, Classification

1. INTRODUCTION

Speaker recognition systems are classified into speaker verification (SV) systems and speaker identification (SI) systems. The task of SV system is to verify the claimed identity of a person from his voice, while the SI system decides who the speaking person is from a database of speakers [1-2].

SI systems can be also classified into text-dependent or text-independent depending on whether the identification based on known utterance or for any given utterance. The SI system consists of two stages:

- Speaker enrolment or speaker modeling, in which features are extracted from all speakers and models are built for them.
- Speaker recognition, in which features are extracted from the speaker under test and a model is built for and compared with models of all speakers in the data set to find the closest speaker (matching).

One of the most successful techniques in speaker recognition is the technique that uses the mel-frequency cepstrum coefficients (MFCC) as a feature set and the Gaussian mixture model (GMM) for matching [3-6].

In this paper, the feature set used for modeling the speakers is based on the Zak transform, while the matching is performed using the Euclidean distance measure.

The new technique is compared with the MFCC technique in terms of identification accuracy and complexity. Both techniques are to be introduced in the next section.

2. METHODS

2.1 MFCC Technique

The perception system of human has some interesting facts. Within the human perception system there is a low-pass filter that blocks high frequency signals from being received. That is why human beings can not percept high frequency signal, where some animals do. Another interesting fact about human perception system is being a non-linear system. Human perception system perceives speech signals in a mel scale. A mel is a unit of measure of perceived pitch or frequency of a tone. It does not correspond linearly to the physical frequency of the tone. The mapping between real frequencies and mel scale is approximately linear below 1 KHz and logarithmic above [7].

Based on the non-linearity of the human perception system, mel-frequency emerged as to mimic the human perception system. The feature set named Mel-frequency Cepstrum Coefficients is obtained using information wrapped in a mel-frequency scale. The speech signal is decomposed into series of frames using a suitable window function, and then MFCC is applied to each frame. The coefficients are obtained through mel-scale filters and collectively named a mel-scale filter banks. These filters follow the mel-scale whereby band edges and centre frequencies of the filters are linear for low frequencies (< 1000) and logarithmically increase with increasing frequency [3]. Figure 1 illustrates the process involving the calculation of MFCC [6].

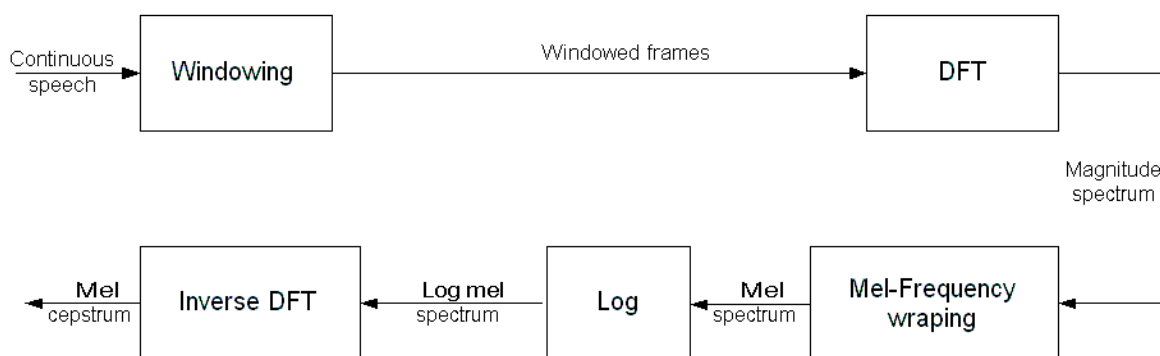


FIGURE 1: Block-Diagram for Computation of Mel-Cepstrum

The pattern-matching task involves computing a match score, which is a measure of the similarity between the input feature vectors and some model. Speaker models are constructed from the features extracted from the speech signal [1]. The comparison could be tested for maximum or minimum score or for a threshold value, dependable on the application.

Due to variability within a speech signal, multi-dimensional Gaussian probability density function (PDF) can be used to represent the signal probabilistically. The Gaussian pdf is state-dependent in that there is assigned a different Gaussian pdf for each acoustic sound class [3]. In this technique the feature set is modelled through GMM, where a speaker model is represented as the measure of the coefficients in terms of means, variances and weights of each mixture. The Gaussian pdf of a feature vector \vec{x} for the i th state is written as [3]:

$$(1)$$

$$b_i(\vec{x}) = \frac{1}{(2\pi)^{\frac{D}{2}} |\Sigma_i|^{\frac{1}{2}}} \exp\left\{-\frac{1}{2}(\vec{x} - \vec{\mu}_i)^T \Sigma_i^{-1} (\vec{x} - \vec{\mu}_i)\right\} \quad (1)$$

where $\vec{\mu}_i$ is the state mean vector, Σ_i is the state covariance matrix, and D is the dimension of the feature vector. The vector $(\vec{x} - \vec{\mu}_i)^T$ denotes the matrix transpose of $\vec{x} - \vec{\mu}_i$, where $|\Sigma_i|$ and Σ_i^{-1} indicate the determinant and inverse of matrix Σ_i respectively. The mean vector $\vec{\mu}_i$ is the expected value of the elements of the feature vector \vec{x} , while the covariance matrix Σ_i represents the cross-correlations (*off-diagonal terms*) and the variance (*diagonal terms*) of the elements of the vector [3].

The speaker model λ represents the set of GMM mean, covariance and weight parameters [3]:

$$\lambda = \{p_i, \vec{\mu}_i, \Sigma_i\} \quad (2)$$

where p_i is the weight, $\vec{\mu}_i$ is the mean and Σ_i is the covariance, for each acoustic class (*mixture*). The probability of a feature vector being in any one of I states (*or acoustic classes*) can be represented as the union of different Gaussian pdfs for a particular speaker [3]:

$$p(\vec{x}|\lambda) = \sum_{i=1}^I p_i b_i(\vec{x}) \quad (3)$$

The job of the GMM is to cluster the coefficients and elaborate all the coefficients extracted from all the frames into a mixture of Gaussian models having different means and variances.

2.2 Discrete Zak Transform

The Fourier transform has been recognized as the great tool for the study of stationary signals and processes where properties are statistically invariant over time.

However, it can not be used for the frequency analysis that is local in time. In recent years, several useful methods have been developed for the time-frequency signal analysis. They include the Gabor transform, Zak transform, and the wavelet transform.

Decomposition of a signal into a small number of elementary waveforms that are localized in time and frequency plays a remarkable role in signal processing. Such a decomposition reveals important structures in analyzing nonstationary signals such as speech and music [8].

Zak transform has been implemented in efficient computation of Gabor's expansion coefficients in a most reliable and completely non-invasive biometric method in iris recognition system [9-10].

For numerical implementations, a Zak transform that is discrete in both time and frequency is required [11].

The discrete Zak transform (DZT) is a linear signal transformation that maps a discrete time signal $x[n]$ onto a 2-D function of the discrete time index n and the continuous normalized frequency variable w . The DZT of $x[n]$ sampled equidistantly at N points can be expressed as the 1-D DFT of the sequence $x[n+kP]$ [12]:

$$Z_x(P, M) = \sum_{k=0}^{M-1} x(n+kP) e^{-jkw2\pi/M}, \quad (4)$$

where $MP=N$. Since the DZT is periodic both in frequency domain w (with the period $2\pi/M$) and in time domain n (with period P), the fundamental zak interval is selected to be $(n = 0,1,\dots,P-1)$ and $(w = 0,1,\dots, M-1)$.

3. DATA

The speech data used in this work are drawn from the ELSDSR (English Language Speech Database for Speaker Recognition) [13]. This ELSDSR database, which is created by the technical university of Denmark, is English spoken by non-native speakers. It contains 23 speakers, 13 male and 10 female. Each speaker has 7 speech files associated with the training and 2 speech files associated with the testing. On average, the duration for reading the training data is 83 s and for reading the test files is 17.6 s.

4. IMPLEMENTATION AND RESULTS

4.1 Implementation

The system uses DZT with $P = 8192$ and $M = 8$. Each speaker is modeled with a matrix of size $(8192, 8)$ by its Zak transform of a speech file of length $(N = 8192*8)$ samples. During the recognition phase, a comparison of the Zak transform matrix of the speaker under test with all matrices (models) of the speakers in the data set is done. The closest speaker (the matched speaker) is identified by the speaker with the minimum Euclidean distance from the speaker under test. The Euclidean distance between two points is defined as:

$$d(x, y) = \sqrt{(x_1 - y_1)^2 + (x_2 - y_2)^2 + \dots + (x_m - y_m)^2} \quad (5)$$

The average of M minimums of M columns of the (M, M) matrix of distances is obtained and used to represent a score to show how close the speaker under test from the speaker of the compared model. The speaker with the minimum score is the identified speaker.

4.2 Results

Table 1 shows the results of identification (efficiency rate) in case of using the first test file or the second test file or both files in the test phase. The mis-identified speakers and the correct order of the speakers are also shown in this table.

Table 2 shows a comparison between MFCC method and the Zak method in speaker identification while either all 7 training files are used in the training phase or only 4 out of them. The Zak method shows the same efficiency rate 100% as the MFCC method if two test files are used.

Table 3 and Table 4 show the complexity comparison between MFCC and Zak methods in terms of modeling and identification times in seconds, respectively. It is clear that the Zak method is faster than MFCC method in both modeling and identification. The time-measurements are obtained using a Fujitsu Siemens computer with Intel Pentium M processor running at 2.00 GHz.

4.3 Modifications

The new technique is implemented also on short-length segments and the Zak transform is found as an average of the Zak transforms of all segments. The signal with $P=8192$ samples is divided into R segments of length P/R . The DZT is found for each segment of length P/R and then the average of the DZT of those R segments is obtained.

The modified Zak method shows equal efficiency results as R varies from 2 to 16. Table 5 shows such consistent results of efficiency of identification, which are better than the results obtained on the full-length P=8192.

The modeling time is increased from 0.312 s to 1.06 s, if R=8 segments is used instead of full-length signal. The modified method is still much faster than the MFCC method in modeling.

Table 6 shows the results of identification execution-time as R varies from 2 to 16. The identification times is less than that obtained with full-length Zak transform method and MFCC method.

Test Files	Efficiency Rate	Identified Speaker	Correct Speaker
File 1	91.3 %	2, 20	3,15
File 2	86.96 %	19, 22, 22	5,13,19
Both	100 %		

TABLE 1. .Results of Identification.

Test Files	All Training Files	All Training Files	First 4 Training Files	First 4 Training Files
	MFCC	Zak	MFCC	Zak
File 1	100 %	91.30 %	95.65 %	91.30 %
File 2	100 %	86.96 %	95.65 %	82.61 %
Both	100 %	100 %	95.65 %	95.65 %

TABLE 2. Comparison with MFCC in terms of Efficiency Rate

Method	All Training Files	First 4 Training Files
Zak	0.320	0.185
MFCC	9.122	6.010

TABLE 3. Comparison with MFCC in terms of Modeling Complexity

Method	Test File 1	Two Test Files
Zak	0.5278	0.5643
MFCC	0.812	1.888

TABLE 4. Comparison with MFCC in terms of Identification Complexity

Test Files	Efficiency Rate	Identified Speaker	Correct Speaker

File 1	95.65 %	10	16
File 2	91.3 %	11, 18	6, 21
Both	100 %		

TABLE 5. Results of Identification of the Modified Zak Method

R	1 Test File	2 Test Files
2	0.1126	0.2048
4	0.1335	0.2126
8	0.1575	0.2377
16	0.2113	0.2874

TABLE 6. Effects of Number of Segments on the Identification Time in Seconds

5. CONCLUSIONS

A novel text-independent speaker identification system is implemented using Zak transform coefficients as a feature set. The method is simple and shows 100% efficiency rate in case of using two files in the test phase in identifying 23 speakers forming the ELSDSR database. Compared to MFCC method, the Zak methods shows a clear advantage in both modeling and identification complexity.

The new method is also improved by applying it on a basis of short--length segments and then an average DZT is computed. The improvement is achieved in both identification efficiency and time while more time is needed for the modeling compared to the full-length Zak method.

6. ACKNOWLEDGMENTS

The authors would like to thank Mrs. Ling Feng from the Technical University of Denmark for providing them with the ELSDSR data.

REFERENCES

1. Campbell, J. P.: "*Speaker recognition: A tutorial*", Proceedings of the IEEE, Vol.85(9), 1437-1462, 1997.
2. Naik, J. M.: "*Speaker verification: A tutorial*", IEEE Communications Magazine, 42-48, January 1990.
3. Quatieri, T. F.: "*Discrete-time speech signal processing: Principles and practice*", Prentice Hall, 2002.
4. Benesty, J., Sondhi, M. M., and Huang, Y.: "*Springer handbook of speech processing*", Springer, 2007.
5. Keshet, J., and Bengio, S.: "*Automatic speech and speaker recognition: Large margin and kernel methods*", John Wiley, 2009.
6. Karpov, E.: "*Real-time speaker identification*", Master Thesis, Department of Computer Science, University of Joensuu, 2003.
7. Deller, J.R., Hansen, J.H.L., Proakis, "*Discrete-Time Processing of Speech Signals*", IEEE Press, New York, NY, 2000.
8. Debnath, L.: "*Wavelet transforms and their applications*", Springer Verlag, 2001.
9. Czajka, A., and Pacut, A.: "*Zak's transform for automatic identity verification*", 4th International Conference on Recent Advances in soft computing RASC2002, Nottingham, United Kingdom, 374-379, December 2002.
10. Daugman, J.: "*Wavelet demodulation codes, statistical independence, and pattern recognition*", Institute of Mathematics and its Applications, Proc. 2nd IMA-IP, 244-260, London, Horwood, 2000.
11. Boelcskei, H., and Hlawatsch, F.: "*Discrete Zak transforms, polyphase transforms, and applications*", IEEE Transaction on Signal Processing, Vol. 45(4), 851--866, April 1997.
12. Janssen, A.: "*The Zak transform: A signal transform for sampled time-continuous signals*", Phillips J. Res., 43, 23--69, 1988.
13. ELSDSR database for speaker recognition, 2004, <http://www.imm.dtu.dk/~lf/eLSDSR.htm>

Wavelet Packet based Multicarrier Modulation for Cognitive UWB Systems

Haleh Hosseini

*Faculty of Electrical Engineering
Universiti Teknologi Malaysia
Johor, 81310, Malaysia*

halehsi@fkegraduate.utm.my

Norsheila Fisal

*Faculty of Electrical Engineering
Universiti Teknologi Malaysia
Johor, 81310, Malaysia*

sheila@fke.utm.my

Sharifah K. Syed-Yusof

*Faculty of Electrical Engineering
Universiti Teknologi Malaysia
Johor, 81310, Malaysia*

kamilah@fke.utm.my

Abstract

Orthogonal frequency division multiplexing (OFDM) is a multi-carrier modulation (MCM) scheme where the sub carriers are orthogonal waves. The main advantages of OFDM are robustness against multi-path fading, frequency selective fading, narrowband interference, and efficient use of spectrum. Recently it is proved that MCM system optimization can be achieved by applying wavelet bases instead of conventional fourier bases. Wavelet packet based MCM (WPMCM) systems have overall the same capabilities as OFDM systems with some improved features. In this research the literature and analytic schemes of WPMCM system is addressed, a wavelet packet based cognitive ultra wideband (UWB) transceiver is proposed, and performance analysis of WPMCM in different wireless multipath channels is investigated. Simulation results show a significant enhancement in terms of spectral efficiency, side-lobes suppression and BER comparing to conventional OFDM.

Keywords: Orthogonal frequency division multiplexing (OFDM), wavelet packet based MCM (WPMCM), cognitive radio (CR), ultra wideband (UWB).

1. INTRODUCTION

Adaptive multi-carrier modulation (MCM) has a flexible spectrum to avoid mutual interference to other users [1]-[3]. MCM increases wireless capacity without increasing bandwidth. It divides data-stream into orthogonal parallel modulated sub-streams with lower bit rate and longer symbol time than the channel delay spread. Increasing the symbol duration leads to a robust system against ISI, channel distortion, impulse noise and fading. In wavelet packet based MCM (WPMCM) systems, the orthogonality is provided by orthogonal wavelet filters (filter banks) [4], and the real wavelet transform converts real numbers to real numbers, hence the complexity of computation is reduced. Moreover, its longer basis functions offers higher degree of side lobe suppression and decreases the effects of narrowband interference, ISI, and ICI [5]. OFDM signals only overlap in the frequency domain while the wavelet packet signals overlap in both, time and frequency. Due

to time overlapping, WPMCM systems don't use cyclic prefix (CP) or any kind of guard interval (GI) that is commonly used in OFDM systems. This enhances the bandwidth efficiency comparing to conventional OFDM systems [6].

Cognitive ultra wideband (UWB) has to exploit variety of spectral opportunity, perform pulse shaping, and adapt its data rate, bandwidth, and transmit power. In a cognitive communication scenario the primary and the cognitive user are subjected to mutual interference when communicate to different receivers (Figure 1), and cognitive radio (CR) needs to avoid or cancel the interference. WPMCM is proposed as a solution for cognitive UWB challenges.

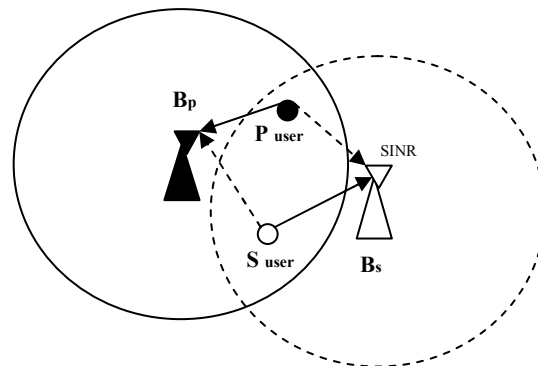


FIGURE 1: A possible arrangement of the primary and secondary receivers, base stations are indicated as B_p and B_s , respectively.

In this paper, the properties of WPMCM system and mathematical scheme are represented, power spectrum and BER are investigated by simulation results, and WPMCM is proposed for cognitive UWB systems. The remainder sections are organized as follows. Section 2 is related works on wavelet based MCM systems. Wavelet packet based MCM properties are described in section 3. System description and analytical relations are provided in section 4. In section 5, cognitive UWB transceiver design is proposed, and simulation results and discussion are described in section 6. We summarize the research in section 7.

2. RELATED WORKS

There is a considerable literature addressing the use of WPMCM and its performance evaluation comparing with conventional method. A closed form formula in [7] is derived to define convolution's counterpart in the wavelet domain, and a wavelet based multicarrier modulation framework presented by discrete wavelet transform (DWT) Mallat's algorithm. Performance analysis of IEEE 802.15.3a channel models for multiband UWB proved that the overhead and the transceiver structure for the WB-MUWB are less complex than those for the FB-MUWB; therefore DWT could be considered as an attractive technique in future multicarrier UWB systems.

In [8] authors studied symbol error rate (SER) of both conventional OFDM and Gabor basis WPMCM in AWGN channel for fast intercity trains, and showed that this new technique with a moderate complexity avoids the spectral efficiency loss. Testing this technique in more realistic channels is an idea to continue their research. For radar applications, Mohseni et.al in [9] replaced the conventional OFDM multicarrier modulation with the WPMCM in order to get a more flexible signal design approach. These designed radar signals have very low side lobe levels in their ambiguity functions and high spectral efficiency. The requirements imposed in the design of usable wavelets and wavelet packets for multicarrier modulation are studied in [10]. According to this article, for perfect reconstruction of data the wavelets have to satisfy bi-orthogonal property. Another real time application of the system is reported in [11] where WPMCM for V-BLAST [12] (vertical Bell laboratories layered space time) is discussed. According to [11] the bit error rate

(BER) performance of the wavelet based V-BLAST system is superior to their Fourier based counterparts.

The major drawback of MCM systems is the peak-to-average power ratio (PAPR) problem. High peaks of the transmitted signal drive the power amplifiers operating near nonlinear saturation regions which degrade the power efficiency and system performance. Hence, it is necessary to transmit signals with lower PAPR because of operating range of power amplifiers. In [13] authors reported reducing in PAPR by a Haar WPMCM system with Hadamard spreading codes. WPMCM system is also sensitive to time synchronization errors resulting from its overlapping symbols in the time domain. OFDM can easily exploit CP to reduce the effects of timing error or dispersive channel. Furthermore, the ISI in OFDM is generated by overlapping of two successive symbols, while in the case of WPMCM, ISI is generated by overlapping of a number of consecutive symbols. Hence, WPMCM is very sensitive to even small timing differences between transmitter and receiver. In [14] the performance of wavelet packet modulation (WPM) systems using several well known wavelets in the presence of timing offset is compared with OFDM. As a future work authors proposed to design wavelet and scaling filters that would minimize the interference energy from timing error. They also suggested using complex wavelets to reduce WPM time shift sensitivity, and designing a robust synchronization scheme to tackle large timing offsets.

Channel estimation is another challenge to be tackled by researchers. In traditional OFDM system, channel estimation is performed by pilot symbol assisted modulation (PSAM) with pilot interpolation in time domain or frequency domain. More pilots, lower bandwidth efficiency and higher system complexity. The channel estimation issue for WPM system has been addressed in [15] and a novel pilot arrangement is designed based on wavelet packet theory for WPM system to achieve higher speed transmission with lower bit error rates. In [5] channel estimation for WPM is surveyed and indicated that ANNs (Artificial Neural Networks) method is more proper than LMMSE estimation. As their future work, authors proposed development of wavelet theory and post-equalization to cancel the interference caused by overlapping symbols.

3. WAVELET PACKET BASED MCM FEATURES

The wavelet basis functions are localized in time (or space) and frequency, and have different resolutions in these domains. Wavelet transforms are broadly classified as continuous and discrete wavelet transforms. The continuous wavelet transform (CWT) of a continuous signal $x(t)$ is defined as the sum of all time of the signal multiplied by scaled, shifted versions of the wavelet waveforms. Discrete wavelet transform (DWT) analyzes the signal at different frequency bands with different resolutions by decomposing the signal into an approximation containing coarse and detailed information. DWT employs two sets of functions, known as scaling and wavelet functions, which are associated with low pass and high pass filters. The decomposition of the signal into different frequency bands is simply obtained by successive high pass and low pass filtering of the time domain signal. Wavelet packet transform (WPT) decomposes the high frequency bands which are kept intact in the DWT; hence it obtains richer resolution. Some advantages of wavelet transform are described as follows.

3.1. Multi-rate Property

The main property of the WPT is the semi-arbitrary division of the signal space. WPT still leads to a set of orthogonal functions, even if the construction iterations are not repeated for all sub-branches. From a multicarrier communication system perspective, this maps into having subcarriers of different bandwidths and symbol length to create a multi-rate system and enhance the quality of service (QoS) of wireless systems.

3.2. Configurable Transform Size

The iterative nature of the wavelet transform allows for a configurable transform size and hence a configurable number of carriers. This facility can be used, for instance, to reconfigure a transceiver according to a given communication protocol; the transform size could be selected

according to the channel impulse response characteristics, computational complexity or link quality.

3.3. Noise and Interference Suppression

By flexible time-frequency resolution, the effect of noise and interference on the signal can be minimized. Wavelet based systems are capable of avoiding known channel disturbances at the transmitter, rather than waiting to cancel them at the receiver. In [16] a WPMCM transmission system, for multi-rate integrated service is demonstrated. The performance of this system under impulse noise and single tone interference is reported to be superior to existing Fourier based variants. WPT digital modulated signals are mapped into their own Time-Frequency Atoms (t-f atoms) which will be utilized in multiplexing of transport orthogonally. Tone interference and impulse noise cause distributed effects in the WPM system.

3.4. Robustness against ISI and ICI

The performance of MCM system depends on the set of waveforms that the carriers use. The wavelet scheme reduces the sensitivity of the system to harmful channel effects like Inter-symbol interference (ISI) and Inter-carrier interference (ICI). Authors in [18] replaced the fourier-based complex exponential carriers of a multicarrier system with orthonormal wavelets. The wavelets are derived from a multistage tree-structured Haar and Daubechies orthonormal quadrature mirror filter (QMF) bank. The authors in [17] compared both OFDM and WPMCM in the context of PLCs and proved that WPMCM has higher transmission efficiency, deeper notches, robustness to narrowband interference (NBI) or impulsive noise, and lower circuit cost as fewer carriers than in conventional or windowed OFDM can be used. An improved performance with respect to reduction of the power of ISI and ICI is reported in Table 1 that makes comparison between orthonormal Haar wavelets and conventional OFDM. This work is extended in [19] with empirical investigations on a model obtained from the measurements of a practical high speed and low-voltage power line communication channel (PLC), the research exhibits superiority of WPMCM to traditional OFDM especially regarding to ISI and ICI mitigation.

Conventional OFDM	IS _{lav} [dB]	-1.07	-0.72	-0.54
	IC _{lav} [dB]	-6.60	-8.16	-9.31
Haar-WPMCM	IS _{lav} [dB]	-2.41	-1.62	-1.23
	IC _{lav} [dB]	-7.49	-12.94	-18.67
Channel excess delay		T	T	T
Number of carriers		8	12	16

TABLE 1: Averaged normalized power of interference for MCM systems.

4. SYSTEM DESCRIPTION

At the transmitter the data stream $X = (x[1], x[2], \dots, x[n], \dots, x[N])$, is first converted from serial to parallel sequences S_k and then modulated with M -array inverse wavelet packet transform (IWPT). Figures 2a and 2b, show the wavelet packet based MCM transceiver operating Mallat's fast algorithm [20].

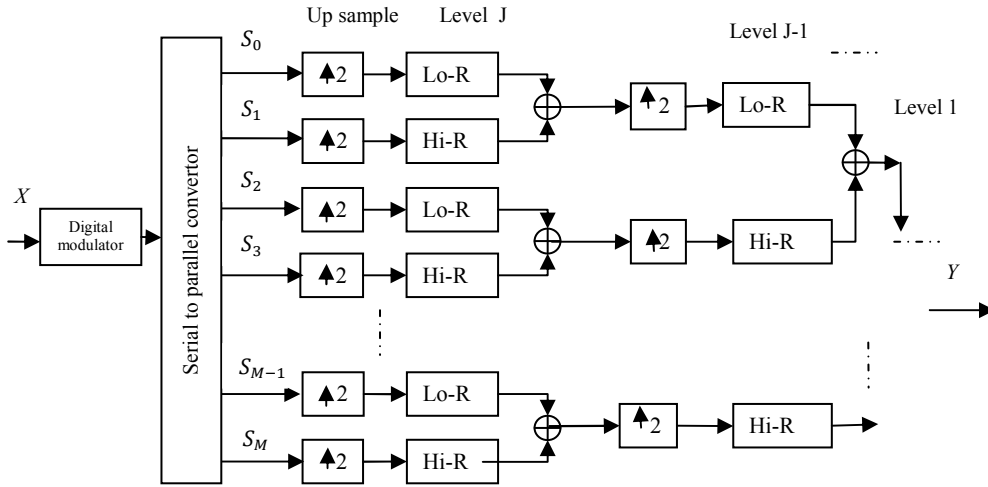


FIGURE 2a: Wavelet packet based MCM transmitter part, including reconstruction filters.

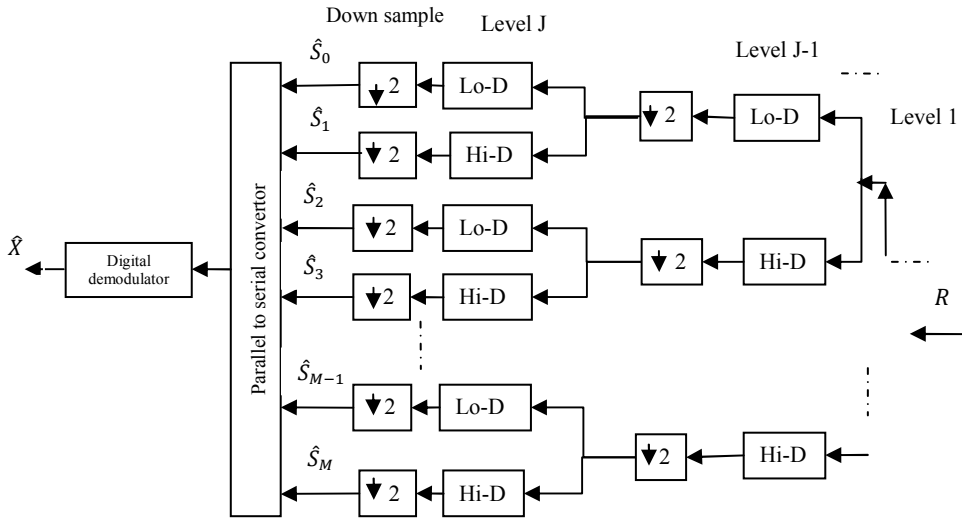


FIGURE 2b: Wavelet packet based MCM receiver part, including decomposition filters.

The transmitted signal Y , is composed of successive K symbols, as the sum of M amplitude modulated waveforms by ϕ_k . It can be expressed using matrix notations as:

$$Y = \sum_k S_k \cdot \phi_k \tag{1}$$

where $Y = (y[1], y[2], \dots, y[n], \dots, y[N])$, is transmitted signal, $S_k = (s_0[k], s_1[k], \dots, s_m[k], \dots, s_{M-1}[k])$, is constellation encoded k -th data symbol, and

$$\phi_k = \begin{pmatrix} \varphi_0[1 - kM] & \dots & \varphi_0[N - kM] \\ \vdots & \varphi_m[n - kM] & \vdots \\ \varphi_{M-1}[1 - kM] & \dots & \varphi_{M-1}[N - kM] \end{pmatrix} \tag{2}$$

is the waveforms matrix which $\varphi_m[n]$ are mutually orthogonal to reduce the symbol errors, i.e.

$$\varphi_i[n] * \varphi_j[n] = \delta[i - j], \quad (3)$$

where * indicates a convolution operation and δ represents the Dirac function.

The relationship between the number of iterations J and the number of carrier waveforms M is given by $M = 2^J$.

In the wavelet packet scheme, we limit our analysis to subcarrier waveforms defined through a set of FIR filters, and implemented by Mallat's fast algorithm [21] with less complexity for wireless communication. In orthogonal wavelet systems, quadrature mirror filter pair (QMF) consists of the scaling filter h_{lo}^{rec} and dilatation filter h_{hi}^{rec} , and knowledge of the scaling filter and wavelet tree depth is sufficient to design the wavelet transform. The scaling filter h_{lo}^{rec} and dilatation filter h_{hi}^{rec} , and the corresponding reversed filters h_{lo}^{dec} and h_{hi}^{dec} , are used to form a wavelet packet tree. These filters satisfy following conditions:

$$\sum_{n=-\infty}^{\infty} h_{lo}^{rec}[n] = 2, \quad (4)$$

$$\sum_{n=-\infty}^{\infty} h_{lo}^{rec}[n]h_{lo}^{rec}[n - 2q] = 2\delta(q), \quad (5)$$

$$h_{hi}^{rec}[n] = (-1)^n h_{lo}^{rec}[\lambda - n - 1], \quad (6)$$

where λ is the span of the filters.

The carrier waveforms are obtained by iteratively filtering the signal into high and low frequency components. The waveforms $\varphi_m[n]$ are derived by J successive iterations as the following recursive equations:

$$\begin{cases} \varphi_{j,2m}[n] = h_{lo}^{rec}[n] * \varphi_{j-1,m}[\frac{n}{2}] \\ \varphi_{j,2m+1}[n] = h_{hi}^{rec}[n] * \varphi_{j-1,m}[\frac{n}{2}] \\ \varphi_{0,m}[n] = \begin{cases} 1, & n = 1 \\ 0, & else \end{cases} \end{cases} \quad (7)$$

where j is the iteration index, $1 \leq j \leq J$, and m the waveform index $0 \leq m \leq M - 1$. Using usual notation in discrete signal processing $\varphi_{j,m}[\frac{n}{2}]$ denotes two version up-sampling of $\varphi_{j,m}[n]$.

The type of WPT algorithm depends on the choice of mother wavelet, the number of levels of expansion, and signal specifications such as periodic, non-periodic, extended and finite WPT. Time and frequency domain localizations are not independent and a waveform with higher frequency domain localization can be obtained with longer time support. Furthermore, short duration waveforms have shorter symbol duration than the channel coherence time, limit the modulation-demodulation delay, and require less memory and less computation.

For the evaluation of a wireless channel, we assume a channel H , with L multi-paths, $H = (h[0], h[1], \dots, h[l], \dots, h[L - 1])$ and received signal at the output of the channel can be written as:

$$R = H.Y + V, \quad (8)$$

where $R = (r[1], r[2], \dots, r[n], \dots, r[N])$, is the received signal, and $V = (v[1], v[2], \dots, v[n], \dots, v[N])$, is additive white Gaussian noise (AWGN).

5. TRANSCIVER DESIGN

Our proposed WPMCM System framework including channel state information (CSI) feedback is illustrated in figures 3. The information bits are firstly grouped and mapped into MPSK or M-QAM. Then the serial data stream is transformed to N parallel lines, where N is the number of subcarriers which is dependent on channel state. So pilots can be inserted into the N lines of signals with particular pilot arrangement strategy, then obtained N lines of signals can be modulated through inverse wavelet packet modulation (IWPM). In the receiver time and frequency diversity are exploited in the system, the maximal ratio combining (MRC) technique is used to combine different diversity branches.

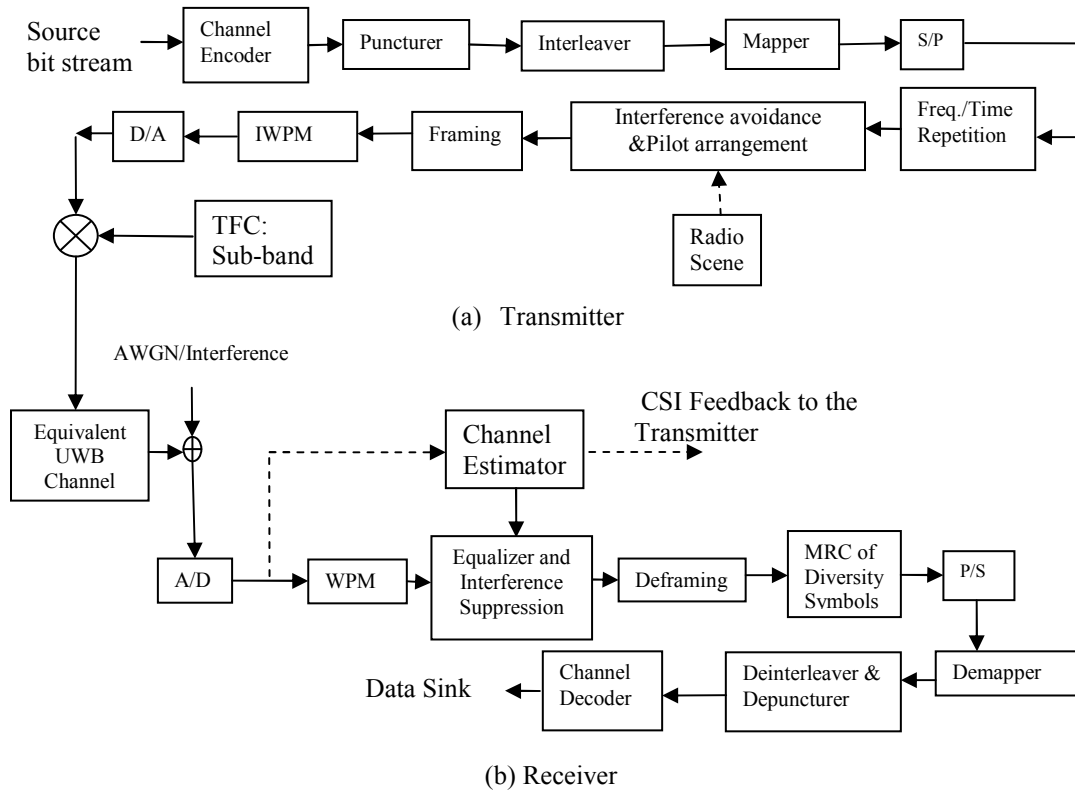


FIGURE 3: Cognitive multiband UWB transceiver via WPMCM.

A multiband UWB system is provided with symbols of duration T, bandwidth 528 MHz, and 128 samples to be transmitted in different sub-bands. For the wavelet based system cyclic prefix is replaced by data bits. Multiple-access can be introduced in the form of time-frequency hopping codes similar to multiband OFDM. Wavelet packet basis and filter pairs are selected due to the type of system application. In the case of MCM, wavelet packet bases are time limited and smooth, well confined in frequency, and orthogonal or linearly independent.

6. RESULTS AND DISCUSSION

In simulation part, we consider 128 wavelet packet equally spaced carriers to be adaptively deactivated for transmission spectrum shaping according to the primary users band (Figure 4).

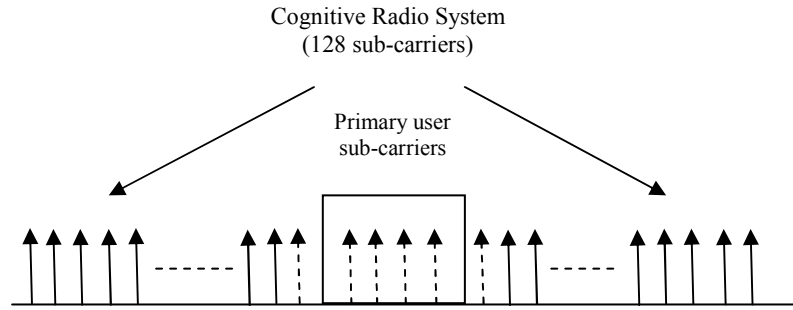


FIGURE 4: CR coexistence with primary user Characteristics, solid lines show active subcarriers and dot lines indicate deactivated subcarriers in the band of or adjacent to primary user.

We assume a WPMCM system which is presented in Figure 5. The information bits are firstly modulated by 16-QAM constellation mapping. Then the serial data stream is transformed to 128 parallel subcarrier lines, pilot symbols are inserted and signals are modulated through IWPT. For the wavelet packet based system, cyclic prefix is replaced by data bits. At the receiver side, the zero forcing equalizer is provided to compensate the effects of channel distortion and WPT block is applied for demodulation of data.

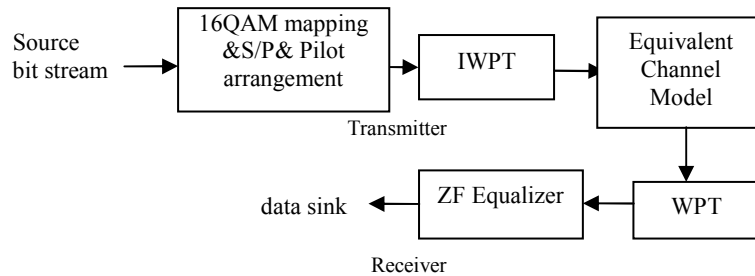


FIGURE 5: WPMCM transceiver for simulation.

In conventional OFDM large side-lobes result in out-of-band (OOB) radiations, thus, coexistence of primary and secondary users depends on side-lobes suppression. Figures 6(a) compares power spectrum density (PSD) of conventional OFDM and WPMCM. According to the graphs, WPMCM enhances the side-lobes suppression effectively accompanied by high spectral efficiency caused by removing the cyclic prefix. These figures illustrate that the occupied bandwidth of WPMCM is far less than OFDM. PSD of zero-padded WPMCM shown in figure 6(b) has minor side-lobes improvement comparing to WPMCM.

Simulation results of Figures 7(a, b and c) compare the bit error rate (BER) of conventional OFDM and WPMCM signal with 1 level wavelet packet tree with Sym4 family, versus the Signal-to-Noise Ratio (SNR) in the presence of different channel conditions. According to the Figure 7(a), WPMCM signal has almost the same BER as conventional OFDM, but for zero-padded WPMCM the BER is lower and performance is improved for all channel conditions with the cost of spectral efficiency. For zero padded WPMCM in AWGN channel, improvement at BER of 10^{-4} is 1dB with respect to conventional OFDM. In the two next cases, (Figures 7b,7c), we consider a two taps channel with additional AWGN effect and zero forcing equalizer in the receiver. Figure 7(b) shows that both WPMCM and zero-padded WPMCM have better BER comparing to OFDM for SNR higher than 15 dB. The performance improvement at 10^{-3} is 6 dB and 7 dB for WPMCM and zero padded WPMCM respectively. In figure 7(c), BER performance doesn't change significantly with various choices of wavelet filter families, but at high SNR situation, two level wavelet packet trees represent superior performances to one level wavelet packet trees.

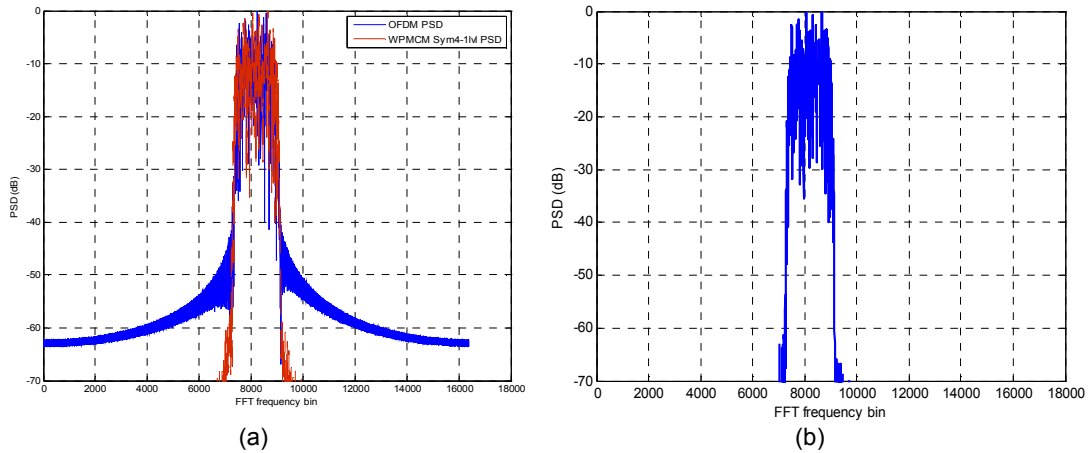


FIGURE 6: Power spectral density (obtained by FFT length of 16384) of (a) conventional OFDM and 1 level WPMCM-Sym4, (b) zero padded 1 level WPMCM-Sym4.

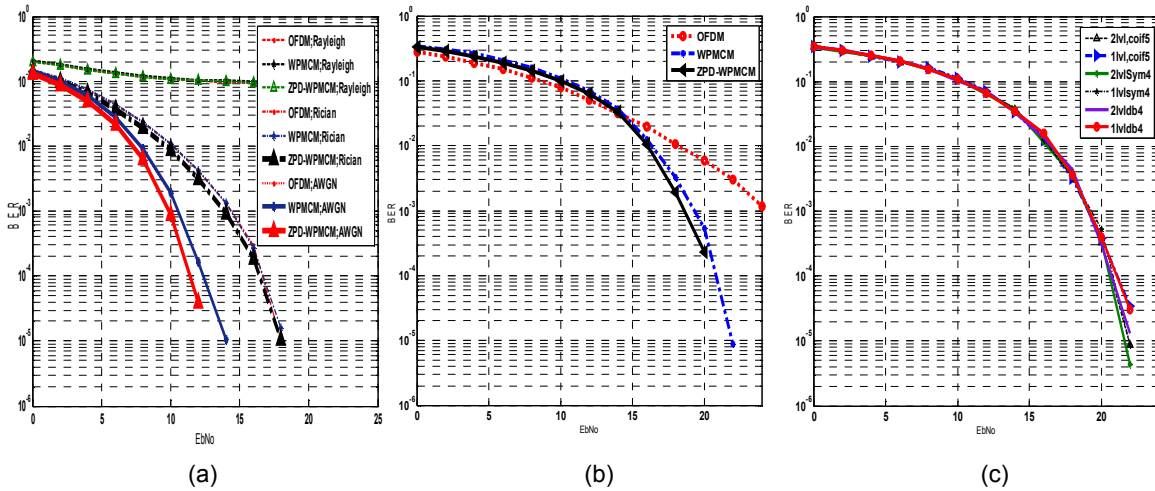


FIGURE 7: BER comparison between conventional OFDM and WPMCM-Sym4 for (a) AWGN, Rayleigh and Rician channel conditions, (b) in the presence of a two taps channel distortion and AWGN,(c) different Wavelet families and tree levels.

7. CONCLUSION

In this research wavelet packet based multicarrier modulation is recommended for cognitive multiband UWB systems as an efficient solution to meet adaptive and cognitive goals. Literature is surveyed, and analytical approach of WPMCM transceiver is addressed. Power spectrum density graphs shows that WPMCM has high spectral efficiency accompanied by significant side-lobes suppression. Finally we investigated the BER performance and power spectral density of WPMCM under different channel models and wavelet families. BER improvement is achieved by WPMCM comparing to the conventional OFDM. As future work, we compare the conventional OFDM and wavelet based MCM-UWB systems under standard IEEE 802.15.3a channel models (CM1-CM4) for wireless personal area networks (WPAN). Study on narrowband interference mitigation of WPMCM UWB systems is the next open contribution.

8. REFERENCES

1. T.A. Weiss, F.K. Jondral. "Spectrum Pooling: An Innovative Strategy for the Enhancement of Spectrum Efficiency", IEEE Communications Magazine, 42:8-14, 2004.
2. M.K. Lakshmanan, I. Budiarto and H. Nikookar. "Maximally Frequency Selective Wavelet Packets Based Multi-Carrier Modulation Scheme for Cognitive Radio Systems", The 50th IEEE Global Communications Conf.(Globecom), Washington DC, USA, 2007.
3. M.K. Lakshmanan, H. Nikookar. "Optimum Wavelet Packet Construction for Multicarrier-based Cognitive Radio System", The 10th Int. Symp. on Wireless Personal Multimedia Communications, Jaipur, India, 2007.
4. G. Strang, T. Nyugen. "Wavelets and Filter Banks", Wellesley/Cambridge Press, 1996.
5. X.Wu, F. Tian, J. Liu. "Efficient Spectrum Multiplexing Using Wavelet Packet Modulation and Channel Estimation Based on ANNs", Int. Conf. on Audio, Language and Image Processing, Shanghai, China, 604-608, 2008.
6. M.K. Laksmanan, H. Nikookar. "Review of wavelets for digital wireless communication", Wireless Pers. Commun. 37:387-420, 2006.
7. R. Dilmaghani, M. Ghavami. "Comparison between wavelet-based and Fourier-based multicarrier UWB systems", IET Commun., 2(2):353-358, 2008.
8. T. Boukour, M. Chennaoui, A. Rivenq, J.M. Rouvaen, M. Berbineau. "A New WOFDM Design for High Data Rates in the case of Trains Communications", IEEE Int. Symp. on Signal Processing and Information Technology(ISSPIT), Athenes, Greece, 2005.
9. R. Mohseni, A. Sheikhi, M. A. Masnadi Shirazi. "UWB Radars Based on Wavelet Packet OFDM Signals", IEEE Int. Conf. on Ultra-Wideband, Hannover, 2:89-92, 2008.
10. C.V. Bouwel, et.al. "Wavelet Packet Based Multicarrier Modulation", IEEE Benelux Symposium on Communications and Vehicular Technology, Leuven, Belgium, 2000.
11. Z. Rafique, N. Gohar, M.J. Mughal. "Performance Comparison of OFDM and WOFDM Based V-BLAST Wireless Systems", IEICE Transactions on Communications, E88-B (5):2207-2209, 2005.
12. P.W. Wolniansky, et.al. "V-BLAST: An Architecture for Realizing Very High Data Rates Over the Rich-Scattering Wireless Channel", ISSSE-98, Pisa, Italy, 1998.
13. K. Anwar, et.al. "PAPR Reduction of OFDM Signals Using Iterative Processing and Carrier Interferometry Codes", IEEE Int. Symp. on Intelligent Signal Processing and Communications System (ISPACS), Seoul, Korea, 48-51, 2004.
14. H. Nikookar, M.K. Lakshmanan. "Comparison of sensitivity of OFDM and Wavelet Packet Modulation to time synchronization error", The 19th Int. Symp. on Personal, Indoor and Mobile Radio Communications(PIMRC2), Athens, greece,1-6, 2008.
15. M. Yang, Z. Liu, J.Dai. "Frequency Selective Pilot Arrangement for Orthogonal Wavelet Packet Modulation Systems", Int. Conf. on Computer Science and Information Technology(ICCSIT), Singapore, 2008.
16. W. Yang, et.al. "A Multirate Wireless Transmission System Using Wavelet Packet Modulation", IEEE 47th Vehicular Technology Conf., Phoenix, AZ, USA, 1: 368-372, 1997.
17. S. Galli, H. Koga, N. Kodama. "Advanced Signal Processing for PLCs: Wavelet-OFDM", IEEE Int. Symp. on Power Line Communications and Its Applications, 187-192, 2008.
18. B.G. Negash, H. Nikookar. "Wavelet-Based Multicarrier Transmission Over Multipath Wireless Channels", IEE Electronics Letters, 36(21):1787-1788, 2000.
19. Y. Zhang, S. Cheng. "A Novel Multicarrier Signal Transmission System Over Multipath Channel of Low-Voltage Power Line", IEEE Transactions on Power Delivery,19(4):1668-1672, 2004.
20. A. Jamin, P. Mahonen. "Wavelet packet Modulation for Wireless Communications", Wireless Communications & Mobile Computing Journal, John Wiley and Sons Ltd., 5(2):123-137, 2005.
21. S. Mallat. "A wavelet tour of signal processing", 2nd ed. Academic Press, 1999.

DSP Based Implementation of Scrambler for 56Kbps Modem

Davinder Pal Sharma

*Department of Physics
University of the West Indies
St. Augustine, Trinidad & Tobago*

davinder.sharma@sta.uwi.edu

Jasvir Singh

*Department of Electronics Technology
Guru Nanak Dev University
Amritsar -143105, India*

j_singh00@rediffmail.com

Abstract

Scrambler is generally employed in data communication systems to add redundancy in the transmitted data stream so that at the receiver end, timing information can be retrieved to aid the synchronization between data terminals. Present paper deals with simulation and implementation of the scrambler for 56Kbps voice-band modem. Scrambler for the transmitter of 56Kbps modem was chosen as a case study. Simulation has been carried out using Simulink of Matlab. An algorithm for the scrambling function has been developed and implemented on Texas Instrument's based TMS320C50PQ57 Digital Signal Processor (DSP). Signalogic DSP software has been used to compare the simulated and practical results.

Keywords: Scrambler, 56Kbps Modem, Matlab, Signalogic, Digital Signal Processor.

1. INTRODUCTION

Often, it is required by the user to ensure that the transmitted signal should have sufficient randomness or activity so that timing recovery, adaptive equalization and echo cancellation can be reliably performed. Mostly users type characters on PC relatively slow due to which computer terminal transmits null characters most of the time. A long sequence of null characters results in a highly correlated line signal. Such signals can foil timing recovery and other functions, all of which assume that the transmitted symbols are uncorrelated. Scrambling is intended to minimize strong correlations among the information bits so as to make them appear more random. It is a method of achieving dc balance (dc null) and eliminating long sequences of zeros to ensure timing recovery without redundant line coding. Scrambler does not add anything in signal, as it is not based on redundancy. Scrambler performs one-to-one mapping between input data bits and coded data bits. The objective is to map the bit sequences, which are problematic and likely to occur, into a coded sequence that looks more random and less problematic.

Scrambler is a digital device, which maps a data sequence into a channel sequence. If the data sequence is periodic, it converts it into a periodic channel sequence with period, which is many times the data period. A simple scrambler adds a Maximum-Length Shift-Registers (MLSR) sequence to the input bit stream to randomize or whiten the statistics of the data, making it more random. Scrambler consists of linear sequential filters with feedback paths, counters, storage

elements and peripheral logic in their discrete form. The counters, storage elements and peripheral logic, monitor the channel sequence but react infrequently so that the scrambler behaves principally as linear sequential filter [1].

There are many applications of scrambler. This is used for encryption of data in security systems, to remove non-linearity of common carrier systems which causes inter-channel interference and to remove systematic jitter caused by self-retiming circuits in base-band Pulse Code Modulation (PCM) systems. In data communication systems, main purpose of the scrambler is to add redundancy in the transmitted data stream so that at the receiver, timing information can be retrieved from received data i.e. to aid the synchronization between two modems. The present study deals with the implementation of the scrambler used for synchronization purpose.

2. THEORETICAL BACKGROUND

In the beginning, scrambler was used to reduce the effect of jitter in the PCM systems. Jitter is a very serious problem as it reduces the Signal-to-Noise Ratio (SNR) and causes more errors to be introduced at the receiver. In addition, jitter also effects the functioning of the repeaters, which has a commutative effect. The proceeding timing circuits generates systematic jitter, which degrades the transmission quality because the r.m.s. value of the jitter increases in proportion to the square root of the number of repeaters. A self-retiming circuit is used in conventional base-band PCM systems to minimize the jitter in which a timing waveform is extracted from an equalized pulse train [2]-[3].

There are certain impairments that vary with the statistics of the digital source in digital transmission systems and these statistics of the data source is related to the problem of timing recovery, equalization and cross talk. One of the methods to isolate the system performance from the source statistics is to use redundant transmission codes. These codes could not provide complete isolation however they generate additional problems by increasing the symbol rate. Alternative method to cope up with this problem is scrambling, which whitens the statistics of digital source. Any source is said to white if it generates statistically independent and equiprobable symbols using which system impairment can be easily analyzed. All the first order and second order statistics of any binary source can be whiten to any degree at the cost of an arbitrarily small controllable rate [4].

3. BASIC SCRAMBLING ACTION

Data transmission through any communication system will be errorless if the timing of each device attached to the system is accurate enough. But it is difficult to ensure the accuracy of the timing in a larger system having many devices or having very large data packets. The solution to this problem of highly accurate clocks can be found by using synchronous communication techniques. In synchronous systems, it is necessary to extract timing information from the received data, which in turn reduces the burden of internal clock circuitry. There are many methods using which timing information from the received data can be retrieved. Line coding techniques like Return to Zero coding and Manchester coding are the few familiar techniques that may be used for this purpose [1]. The problem with the usage of these line-coding techniques is that the timing benefits come at the expense of bandwidth, so these techniques are not used in Public Switched Telephone Network (PSTN), which is severely band-limited network, so one has to choose other options. Scrambling is a technique that can be used in conjunction with simpler line coding algorithms such as simple binary and RS232C protocol to achieve above-mentioned goal without sacrificing the bandwidth requirement.

In digital system, it is common practice to encounter long strings of 1's and 0's within the transmitted data that results in constant output levels. Timing information cannot be retrieved from such outputs because there will be no state-transition during these sequences which may result in transmission errors at the receiver. Scrambler can eliminate this problem by detecting undesirable sequences of bits and inserting state transitions in a pseudo random manner. If there is a long sequence of 1's, 0's will be pseudo randomly inserted in to the stream. It ensures that the probability of receiving a '1' is equal to the probability of receiving '0' and minimizes the probability of periodic or repetitive data transmission, which in turn make clock recovery easier [5]. Simple scrambling action of a scrambler is shown in Fig. (1). While it may not be possible to prevent the occurrence of all undesirable sequences with absolute certainty, at least most of the common replications in the input data stream can be removed by the use of a scrambler. It has been found that the transmission of short repetitive patterns could play havoc with both the equalizer and timing recovery systems [2].

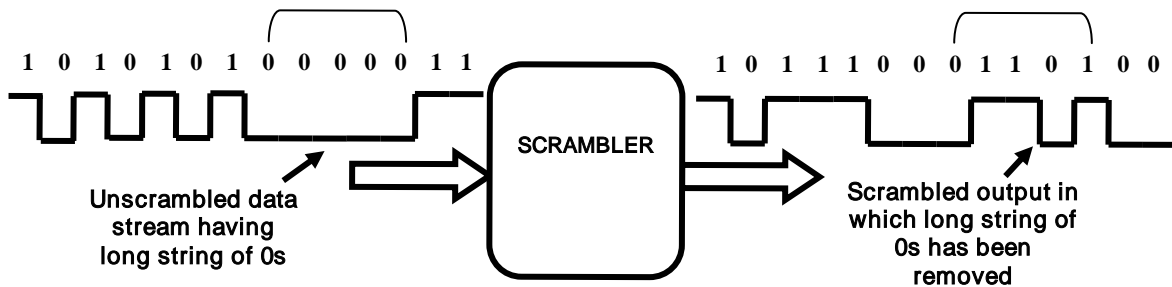


FIGURE 1: Scrambling Action

4. SYSTEM DESIGN

There are many ways to implement scrambler but all rely on the same basic building blocks of linear feedback shift registers and modulo-2-addition functions. Many researchers have discussed the general theory of implementation of scramblers [2-4], [6-7]. In general, the serial data enters in linear feedback shift register, where each stage in the register delays the signal by one time unit as shown in Fig. (2). The delayed version of the output signal is then fed back and

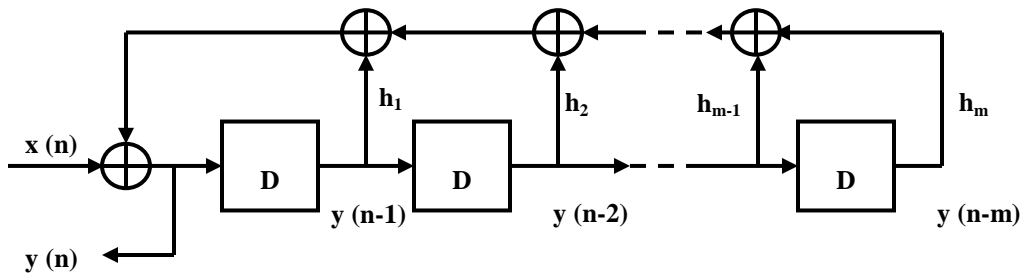


FIGURE 2: Basic Structure of a Scrambler

modulo-2-addition is performed with the input signal. The scrambler's input and output relation, in general, is given by [1]-[2] :

$$y(n) = x(n) + \sum_{k=1}^m h_k y(n - k) \tag{1}$$

Where $y(n)$ is current output, $y(n-k)$ is the output delayed by k times, $x(n)$ is current input and h_k is system transform function. All the constants and variable in eqn. (1) can only have the values '0' or '1' and all additions performed are modulo-2-additions (exclusive-OR operations). Corresponding state vector $s(n)$ to this eqn. can be written as

$$s(n) = [y(n-1), y(n-2), \dots, y(n-m)]$$

$$= [s_1(n), s_2(n), \dots, s_m(n)] \tag{2}$$

In general scrambler is of two types; Frame synchronized scrambler and self-synchronized scrambler. Frame-synchronized scrambler is used for cryptography purposes whereas self-synchronized scrambler is used for clock or carrier recovery purpose and it is this scrambler, which is used in modem design.

Both scramblers are based upon maximum-length shift-register sequence or M-sequences, which are periodic bit sequences with properties that make them appear to be random. These sequences can be generated using a feedback shift register, which is basically a linear sequential filter with feedback paths. Binary m -stage linear feedback shift register is shown in Fig. (3) [8]. Binary sequence of this maximum length is known as M-sequence or pseudo-random binary sequence because it satisfies several statistical tests for randomness. The auto-correlation function of such sequences resembles with the white noise. While implementing such device, the design problem is to select the shift register taps, which generate a M-sequence. The theory behind it is based on finite fields so it involves algebraic polynomials and finite field arithmetic (modulo-2-addition). Polynomials, which generate 'M' sequences, should be primitive. A polynomial $y(x)$ of degree ' m ' is primitive if it is irreducible i.e. has no factors except 1 and itself and if it divides x^k+1 for $k = 2^m - 1$ and does not divide x^k+1 for $k < 2^m - 1$. Sequence period of such primitive polynomials is $2^m - 1$. Characteristic polynomial for M sequence generator is given by [2, 9]:

$$y = 1 + \sum_{k=1}^m h_k x_k \tag{3}$$

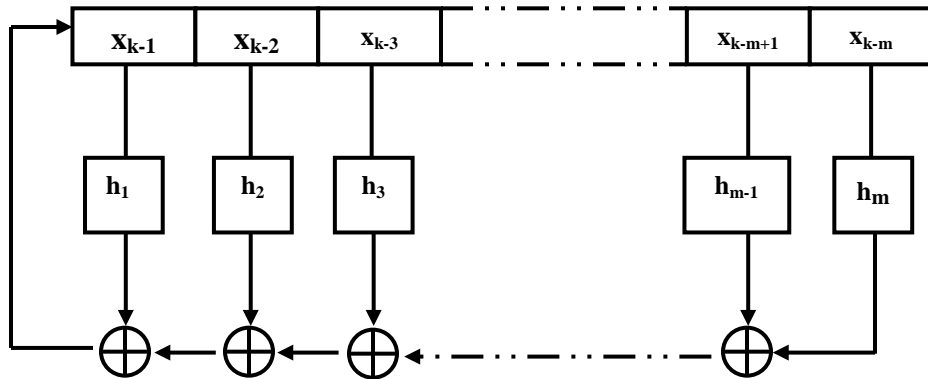


FIGURE 3: Binary m -stage Feedback Shift Register

Let $x(n)$ be the binary sequence at the input of scrambler. Taking D-transform (Huffman transform; like z -transform with $D = z^{-1}$) of the incoming sequence as

$$X(D) = \sum_{n=0}^{\infty} x(n) D^n \tag{4}$$

Then the connecting polynomial for the scrambler given in Fig. (2) can be written as

$$h(D) = 1 + \sum_{k=1}^m h_k D^k \tag{5}$$

Output transform with zero initial state is given by

$$y(n) + \sum_{k=1}^m h_k y(n-k) = x(n) \tag{6}$$

Taking D-transform on both sides of the above equation, we have:

$$Y(D)h(D) = X(D) \tag{7}$$

The output of the scrambler is therefore given by

$$Y(D) = X(D) / h(D) \tag{8}$$

So mathematical operation performed by the scrambler is basically equivalent to dividing the input information sequence by a Generating Polynomial (GP). The polynomial resulting in the fewest feedback connection is often the most attractive for scrambling purpose. Scrambling action of a simple five-tap scrambler specified by the generating polynomial

$$y(x) = 1 + x^{-3} + x^{-5} \tag{9}$$

is shown in Fig. (4).

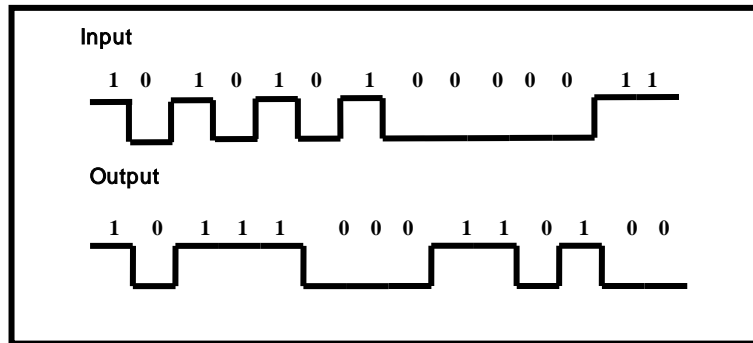


FIGURE 4: Input and Output Waveforms of a Five-tap Scrambler

There are many types of characteristic polynomials that can be used in modems. Some of the popular generating polynomials are those which have been used in the CCITT V.22 and CCITT V.27 protocols. The V.22 polynomial is the one in which seventeen-stage operation is recommended [6]. The CCITT V.27 protocol suggests a seven-stage register. Finally, the CCITT V.29 recommends the 23-stage register to implement generating polynomial. Everyone has his own preference regarding which polynomial to use but all rely on the same basic cells; shift registers and modulo-2-adders.

5. SCRAMBLER IN 56KBPS MODEM

56Kbps modem uses PCM in the downstream (server to client). Clock recovery circuit of the modem generally uses high-Q resonant tank circuit, which averages the clock phase over several bit periods. Clock phase resulting from sampling a constant signal level will attain a static value and if this bit pattern changes to another pattern, the implementation of clock recovery circuit will force the clock phase to change and attain a new value. The serial PCM bit stream reflects the deterministic parts of the signal and this leads to clock phase jitter in the repeater. Its r.m.s. value increases linearly as square root of the number of cascaded repeaters. Since a clock phase change is equivalent to timing jitter, the data eye will not always be sampled at the optimum time and so there will be an increase in bit error probability. Scrambling is one of the effective methods for the suppression of this jitter [10-11].

The data scrambler specified for the transmitter of 56Kbps digital modem is designed using the following generating polynomial [12]:

$$y(x) = 1 + x^{-18} + x^{-23} \tag{10}$$

This is a self-synchronizing scrambler, which means that it will not only provide clocking information throughout the transmission but also will be used to create the signals for the initial handshaking between the modems on the receiving and transmitting end. If there is an error free transmission then one can use the same generating polynomial with the feed-forward shift-register device for de-scrambling but if there is any error then one have to use different polynomial. Block diagram of 56Kbps digital modem’s scrambler is given in Fig. (5).

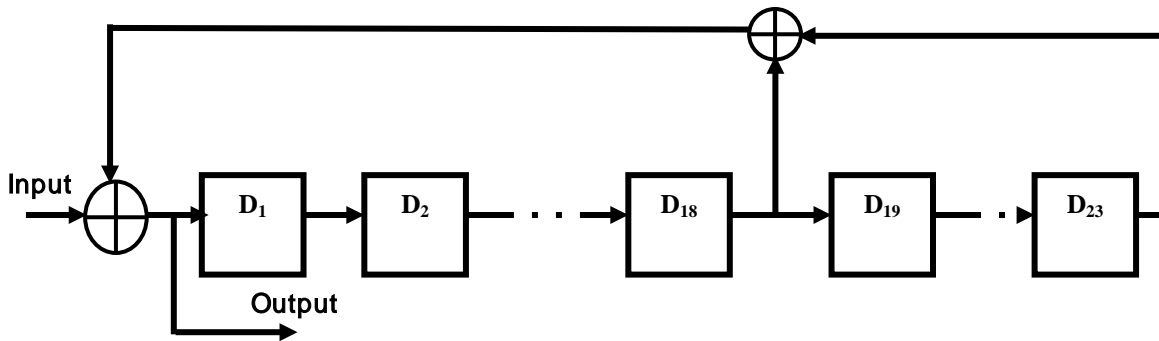


FIGURE 5: Scrambler for 56Kbps Digital Modem

6. SIMULATION OF SCRAMBLER USING MATLAB

Matlab has been used to study the scrambling action in the transmitter of 56Kbps digital modem which uses generating polynomial given by eqn. (10). Using Simulink toolbox of Matlab, a model of scrambler as shown in Fig. (6), corresponding to the eqn. (10) has been developed and its performance against input binary sequences with different probabilities of occurrence of 0’s (**P**) has been evaluated. Model contains a Bernoulli Random Binary Generator (BRBG) block, which generates random number using Bernoulli distribution [13].

The Bernoulli distribution produces zeros with the probability **P** and ones with the probability **1-P**. The Bernoulli distribution has mean value **1-P** and variance **P (1-P)** [14]. The scrambler block scrambles the input signal (the output of BRBG) using scramble polynomial parameter **p**, which

defines the feedback connections in the scrambler i.e. feedback connection from 1st, 3rd and 5th delay elements can be represented as $\mathbf{p} = [0, -3, -5]$ or as $\mathbf{p} = [1 \ 0 \ 0 \ 1 \ 0 \ 1]$.

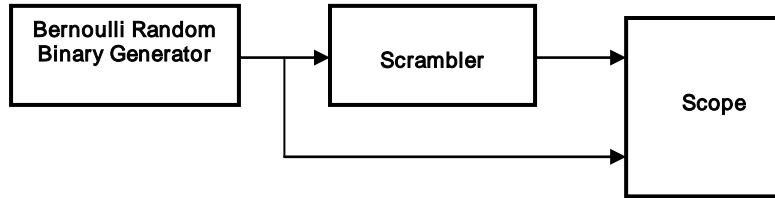


FIGURE 6: Matlab Model to Study the Relation between P and R in a Scrambler

Simulation results corresponding to different values of \mathbf{P} in time domain were obtained and from these results, the number of transitions in input data ($T_{i/p}$) and in output data ($T_{o/p}$) have been calculated. The ratio of $T_{o/p}$ to the $T_{i/p}$ gives the Randomization Parameter \mathbf{R} which can be considered as a measure of performance of the scrambler, \mathbf{R} therefore describes how effectively scrambler randomizes the incoming binary signal. Fig. (7) gives the graphical representation of the results obtained and hence it can be concluded that scrambling action of the scrambler is more effective for the input data sequences having high value of probability of occurrence of zeros or ones i.e. the signal having long sequences of 0s or 1s. Scrambler is less effective for the input data sequences having frequent transitions and moreover no scrambling is needed for such inputs because these sequences have sufficient number of transitions in it, using which clock information can easily be retrieved.

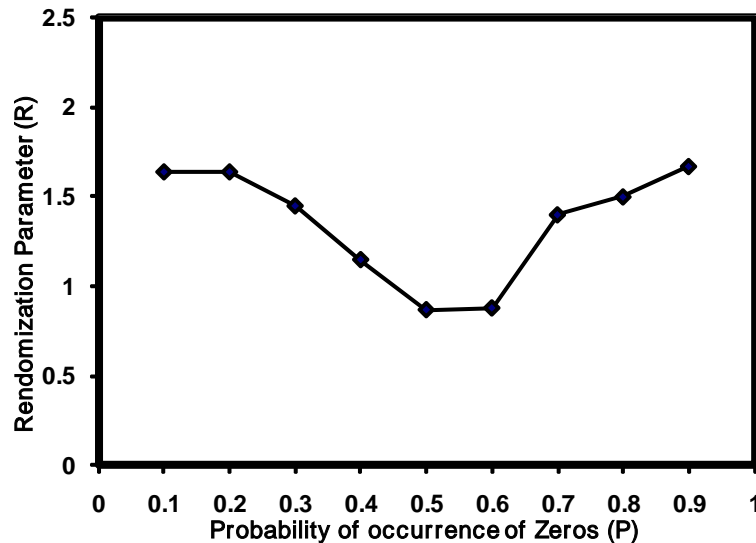


FIGURE 7: Variation of Randomization Parameter (R) With the Probability of Occurrence of (P) For Scrambler With GP Given in Eqn. (10).

7. IMPLEMENTATION OF SCRAMBLER ON DSP CHIP

Scrambler for 56Kbps server (digital) modem has been implemented on TMS320C50PQ57 DSP chip using MICRO-50EB evaluation module. Experimental setup used for the present implementation is shown in Fig. (8). Evaluation module contains a 16 bit fixed point processor TMS320C50PQ57 along with 48-Kiloword (KW) of monitor EPROM, 16KW of program RAM, 32 KW of data RAM & 32KW of I/O RAM. The highly paralleled architecture and efficient instruction set provide speed and flexibility which make the TMS320C50PQ57 DSP to capable of executing about 57 Million Instructions Per Second (**MIPS**). TMS320C50PQ57 DSP optimizes speed by

implementing functions in hardware that other processors implement through micro-code or software. This hardware intensive approach provides high processing power previously unavailable on single chip. Its powerful instruction set, inherent flexibility, high-speed number-crunching capabilities, and innovative architecture have made this high-performance, cost effective processor; the ideal solution to many telecommunications, commercial, industrial and military applications [15].

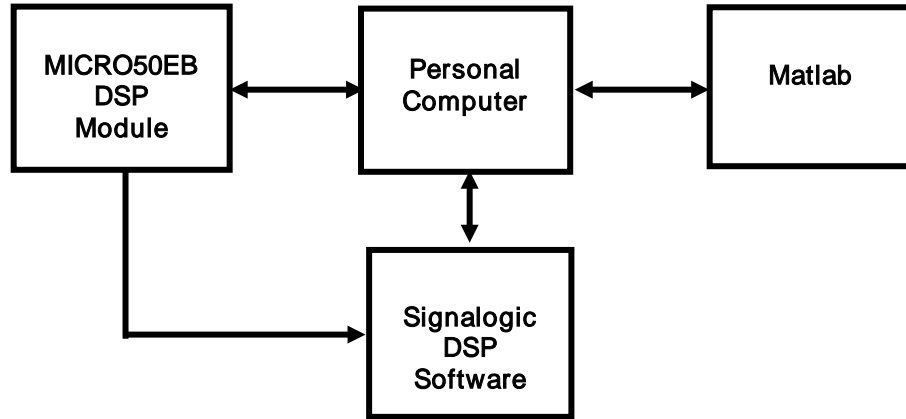


FIGURE 8: Experimental Setup for Soft Implementation of Scrambler of 56Kbps Digital Modem on DSP

7.1. Algorithm for Soft Implementation of the Scrambler

Scrambler has been implemented using the circular buffers of the TMS320C50PQ57 DSP chip. The chip has special memory mapped registers and associated circuitry for two circular buffers. One of the eight auxiliary registers can be used as a pointer into the circular buffer. Circular buffer was implemented on the DSP on-chip memory block. Two memory-mapped registers are associated with each circular buffer that needs to be initialized with the start and end address. Block diagram of I/P sample circular buffer is given in Fig. (9), where $x(n)$ is the input data at a time n , $x(n-1)$ is input data delayed by single time unit and N is length of linear feedback or feed forward shift register. Initialized circular buffer can be used for producing delay and data can be read from any position pointed by the auxiliary register AR-1. Then XOR operation can be performed on delayed samples to achieve scrambling action. Before the initialization of circular buffer we have to initialize the DSP chip and I/O devices [9].

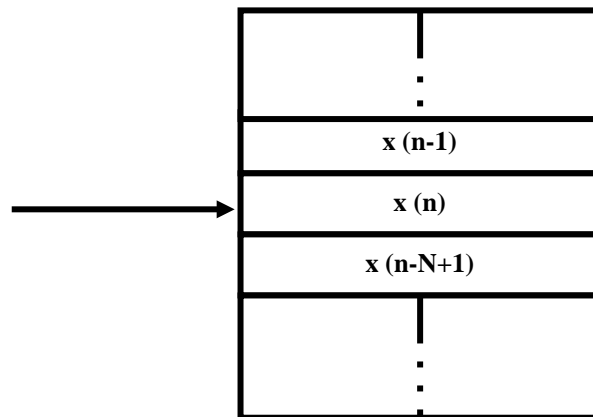


FIGURE 9: Structure of Circular Buffer

In present implementation TLC32044 AIC (Analog Interface Circuit) has been used as I/O device. The supporting algorithm for the initialization of DSP module and algorithm for implementation of scrambler of digital modem is given in Appendix (A) along with the algorithm of main scrambling routine using circular buffer.

Assembly level program (source code) for the scrambler of 56Kbps digital modem has been written using algorithm given in Appendix (A). Source code were loaded into the DSP and output data obtained was stored at appropriate data memory location with the slight modification in the program i.e. one more step of data storage in addition with the data transmission has been included in the main program. Stored data was loaded into the Signalogic DSP Software for time and frequency domain analysis of practically obtained results. In the similar fashion output data obtained from the simulation was loaded in to the software package and simulated and practical results were compared in time as well as frequency domain.

Time domain comparison of scrambler's simulated and practical result is shown in Fig. (10). It can easily be concluded from this figure that the present practical result differs very slightly from the simulated results. The transition which was occurring at 3.375ms in the simulation study has been get shifted to 3.875 in actual practice but this shift does not disturb the scrambling action because total number of transitions are same. Similar study in frequency domain has been carried out for simulated and practical results. Spectral analysis i.e. variation of magnitude with frequency of simulated and practical results is presented in Fig. (11). It is clear from this figure that the practical and simulated results are almost same, which confirms the successful implementation of scrambler on DSP.

Present implementation is more efficient than the earlier implementation reported by Steven A.Tretter, C.J.Buechler and H. Sampath [16]. In the present implementation circular buffer is being used to produce delay and on chip memory of the DSP chip is being used due to which memory requirement as well as execution time have been reduced by using efficient algorithm discussed earlier. Comparison of various implementation parameters like program execution time, program and data memory used for the current and previous study is given in the Table (1).

Implementation	Program Execution Time (μsec)	Program Memory Used (W)	Data Memory Used (W)
Present	3.2	64	23
Previous	5	100	15

TABLE 1: Various Implementation Parameters

8. CONCLUSION

Scrambler for 56Kbps digital modem has been simulated using Matlab and implemented using TMS320C50PQ57 DSP chip during the present study. From the simulation it has been found that scrambling action of proposed scrambler is more effective for the input data sequences having high value of probability of occurrence of zeros or ones i.e. the signal having long sequences of 0s or 1s. Scrambler is less effective for the input data sequences having frequent transitions and more over no scrambling is needed for such inputs because it has sufficient number of transitions in it, from which, clock information can easily be retrieved. In present implementation circular buffer is being used to produce delay and on-chip memory of the DSP chip is used due to which program memory requirement as well as execution time has been get reduced using the efficient algorithm as compared to previous study. Simulated and practical results have been compared

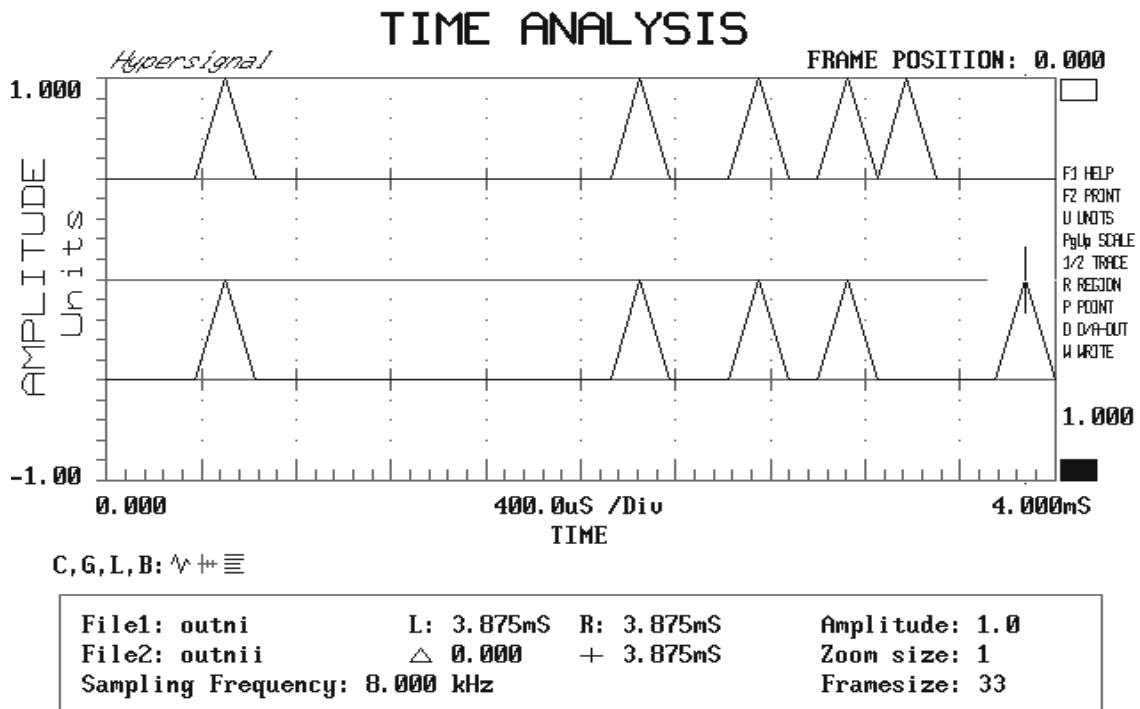


FIGURE 10: Comparison of Simulated and Practical Results of Scrambler in Time Domain

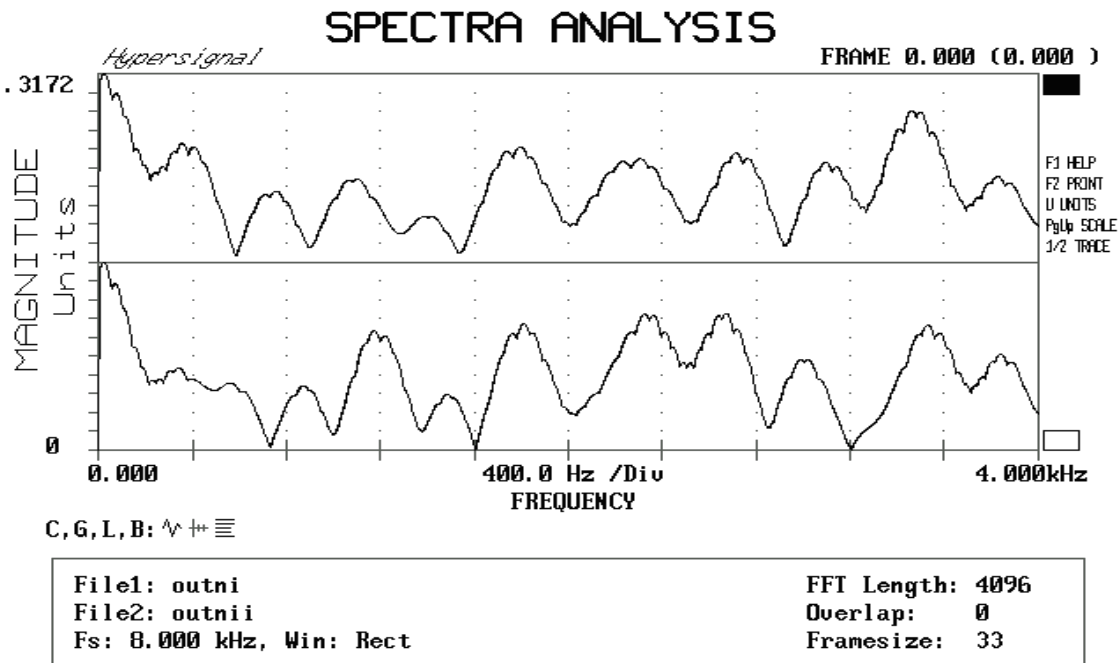


FIGURE 11: Comparison of Simulated and Practical Results of Scrambler in Frequency Domain

using Signalogic DSP Software in time as well as frequency domain and have been found same which confirms the successful implementation of scrambler on DSP.

ACKNOWLEDGEMENTS

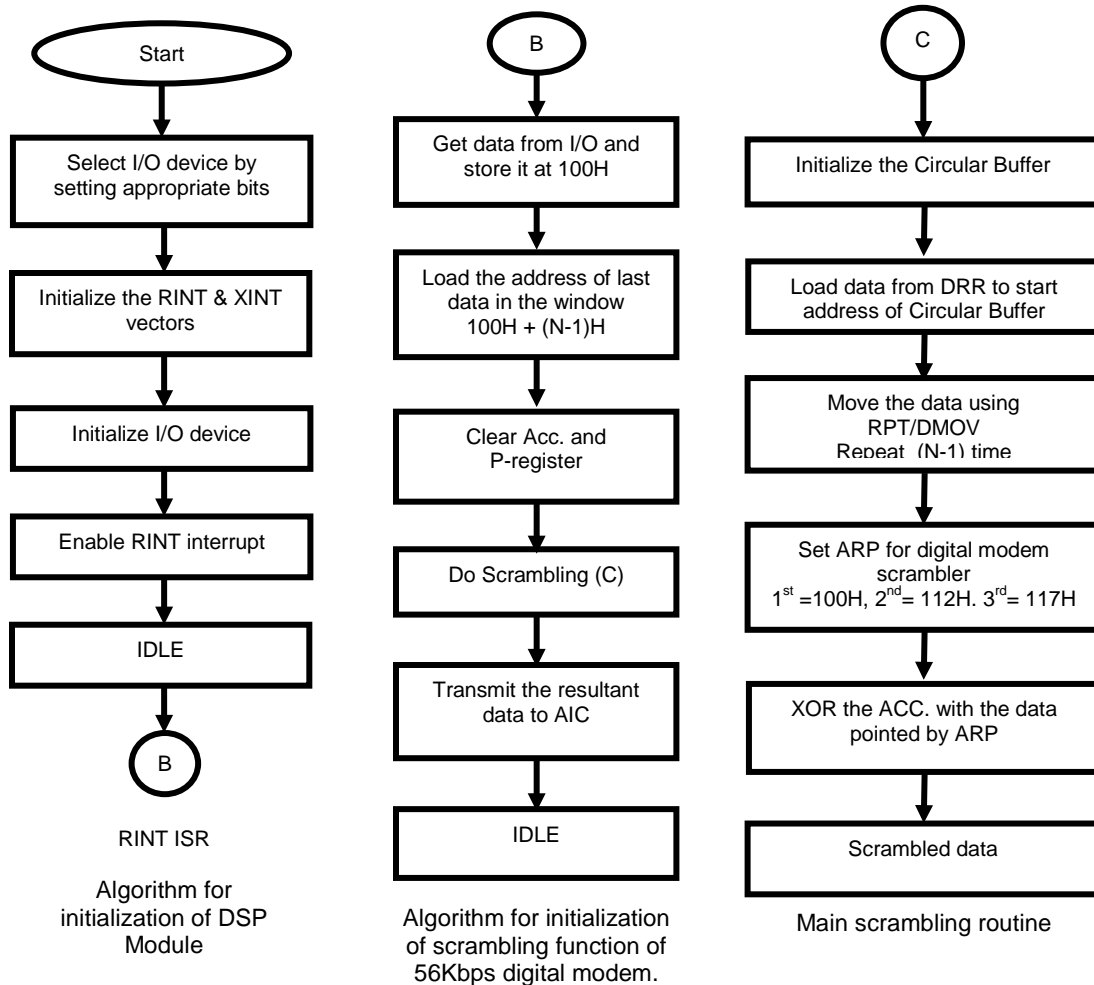
One of the authors Davinder Pal Sharma is thankful to Guru Nanak Dev University, Amritsar, for providing DSP Research facilities at Department of Electronics Technology for present research work.

9. REFERENCES

1. J. G. Proakis, M. Salehi. "*Digital Communications*", McGraw Hill, (2007).
2. R. D. Gitlin, J. F. Hayes. "*Timing recovery and scramblers in data transmission*", Bell System Technical Journal 54(3): 569 – 593, 1975.
3. H. Kasai, S. Senmoto and M. Matsushita, "*PCM jitter suppression by scrambling*", IEEE Trans. on Communications, 22(8): 1114-1122, 1974.
4. A. Huzii, S. Kondo. "*On the timing information disappearance of digital transmission systems*", IEEE Trans. on Communications, 21(4):1072-1074, 1973.
5. R.L. Freeman. "*Practical Data Communications*", John Wiley and Sons Inc., (1995).
6. C. H. Lin et.al. "*Parallel scrambler for high speed applications*", IEEE Trans. on Circuit & Systems-II, 53(7): 558-562, 2006.
7. M. Cluzeau. "*Reconstruction of a linear scrambler*", IEEE Trans. on Computers, 56(9): 1283-1291, 2007.
8. "*Data Scrambler / Descrambler with Look Ahead*", IBM Technical Disclosure Bulletin, 28: 1063-1064, 1985.
9. S. A. Tretter. "*Communication System Design Using DSP Algorithms: With Laboratory Experiments for the TMS320C6713 DSK*", Springer, 163-171 (2008).
10. ITU-T Recommendation V.92. "*Enhancement to Recommendation V.90*", International Telecommunication Union, 2000.
11. D. Y. Kim et. al. "*V.92: The last dial-up modem*", IEEE Trans. On Communications, 52(1): 54-61, 2004.
12. ITU-T Recommendation V.90. "*A digital and analog modem pair for use on the PSTN at data signaling rates of up to 56000 bits/s downstream and 33600 bits/s upstream*", International Telecommunication Union, 1998.
13. "*Simulink User Guide*", The Mathworks Inc. (2009), <http://www.mathworks.com>.

14. G. Zimmermann. "Probabilities of long sequences of identical bits after data scrambling". In Proceeding of IEEE International Conference on Communications, 1990, 1521-1525.
15. "Micro-50 EB user manual", DSP Series, Vi Microsystems Pvt. Ltd., (2000).
16. S. A. Tretter et. al. " V.34 Transmitter and receiver implementation on the TMS320C50 DSP", Digital Signal Processing Solutions, Texas Instruments, USA, 1997.

APPENDIX (A)



Time Domain Analysis and Synthesis Using P^{th} Norm Filter Design

M.Y.Gokhale

Professor and Head of Department of Mathematics,
Maharashtra Institute of Technology, Kothrud,
Pune 38, India

Daljeet Kaur Khanduja

Assistant Professor, Department of Mathematics,
Sinhgad Academy of Engineering, Kondhwa,
Pune 48, India

dkdkhalsa@gmail.com

Abstract

In this paper, a new approach for the design and implementation of FIR filter banks for multirate analysis and synthesis is explored. The method is based on the least P^{th} algorithm and takes into consideration the characteristics of the individual filters. Features of the proposed approach include; it does not need to adapt the weighting function involved and no constraints are imposed during the course of optimization. Mostly, the FIR filter design is concentrated around linear phase characteristics but with the help of minimax solution for FIR filters using the least- P^{th} algorithm, this optimal filter design approach helps us to enhance the properties of LTI systems with good stability. Hence P^{th} norm algorithm will be used in multirate to explore the stability and other properties. We have proposed the band analysis system for analysis and synthesis purpose to explore multirate filter banks. The Matlab toolbox has been used for implementing the filters and its properties are verified with various plots and tables. The results of this paper enable us to achieve good signal to noise ratio (SNR_r) with analysis and synthesis level operations.

Keywords: Analysis, Synthesis, Filter banks, least P^{th} algorithm,

1. INTRODUCTION

Over the last two decades, there has been a steady growth of interest in multirate processing of digital signals. Unlike the single-rate system, the sample spacing in the multirate system can vary from point to point [1]. In multirate filter banks the input signal is divided into channels using band pass filters, and the individual channels are down sampled to rates appropriate to the individual channel bandwidths. The problem of designing filter banks that can provide good frequency resolution while allowing for exact or near perfect reconstruction of the signal is quite challenging because so many dissimilar types of distortion must be minimized and/or eliminated in the same design context. The individual filter issues include the passband size and ripple, stopband size and ripple, transition width and shape, filter phase, filter type (IIR and FIR), filter order, and filter structure. The filter bank issues include the number of bands, frequency coverage, bank efficiency and aliasing, distortion issues include linear distortions (magnitude, phase, and aliasing distortions) and nonlinear distortions (quantization, coding and channel distortions) and the overall processing issues include the system delay and the ability to reject processing distortions [2]. There are several important issues to consider that impact the performance and cost effectiveness of analysis/synthesis filter banks in practical applications. First, the quality of the individual filters in both banks should be good. Typically, this means having high stop band attenuation, good transition band properties and/or good impulse response characteristics. Second, the overall analysis/

synthesis system should reconstruct the input with negligible distortion in the absence of quantization. Third, the filter banks should have an efficient implementation. This impacts the speed of the system as well as the cost. Finally, the overall system delay should be considered. A variety of methodologies based on time domain as well as frequency domain representations are now available [2], [3], [4], but all of these methods have limitations. This paper discusses a new approach using the least P^{th} algorithm to explore the stability and various properties by using the Matlab toolbox for designing various filter banks. The resulting design methodology is uniquely flexible and powerful. By imposing appropriate constraints, a very broad class of FIR analysis /synthesis systems can be designed.

The most efficient tools for the minimax design of FIR digital filters are the Parks-McClellan algorithm and its variants [5]-[7]. However, they only apply to the class of linear phase FIR filters. In many applications, nonlinear phase FIR filters (e.g. those with low group delay) are more desirable. For the minimax design of FIR filters with arbitrary magnitude and phase response several methods are available in the literature. Among others, we mention the weighted least-squares approach [8] in which the weighted function is adapted until a near equiripple filter performance is achieved; the constrained optimization approach [9] in which the design is formulated as a linear or quadratic programming problem; the semidefinite programming approach [10] where the design is accomplished by minimizing an approximation – error bound subject to a set of linear and quadratic constraints that can be converted into linear matrix inequalities. For the 1-D case, minimax design of 1-D FIR filters has been largely focused on the class of linear phase filters. This paper presents a least- P^{th} approach to the design problem. Least – P^{th} optimization as a design tool is not new. It was used quite successfully for the minimax design of IIR filters. However, to date least- P^{th} based algorithms for minimax design of non linear phase 1-D FIR filters have not been reported. In the proposed method, a (near) minimax design is obtained by minimizing a weighted L_p error function without constraints, where the weighting function is fixed during the course of optimization and the power p is taken as an even integer. The proposed method does not need to update the weighting function, and it is an unconstrained convex minimization approach. The approach developed here has some advantages over the method discussed in [2] in terms of computational efficiency, filter quality, implementation structure, mathematical verification of the properties such as causality, stability, etc using the pole zero and magnitude plots.

In section 2, time domain analysis is described. In section 3, basic tools such as decimators, interpolators and multirate filter banks are reviewed. In section 4, the design procedure for implementing the filter banks is presented. Section 5 discusses the design examples to illustrate the effectiveness of the design procedure. Finally some concluding remarks are drawn in Section 6.

2. TIME DOMAIN ANALYSIS

Linear Time Invariant (LTI) systems can be characterized in the time domain by its response to a specific signal called the impulse. This response is called the impulse response of the filter. The impulse response of the filter is the response of the filter at time n to a unit impulse $\delta(n)$ occurring at time 0 and is most often denoted by $h(n)$. The impulse sequence is denoted by $\delta(n)$ and is defined by

$$\begin{aligned}\delta(n) &= 1, \quad n = 0 \\ &= 0, \quad n \neq 0\end{aligned}$$

If the input is the arbitrary signal $x(n)$ that is expressed as a sum of weighted impulses, that is,

$$x(n) = \sum_{k=-\infty}^{\infty} x(k)\delta(n-k)$$

Then the response of the system to $x(n)$ is the corresponding sum of weighted outputs, that is

$$\begin{aligned}
 y(n) = T[x(n)] &= T\left[\sum_{k=-\infty}^{\infty} x(k)\delta(n-k)\right] \\
 &= \sum_{k=-\infty}^{\infty} x(k)T[\delta(n-k)] \\
 &= \sum_{k=-\infty}^{\infty} x(k)h(n,k)
 \end{aligned} \tag{1}$$

Equation (1) is an expression for the response of a linear system to any arbitrary input sequence $x(n)$. This expression is a function of both $x(n)$ and the responses $h(n,k)$ of the system to the unit impulses $\delta(n-k)$ for $-\infty < k < \infty$. In fact, if the response of the LTI system to the unit impulse sequence $\delta(n)$ is denoted as $h(n)$, that is

$$h(n) \equiv T[\delta(n)]$$

Then by the time – invariance property, the response of the system to the delayed unit impulse sequence $\delta(n-k)$ is

$$h(n-k) = T[\delta(n-k)]$$

Consequently the formula in equation (1) reduces to

$$y(n) = \sum_{k=-\infty}^{\infty} x(k)h(n-k) \tag{2}$$

Now the LTI system is completely characterized by a single function $h(n)$, namely, its response to the unit impulse sequence $\delta(n)$. The formula in equation (2) that gives the response $y(n)$ of the LTI system as a function of the input signal $x(n)$ and the impulse response $h(n)$ is called the convolution sum and we say the input $x(n)$ is convolved with the impulse response $h(n)$ to yield the output $y(n)$. Since LTI systems are characterized by their impulse response $h(n)$, in turn $h(n)$ allows us to determine the output $y(n)$ of the system for any given input sequence $x(n)$ by means of the convolution summation,

$$y(n) = \sum_{k=-\infty}^{\infty} h(k)x(n-k) \tag{3}$$

In general, any LTI system is characterized by the input –output relationship in Equation (3). Moreover the convolution summation formula in Equation (3) suggests a means for the realization of the system. In case of FIR systems, such a realization involves additions, multiplications and a finite number of memory locations. Consequently, a FIR system is readily implemented directly, as implied by the convolution summation. LTI systems can also be characterized in the time domain by constant coefficient difference equations. The difference equation is a formula for computing an output sample at time n based on past and present input samples and past output samples. In general a causal LTI difference equation is

$$\begin{aligned}
 y(n) &= b_0x(n) + b_1x(n-1) + \dots + b_Mx(n-M) + \dots - a_1y(n-1) - a_2y(n-2) - \dots - a_Ny(n-N) \\
 &= \sum_{i=0}^M b_i x(n-i) - \sum_{j=1}^N a_j y(n-j)
 \end{aligned} \tag{4}$$

where x is the input signal, y is the output signal, and the constants $b_i, i = 0, 1, 2, 3, \dots, M$ $a_i, i = 1, 2, \dots, N$ are called the coefficients, integers M and N represent the maximum delay in the input and output respectively. The difference equation (4) is often used as a recipe for numerical implementation in software and hardware.

The basic FIR filter is characterized by the following two equations:

$$y(n) = \sum_{k=0}^{N-1} h(k)x(n-k) \tag{5}$$

$$H(z) = \sum_{k=0}^{N-1} h(k)z^{-k} \tag{6}$$

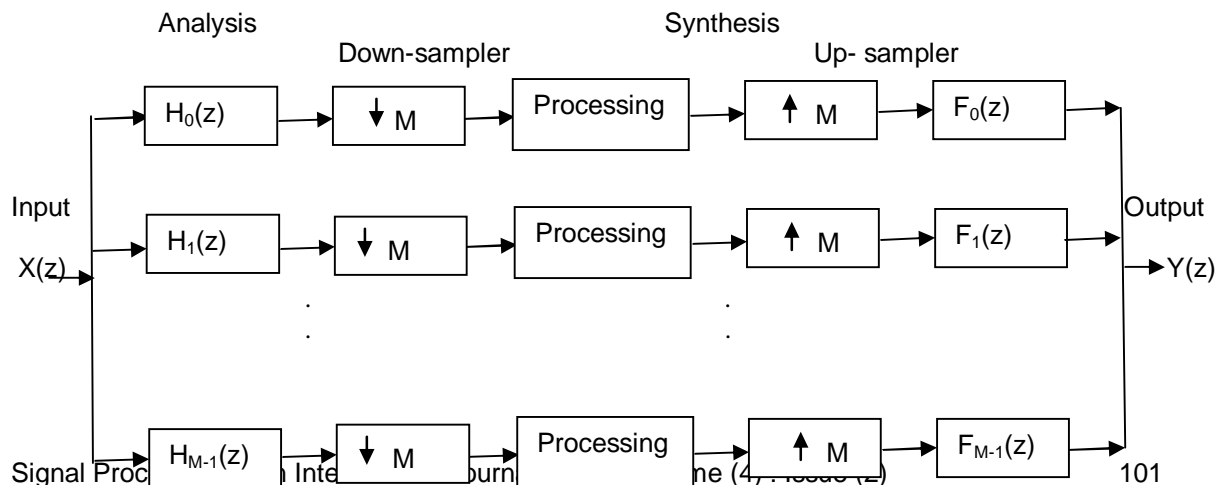
Where $h(k)$, $k=0,1,2,\dots,N-1$, are the impulse response coefficients of the filter, $H(z)$ is the transfer function of the filter and N is the filter length, that is, the number of filter coefficients. Equation (5) is the FIR difference equation. It is a time domain equation and describes the FIR filter in its non recursive form: the current output sample, $y(n)$, is a function only of past and present values of the input, $x(n)$. When FIR filters are implemented in this form that is by direct evaluation of Equation (5) they are always stable. Equation (6) is the transfer function of the filter. It provides a means of analyzing the filter that is for evaluating the frequency response.

3. FILTER BANKS AND MULTIRATE SYSTEMS

To analyze different systems mathematically, it is useful to have some blocks that are common among the systems and furthermore ease the analysis process. In the analysis of the multirate systems and filter banks, the basic building blocks are the interpolators and decimators that alter the sampling frequency at different parts of the system leading to the name "Multirate". These systems provide new and effective tools to represent signals for understanding, processing and compression purposes. Multirate algorithms provide high computational efficiency and hence increase the number of potential applications. The main advantage of using multirate filter banks is the ability of these systems to separate the signal under consideration in the frequency domain into two or more signals or to compose two or more different signals into a single signal. When splitting the signal into various frequency bands, the signal characteristics are different in each band, and various numbers of bits can be used for coding and decoding the sub-signals. In many applications, the processing unit is used for treating the sub-signal in order to obtain the desired operation for the output signal of the overall system.

A filter bank is a collection of filters that are divided in two groups, the analysis filters and the synthesis filters. Analysis filters divide the incoming signal into sub-bands, while the synthesis filters merge the sub-bands in one signal. When the signal is divided into sub-bands, it is possible to process each sub-band separately. The analysis side also includes downsampling while the synthesis side includes upsampling. In the simplest form, the down-sampler reduces the input sample rate by an integer factor, M , by retaining only every M^{th} sample. On the other hand, the up-sampler increases the input sample rate by an integer factor, M , by inserting $M-1$ zeros between consecutive samples. Figure (1) shows a typical structure of an M channel Filter bank.

FIGURE1: M CHANNEL FILTER BANK



4. DESIGN FORMULATION

4.1. The P^{th} Norm and Infinity Norm

Least P^{th} norm provides optimal non linear phase designs that can minimize any norm from 2 (minimum error energy) to infinity (minimax / equiripple error)

The P^{th} norm and infinity norm of a n vector $v = [v_1, v_2 \dots v_n]^T$ are defined as

$$\|v\|_p = \left(\sum_{i=1}^n |v_i|^p \right)^{\frac{1}{p}}$$

And $\|v\|_\infty = \max_i (|v_i|, \text{ for } 1 \leq i \leq n)$. If p is even and the vector components are real numbers, then

$$\|v\|_p = \left(\sum_{i=1}^n v_i^p \right)^{\frac{1}{p}}$$

It is well known that [11] the P^{th} norm and the infinity norm are related by

$$\lim_{p \rightarrow \infty} \|v\|_p = \|v\|_\infty \quad (7)$$

$p \rightarrow \infty$

To get a sense of how $\|v\|_p$ approaches $\|v\|_\infty$, we compute for $v = [1 \ 2 \ 3 \ \dots \ 50]^T$

Its p^{th} norm $\|v\|_2 = 207.18$, $\|v\|_{10} = 58.80$, $\|v\|_{50} = 50.44$, $\|v\|_{100} = 49.07$

$\|v\|_{200} = 49.02$, and of course $\|v\|_\infty = 49$

For an even p , the P^{th} norm is a differentiable function of its components but the infinity norm is not.

So, when the infinity norm is involved in a (design) problem, one can replace it by P^{th} norm (with p even) so that powerful calculus based tools can be used to help solve the altered problem. Obviously, with respect to the original design problem the results obtained can only be approximate. However as indicated by equation (7), the difference between the approximate and exact solutions become insignificant if power of p is sufficiently large.

4.2. Description Of The Design Procedure

To design a filter that meets the performance needs, such as having the required pass bands, stop bands, or transition regions, and is also the optimal solution, the optimal solution filter minimizes a measure of the error between the desired frequency response and the actual filter response using the least P^{th} norm algorithm. Consider two filter frequency response curves;

$D(w)$ -- The response of ideal filter, as defined by signal processing needs and specifications.

$H(w)$ -- The frequency response of the filter implementation to be selected.

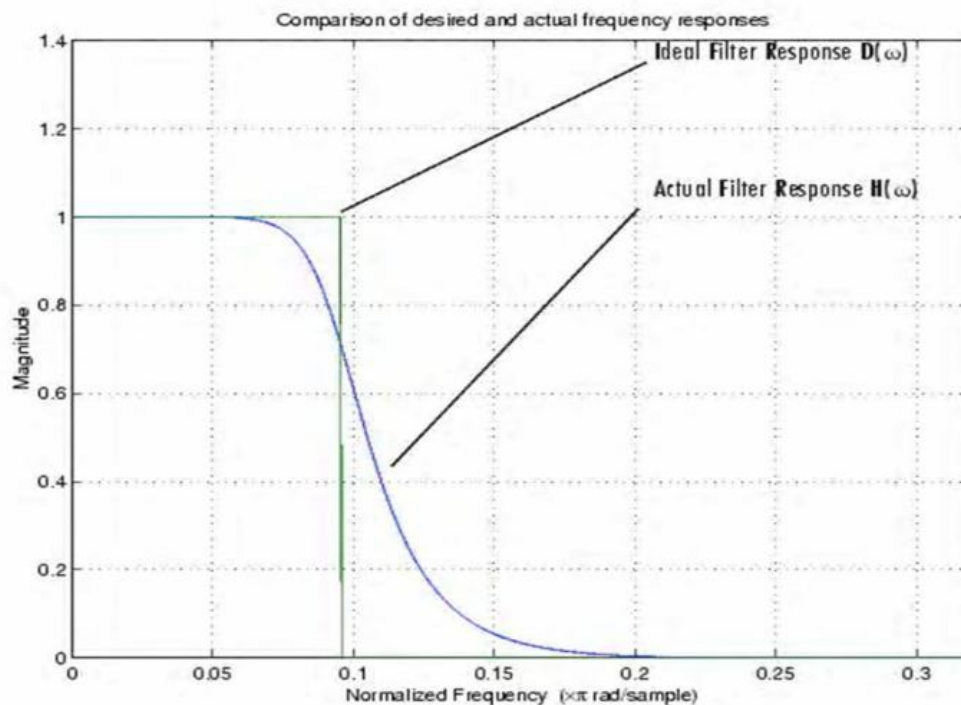
In figure (2), the response curves for $D(w)$ and $H(w)$, both low pass filters are shown. Least P^{th} algorithm seeks to make $H(w)$ match $D(w)$ as closely as possible by a given measure of closeness. More precisely, we define a weighted error

$$E(w) = W(w)[H(w) - D(w)]$$

where $E(w)$ is the error between the ideal and actual filter response values and $W(w)$ is the weighting function. The optimal filter design problem is to determine $H(w)$ that minimizes some measure or norm of $E(w)$ given a particular weighting function $W(w)$ and a desired response $D(w)$. $W(w)$, the weighting function, determines which portions of the actual filter response curve are most important to the filter performance, whether pass band response or attenuation in the stop band. Usually, to measure the error

the L_p norm is used. This norm is given by $\int_{\Omega} [E(w)]^p$ and this is the quantity to be minimized.

FIGURE 2: RESPONSE CURVES FOR IDEAL AND ACTUAL LOWPASS FILTERS



Since the minimization in the ∞ norm is complicated, the minimization under the 2 norm is used in the design procedure. L_2 norm minimizes the energy of the ripples, resulting in a small “total” error and attenuates the energy of a signal as much as possible. The usefulness of the L_2 norm in practice is due to the fact that it can easily be found also in the frequency domain (Parseval Theorem). The L_p norm is computed over a region Ω that uses a subset of the positive Nyquist interval $[0, \pi]$. Ω covers the positive Nyquist interval except for certain frequency bands deemed to be “don't care” regions or transition bands that are not included in the optimization. The optimal filter design problem is to find the filter whose magnitude response, $|H(w)|$ minimizes

$$E(w) = \int_w [W(w)(|H(w)| - D(w))]^p dw \tag{8}$$

for a given $\Omega, p, W(w)$ and $D(w)$.

Up to a given tolerance, FIR filter that approximates a rather arbitrary frequency response $D(w)$ in the minimax sense can be obtained by minimizing $E(w)$ in equation (8) with a sufficiently large p .

5. DESIGN EXAMPLES

FIGURE 3 : BLOCK DIAGRAM USING PTH NORM FILTER DESIGN

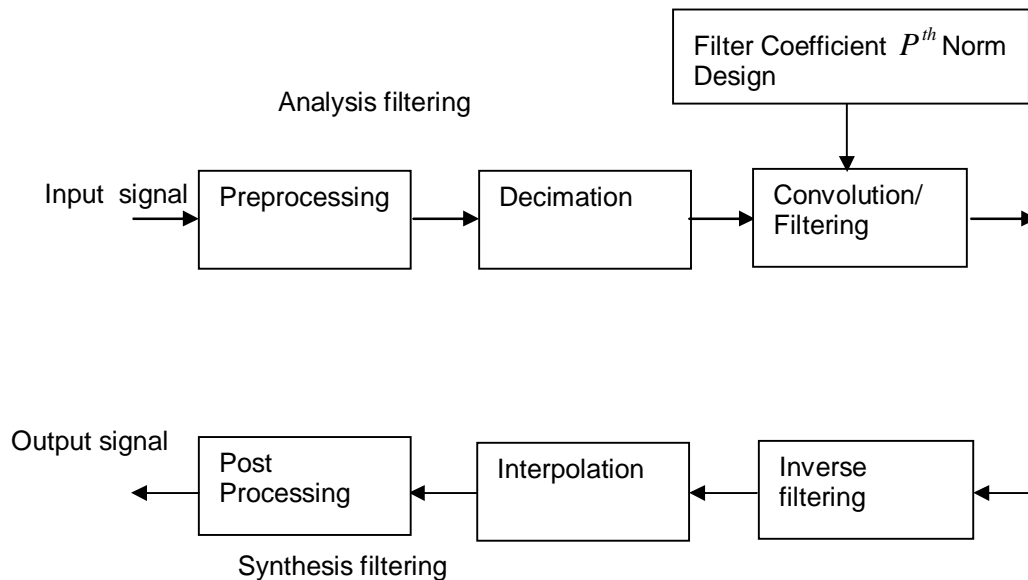


Figure 3 shows proposed system used in application for P^{th} norm filter. A random input signal is preprocessed to remove unwanted parameters, then; decimation is used for multirate analysis purpose. Then P^{th} norm filter coefficients are applied to achieve the analysis parts. For reconstruction, using inverse filtering and interpolation the input signal is reconstructed to calculate reconstruction error to verify the system functionality.

The proposed design procedure can be used to design a wide variety of analysis/ synthesis filter banks with different structural and performance constraints. The imposition of constraints impacts the quality of the resulting overall analysis /synthesis system .The purpose of this section is to illustrate the effectiveness of the design procedure through a series of related examples. In all, four examples are included – three five band systems and one 16-band system. For comparative purposes, the magnitude responses of analysis and synthesis filters are presented. To check the perfect reconstruction quality of the designed filter bank the signal- to- reconstruction noise ratio (SNR_r) which in decibel units is defined as

$$SNR_r = 10 \log_{10} \left(\frac{\text{signal energy}}{\text{reconstruction noise energy}} \right)$$

$$= 10 \log_{10} \left(\frac{\sum_n x^2(n)}{\sum_n (x(n) - \hat{x}(n+k))^2} \right)$$

was used as a measure of reconstruction performance where $x(n)$ and $\hat{x}(n)$ are the input and output signals and k is the system delay. The reconstruction performance is examined by calculating the (SNR_r) for two types of input signals, namely, a ramp input (8000 samples) and a random input (8000 samples) which are denoted by $SNR_r 1$ and $SNR_r 2$.

1. Basic Five –Band System

In the basic five band system example, a simple structure is imposed on the analysis filters of the system. In this case, the fourth and fifth filters, $h_4(n)$ and $h_5(n)$ are defined to be time reversed and frequency shifted versions of the second and first analysis filters, $h_2(n)$ and $h_1(n)$, respectively. The system filters are 55- tap and the system delay is 54 samples. Thus,

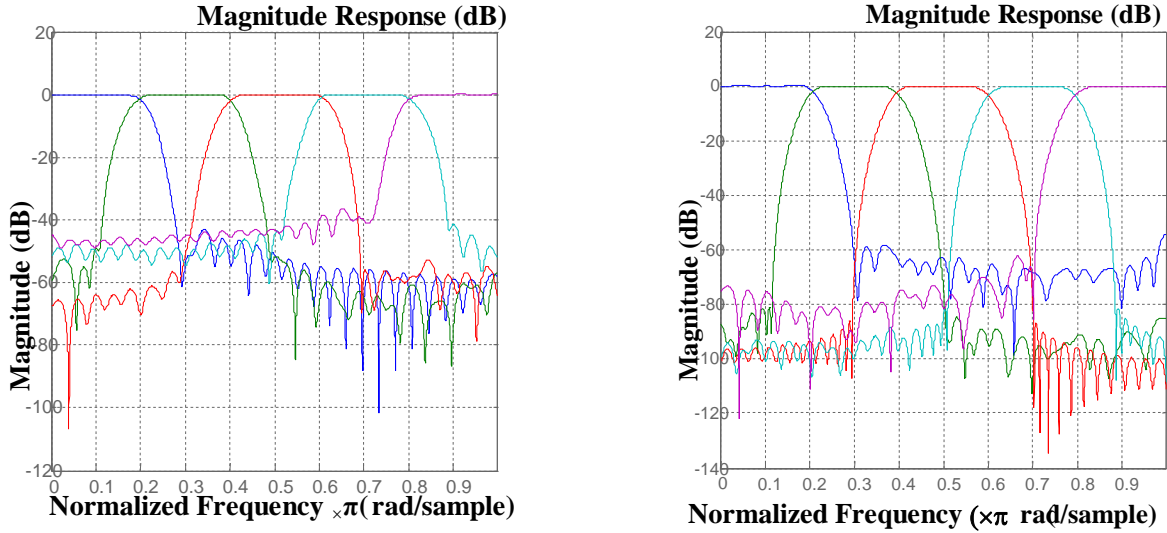
$$h_4(n) = (-1)^n h_2(N-1-n) \tag{10}$$

$$h_5(n) = (-1)^n h_1(N-1-n) \tag{11}$$

In this example, the low pass filter for the analysis section $w_p = 0.1641$ and $w_s = 0.2827$ (Normalized 0 to 1) The second band is a band pass filter with $w_{p_1} = 0.2345$ and $w_{p_2} = 0.3809$, $w_{s_1} = 0.1086$ and $w_{s_2} = 0.5012$. The third band is also a band pass filter with $w_{p_1} = 0.4334$ and $w_{p_2} = 0.5782$, $w_{s_1} = 0.2998$ and $w_{s_2} = 0.6910$. The remaining filters in the bank can be obtained by frequency shifts and time reversals described in (10) and (11). Similarly, for the synthesis section, the low pass filter has $w_p = 0.1527$ and $w_s = 0.2944$. The second band is a band pass filter with $w_{p_1} = 0.2349$ and $w_{p_2} = 0.3532$, $w_{s_1} = 0.1176$ and $w_{s_2} = 0.5030$. Similarly, for the third and fourth band, $w_{p_1} = 0.4583$ and $w_{p_2} = 0.5533$, $w_{p_1} = 0.6517$ and $w_{p_2} = 0.7575$ respectively and $w_{s_1} = 0.2966$ and $w_{s_2} = 0.7001$, $w_{s_1} = 0.5097$ and $w_{s_2} = 0.8834$ respectively. The fifth band is a high pass filter with $w_s = 0.7058$ and $w_p = 0.8846$

Figure(4) shows the frequency response of the analysis and synthesis filters for the resulting five – band system. The reconstruction error and signal to noise ratios of the five band systems are presented in Table 1. Table 2 contains the coefficients of the first three analysis and synthesis filters.

FIGURE 4(a) Analysis and(b) Synthesis filters of the basic five band system with 55 tap analysis and synthesis filters and a system delay of 54 samples(Table 2)



2. Low Delay Five –Band System

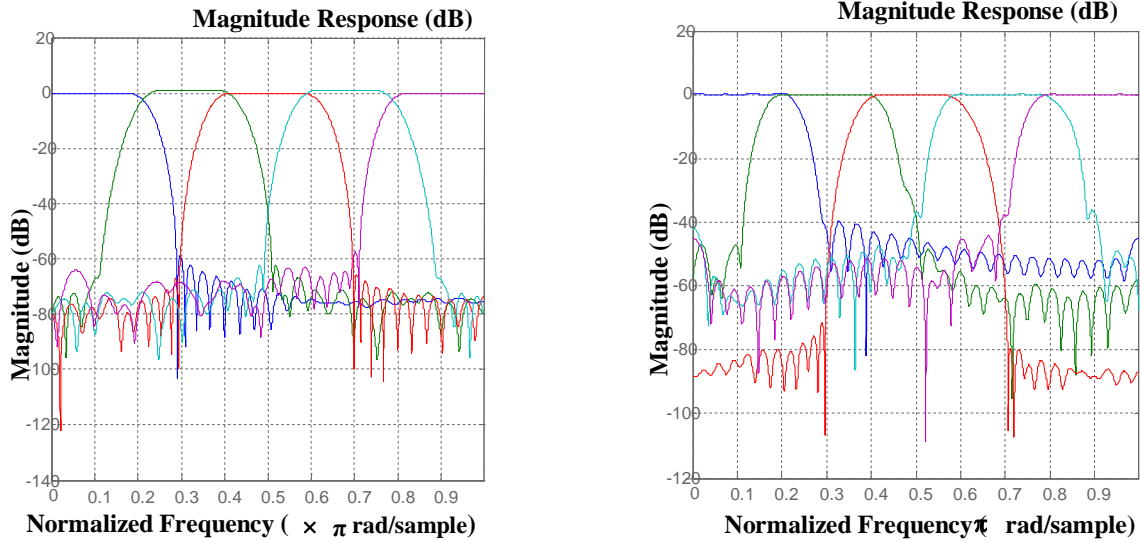
Due to filtering operations that are performed on the signal passing through the filter bank, a delay between the input and the output signals is introduced. In many applications, it is desirable to keep this delay as short as possible. In this example, the design system’s flexibility in adjusting the reconstruction delay of the system was utilized and the system delay is chosen to be 28 samples. In this system, the fourth and fifth band analysis filters were selected to be the frequency shifted versions of the first two analysis filters as

$$h_4(n) = (-1)^n h_2(n) \quad (12)$$

$$h_5(n) = (-1)^n h_1(n) \quad (13)$$

For this example, three minimum phase filters were used as starting point filters since they have been found to be good starting point filters for low delay systems. For this case, for the analysis section, the first band which is a low pass filter has $w_p = 0.1767$ and $w_s = 0.2871$. The second and the third band pass filters have $w_{p_1} = 0.4205$ and $w_{p_2} = 0.5752$, $w_{p_1} = 0.2725$ and $w_{p_2} = 0.3657$ respectively and $w_{s_1} = 0.2977$ and $w_{s_2} = 0.6955$, $w_{s_1} = .1059$ and $w_{s_2} = 0.5017$ respectively. Similarly for the synthesis section, the low pass filter has $w_p = 0.1832$ and $w_s = 0.2940$ respectively. The second, third and fourth band filters have $w_{p_1} = 0.2095$ and $w_{p_2} = 0.3881$, $w_{p_1} = 0.4297$, $w_{p_2} = 0.5481$, $w_{p_1} = 0.6128$, $w_{p_2} = 0.7864$ respectively and $w_{s_1} = 0.1136$, $w_{s_2} = 0.5036$, $w_{s_1} = 0.2990$, $w_{s_2} = 0.7039$, $w_{s_1} = 0.5078$, $w_{s_2} = 0.8867$ respectively. The fifth band is a high pass filter with $w_s = 0.7060$ and $w_p = 0.7996$. Figure (5) shows the frequency response of the resulting analysis and synthesis filters. The reconstruction error and signal to noise ratios of this system are given in Table 1. Table 3 contains the coefficients of the analysis and synthesis filters.

FIGURE 5: (a) Analysis and (b) Synthesis filters of the low delay five-band system with 55-tap filters and a system delay of only 28 samples (Table 3)



3. COSINE MODULATED FIVE –BAND SYSTEM

Cosine modulated filter banks are widely used and known to be highly efficient since each of the analysis and synthesis filters can be implemented with the aid of only one prototype filter and a Discrete Cosine Transform. In the cosine modulated five band systems, the analysis filters were chosen to be a cosine modulated version of a baseband filter. The baseband filter $h_0(n)$ had a nominal cutoff of $\frac{\pi}{10}$ and the analysis filters were defined as

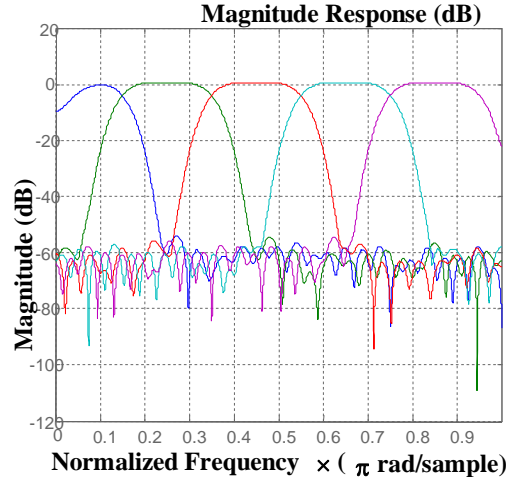
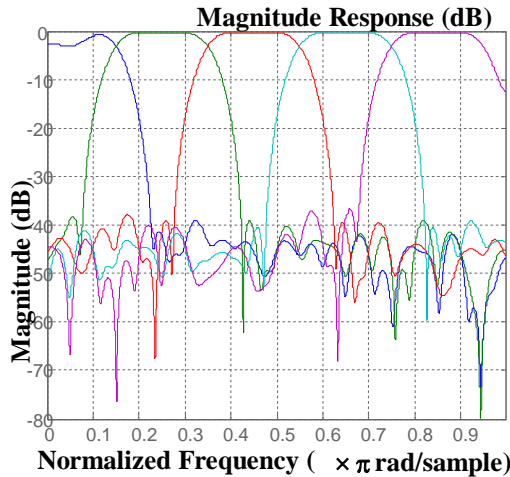
$$h_k(n) = h_0(n) \cos \left[\left(k - \frac{1}{2} \right) \frac{n\pi}{M} \right] \quad k= 1, 2 \dots M \quad (14)$$

and the synthesis filters were defined as

$$g_k(n) = g_0(n) \cos \left[\left(k - \frac{1}{2} \right) \frac{(n - n_0)\pi}{M} \right], \quad k= 1, 2 \dots M \quad (15)$$

where $g_0(n)$ is the baseband synthesis filter and n_0 is an integer whose value depends on the length of the filters and the total system delay. In this example n_0 is 5. Figure (6) shows the frequency response of the analysis and synthesis filters. The reconstruction error and signal to noise ratios of the five band systems are presented in Table 1. Table 4 contains the coefficients of the analysis baseband and synthesis baseband filters.

FIGURE.6 (a) Analysis and(b)Synthesis filters of the system with cosine modulated 55-tap analysis and synthesis filters and a system delay of 54 samples.($n_0=5$) (Table 4)



4. COSINE MODULATED 16-BAND SYSTEM

To illustrate the possibility of designing large systems, a 16-band example with 96-tap analysis and synthesis filters is designed. This system is also based on cosine modulation and the system delay is 95.

For this case, the baseband filter has a cut off frequency of $\frac{\pi}{32}$ and n_0 is 1. Figure (7) shows the frequency response of the analysis and synthesis filters. Table 5 contains the coefficients of the analysis baseband and synthesis baseband filters.

FIGURE7 (a) Analysis and (b) Synthesis filters of the cosine modulated 16 band systems with 96 tap filters (Table5)

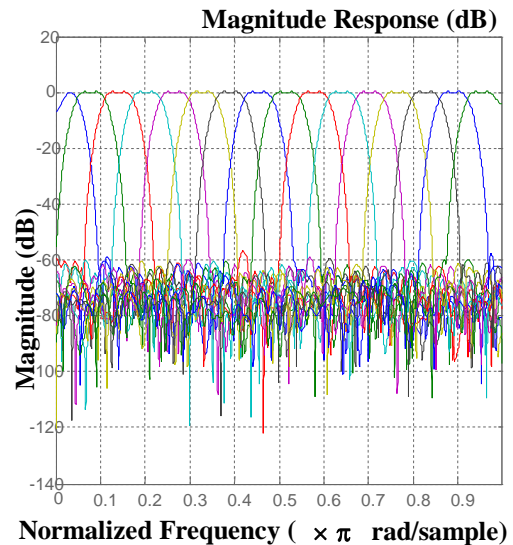
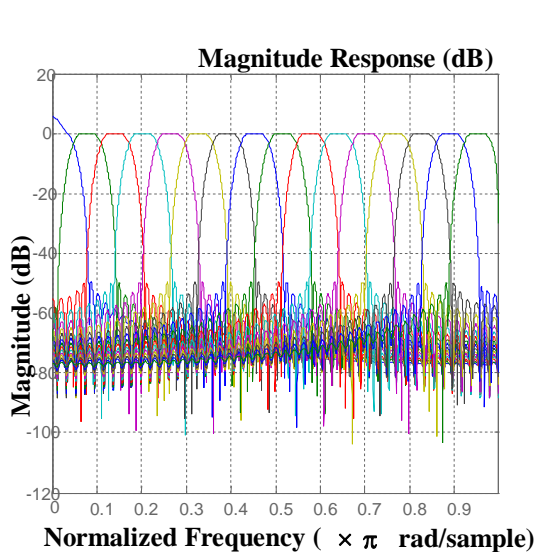


TABLE 1: Some System Specifications for the Five-Band Systems

	Basic System	Low Delay	Cosine Modulated
Filter Length	55	55	55
Reconstruction Error	0.2501	0.1916	0.0022
SNR_r1	100dB	97dB	87dB
SNR_r2	100dB	97dB	87dB
System Delay	54	28	54

Reconstruction error is calculated by considering the 8000 samples. The reconstruction error has also been tested with increasing number of samples which is an acceptable range that is minimum.

6. CONCLUSION

In this paper a new least P^{th} norm approach for FIR filter design is presented which provides optimal non linear phase designs that can minimize any norm from 2 (minimum error energy) to infinity (minimax / equiripple error). The resulting design procedure is very flexible and allows the direct imposition of many combinations of constraints and the realization of many different types of tradeoffs. The necessary assumptions and the design procedure for designing the filter have been explained. Four design examples have been included to illustrate the design procedure. The criteria used for the designed filter keeping in mind the properties of filter design are not violated, that is, in other words we have verified the mathematical results with *MATLAB* tool for filter design and analysis and verified for filter stability using the pole-zero plot, and the causality property using the impulse response. However this chapter helps to achieve the multirate analysis and synthesis approach which helps its application paradigm. In [2], a time domain design algorithm is described for the design of FIR filter bank systems. However, the design process involves calculating the pseudo inverse of large matrices, which is time consuming. In the design methods proposed here there is no need to calculate inverses of matrices. This leads to improvement in the computational efficiency during the implementation of the system. From Table 2.1, it can be seen that all the SNR_r ratios are over 80 dB, which are good enough for many applications. The tables show the filter coefficients and its responses and analysis and synthesis quality is verified with the help of SNR_r , which is good as shown in the result tables. Hence we conclude that the P^{th} norm filter can be used for efficient multirate analysis and synthesis purpose.

REFERENCES

- [1] P.P. Vaidyanathan, "Multirate digital filters, filter banks, polyphase networks and Applications: A tutorial." Proc. IEEE, pp. 56-93. Jan1990.
- [2] K. Nayebi. T. Barnwell and M. Smith "Time domain filter bank analysis: A new design Theory. " IEEE Trans. Signal Processing. pp.1412-1429, June 1992.
- [3] M. Smith and T. Barnwell. "A new filter bank theory for time frequency representation." IEEE Trans. Acoustic Speech Signal processing .vol.ASSP-35 .no.3, pp 314-327. March 1987.
- [4] M. Vetterli. "A theory of multirate filter banks." IEEE Trans. Acoustic Speech signal Processing .vol.ASSP – 35.pp 356-372. March 1987.
- [5] T.W. Parks and J.H. Mc.Clellan, "Chebyshev approximation for nonrecursive digital filters with linear phase." IEEE Trans. Circuit Theory, vol19, pp189-194, 1972.
- [6] T.W.Parks and C.S.Burrus, Digital Filter Design, Wiley, New York, 1987
- [7] A. Antoniou, Digital Filters; Analysis, Design and applications, Second Edition, Mc Graw – Hill, New York 1993
- [8] Y.C.Lim, J.H.Lee, C.K. Chen, and R-H Yang, "A weighted least squares approximation for quasi-

- equiripple FIR and IIR digital filter design," IEEE Trans. Signal Processing, vol 40, pp.551-558, 1992
- [9] M.C.Lang, "Chebyshev design of FIR filters with arbitrary magnitude and phaseResponses," EUSIPCO'96, vol.3, pp.1757-1760, Trieste, Italy 1996.
- [10] W.S.Lu, "Design of nonlinear phase FIR digital filters: A semidefinite programming Approach," Proc. ISCAS vol III, pp. 263-266, May1999
- [11] G.H.Golub and C.F. Van Loan, Matrix Computation, Second Edition, the Johns Hopkins University Press, 1989.

TABLE 2 The Filter Coefficients of the Basic Five-Band System with 55-Tap Filters and 54 Samples of Delay

$h_1(n)$	$h_2(n)$	$h_3(n)$	$g_1(n)$	$g_2(n)$	$g_3(n)$	$g_4(n)$	$g_5(n)$
-0.00028	-0.00086	0.00079	-0.00052	0.00000	-0.00010	0.00010	0.00005
0.00179	-0.00055	-0.00118	-0.00018	0.00028	-0.00004	-0.00025	-0.00024
0.00390	0.00183	-0.00092	0.00026	0.00122	0.00038	-0.00006	0.00055
0.00659	0.00274	0.00271	0.00114	0.00227	0.00045	0.00133	-0.00101
0.00914	-0.00082	-0.00105	0.00170	0.00100	-0.00048	-0.00253	0.00170
0.01103	-0.00358	-0.00548	0.00185	-0.00486	-0.00202	0.00106	-0.00247
0.01094	0.00156	0.00570	0.00089	-0.01216	-0.00078	0.00394	0.00326
0.00757	0.01014	0.00702	-0.00133	-0.01070	0.00588	-0.00835	-0.00369
0.00016	0.00615	-0.01036	-0.00471	0.00683	0.00528	0.00583	0.00356
-0.00947	-0.01356	-0.00318	-0.00769	0.02996	-0.01259	0.00394	-0.00272
-0.01808	-0.02811	0.00888	-0.00854	0.03177	-0.01407	-0.01223	0.00156
-0.02183	-0.01523	-0.00937	-0.00482	-0.00248	0.02061	0.01049	-0.00104
-0.01849	0.01479	0.00483	0.00425	-0.04680	0.02504	-0.00160	0.00257
-0.00774	0.02857	0.02963	0.01780	-0.04990	-0.02538	-0.00368	-0.00736
0.00777	0.01472	-0.02885	0.03160	0.00482	-0.03133	0.00247	0.01545
0.02318	-0.00049	-0.04936	0.04008	0.06295	0.02019	-0.00408	-0.02508
0.03188	0.00596	0.05160	0.03731	0.04863	0.02284	0.01345	0.03271
0.02855	0.01727	0.05431	0.02068	-0.03852	0.00047	-0.01819	-0.03438
0.01153	0.00247	-0.05419	-0.00759	-0.10023	0.00845	0.00454	0.02746
-0.01477	-0.02925	-0.03254	-0.03897	-0.04393	-0.03668	0.01689	-0.01300
-0.04073	-0.03751	0.02141	-0.06127	0.09353	-0.06186	-0.01957	-0.00362
-0.05390	-0.01337	-0.01495	-0.06168	0.16398	0.08060	0.00151	0.01358
-0.04417	-0.00134	0.04521	-0.03290	0.07047	0.12452	0.00285	-0.00763
-0.00752	-0.02725	0.07396	0.02355	-0.11024	-0.11847	0.02791	-0.01982
0.05103	-0.04110	-0.12571	0.09609	-0.20118	-0.17495	-0.05354	0.06735
0.11866	0.02507	-0.12172	0.16608	-0.11659	0.13660	0.00961	-0.12526
0.17794	0.13941	0.18909	0.21378	0.05184	0.19293	0.09474	0.17803
0.21289	0.16984	0.13991	0.22604	0.14821	-0.12833	-0.15167	-0.20941
0.21406	0.03603	-0.20962	0.20008	0.11738	-0.17042	0.06661	0.20817
0.18216	-0.16648	-0.12463	0.14551	0.03085	0.09765	0.11155	-0.17275
0.12732	-0.24591	0.18139	0.07977	-0.02625	0.11649	-0.21520	0.11195
0.06574	-0.12170	0.08776	0.02207	-0.04409	-0.05704	0.13380	-0.04200
0.01345	0.08371	-0.12135	-0.01430	-0.05647	-0.05275	0.05910	-0.01935
-0.01870	0.18187	-0.04759	-0.02511	-0.06624	0.02089	-0.18239	0.05876
-0.02844	0.11586	0.05737	-0.01638	-0.04277	0.00201	0.13937	-0.07151
-0.02115	-0.00788	0.01924	0.00051	0.01780	0.00132	-0.00361	0.06177
-0.00692	-0.06179	-0.01320	0.01355	0.06977	0.02270	-0.08522	-0.03975
0.00476	-0.03122	-0.00679	0.01577	0.06838	-0.00828	0.07329	0.01688
0.00843	0.00684	-0.00242	0.00677	0.02203	-0.02247	-0.01874	-0.00145
0.00447	-0.00116	0.00462	-0.00817	-0.02229	0.00511	-0.00653	-0.00359
-0.00287	-0.02966	-0.00296	-0.02187	-0.03408	0.00843	-0.00205	0.00036
-0.00815	-0.02791	-0.00474	-0.02843	-0.02252	0.00103	0.00436	0.00620
-0.00819	0.00770	0.01424	-0.02616	-0.01036	0.00646	0.01580	-0.01126
-0.00280	0.03515	0.00355	-0.01698	-0.00421	-0.00516	-0.03299	0.01207
0.00517	0.02512	-0.02065	-0.00564	0.00263	-0.01433	0.02229	-0.00874
0.01206	-0.00636	0.00003	0.00370	0.01141	0.00584	0.00656	0.00331
0.01448	-0.02364	0.01819	0.00822	0.01437	0.01426	-0.02450	0.00169
0.01136	-0.01380	-0.00271	0.00814	0.00752	-0.00424	0.01864	-0.00466
0.00410	0.00586	-0.01124	0.00490	-0.00269	-0.00974	-0.00160	0.00521
-0.00378	0.01439	0.00364	0.00114	-0.00743	0.00218	-0.00862	-0.00403
-0.00942	0.00787	0.00439	-0.00159	-0.00511	0.00482	0.00741	0.00224
-0.01155	-0.00149	-0.00235	-0.00246	-0.00070	-0.00076	-0.00183	-0.00084
-0.01018	-0.00536	-0.00058	-0.00221	0.00143	-0.00163	-0.00129	0.00001
-0.00688	-0.00351	0.00073	-0.00129	0.00115	0.00014	0.00125	0.00021
-0.00227	-0.00102	-0.00007	-0.00004	0.00033	0.00030	-0.00037	-0.00017

TABLE 3 The Filter Coefficients of The Low Delay Five-Band System With 55-Tap Filters and 28 Samples of delay.

$h_1(n)$	$h_2(n)$	$h_3(n)$	$g_1(n)$	$g_2(n)$	$g_3(n)$	$g_4(n)$	$g_5(n)$
0.00190	0.00175	0.00298	0.00108	-0.00295	0.00071	-0.00528	0.00179
0.00805	0.00636	-0.00027	-0.00425	-0.00587	-0.00031	0.01147	-0.00658
0.02201	0.00711	-0.01557	-0.00857	-0.00062	-0.00351	-0.00038	0.01183
0.04667	-0.00836	0.00110	-0.01285	0.01766	0.00128	-0.03232	-0.01701
0.08248	-0.03651	0.04663	-0.01696	0.03382	0.00910	0.05183	0.01976
0.12562	-0.04130	-0.00236	-0.01997	0.01981	-0.00289	-0.01530	-0.01840
0.16758	0.01352	-0.10054	-0.01769	-0.02759	-0.01487	-0.06317	0.01430
0.19663	0.09908	0.00325	-0.00791	-0.06528	0.00425	0.09787	-0.01019
0.20140	0.11600	0.16916	0.01025	-0.04579	0.01294	-0.03482	0.01057
0.17545	0.00115	-0.00270	0.03269	0.01418	-0.00358	-0.06085	-0.01710
0.12082	-0.16195	-0.22931	0.05290	0.03997	0.00799	0.06944	0.02867
0.04894	-0.19730	0.00033	0.06150	0.00076	-0.00058	0.01323	-0.03816
-0.02218	-0.03783	0.25098	0.05264	-0.02992	-0.05575	-0.05356	0.03837
-0.07379	0.16834	0.00270	0.02592	0.03148	0.00793	-0.03852	-0.02398
-0.09309	0.21061	-0.21455	-0.00902	0.13803	0.12590	0.15406	-0.00079
-0.07808	0.06019	-0.00423	-0.03698	0.13578	-0.01553	-0.11062	0.02516
-0.03834	-0.10421	0.12603	-0.04068	-0.03700	-0.19814	-0.09645	-0.03228
0.00875	-0.12269	0.00266	-0.01070	-0.23274	0.01909	0.25329	0.01022
0.04494	-0.03228	-0.01833	0.05124	-0.24357	0.24294	-0.18569	0.04443
0.05810	0.02299	0.00140	0.12888	-0.04667	-0.01575	-0.03318	-0.11931
0.04643	-0.00250	-0.06507	0.19858	0.16439	-0.23694	0.18176	0.19249
0.01818	-0.02436	-0.00533	0.23596	0.20420	0.00657	-0.15755	-0.23710
-0.01276	0.01781	0.09451	0.22803	0.08849	0.17779	0.04920	0.23595
-0.03333	0.06859	0.00627	0.17663	-0.02783	0.00362	0.02143	-0.18621
-0.03663	0.05075	-0.07012	0.09989	-0.05216	-0.08784	-0.04292	0.10473
-0.02406	-0.01659	-0.00344	0.02243	-0.02717	-0.00917	0.05808	-0.01769
-0.00359	-0.05152	0.01878	-0.03282	-0.02377	0.00281	-0.06377	-0.04708
0.01468	-0.02693	-0.00114	-0.05565	-0.03777	0.00740	0.02454	0.07500
0.02329	0.00619	0.02513	-0.04901	-0.02607	0.04763	0.03697	-0.06607
0.02027	0.00536	0.00436	-0.02759	0.00866	-0.00047	-0.05407	0.03616
0.00915	-0.00956	-0.04069	-0.00749	0.02090	-0.05475	0.00793	-0.00470
-0.00364	-0.00322	-0.00436	-0.00053	-0.00167	-0.00638	0.03844	-0.01138
-0.01216	0.01748	0.02905	-0.00765	-0.01830	0.03167	-0.02994	0.00793
-0.01354	0.02099	0.00177	-0.02217	0.00277	0.00862	-0.01417	0.00990
-0.00873	0.00249	-0.00648	-0.03265	0.03647	-0.00170	0.03533	-0.02900
-0.00125	-0.01291	0.00111	-0.03149	0.03866	-0.00545	-0.01968	0.03935
0.00491	-0.00987	-0.01013	-0.01677	0.00634	-0.01685	-0.00183	-0.03582
0.00736	0.00017	-0.00235	0.00518	-0.02202	-0.00027	0.00618	0.02298
0.00594	0.00222	0.01388	0.02570	-0.02161	0.01891	-0.00628	-0.00781
0.00233	-0.00171	0.00173	0.03633	-0.00721	0.00463	0.01243	-0.00157
-0.00125	-0.00197	-0.00832	0.03478	-0.00332	-0.01062	-0.01463	0.00358
-0.00319	0.00214	-0.00033	0.02326	-0.00814	-0.00546	0.00156	0.00044
-0.00312	0.00410	0.00113	0.00857	-0.00540	0.00130	0.01269	-0.00483
-0.00171	0.00154	-0.00059	-0.00362	0.00639	0.00337	-0.01172	0.00656
-0.00007	-0.00153	0.00270	-0.00921	0.01167	0.00343	-0.00211	-0.00344
0.00093	-0.00186	0.00065	-0.00877	0.00452	-0.00053	0.01015	-0.00198
0.00109	-0.00051	-0.00273	-0.00432	-0.00354	-0.00344	-0.00667	0.00751
0.00065	0.00030	-0.00027	0.00021	-0.00197	-0.00121	-0.00113	-0.00936
0.00007	0.00028	0.00125	0.00300	0.00377	0.00150	0.00443	0.00783
-0.00027	0.00009	-0.00007	0.00250	0.00402	0.00145	-0.00581	-0.00393
-0.00026	0.00001	-0.00012	-0.00011	-0.00163	-0.00001	0.00588	0.00148
-0.00009	0.00000	0.00007	-0.00327	-0.00511	-0.00087	-0.00356	-0.00033
0.00001	0.00000	-0.00011	-0.00356	-0.00304	-0.00037	-0.00209	0.00024
0.00002	0.00000	0.00000	-0.00221	0.00049	0.00026	0.00589	-0.00110
0.00000	0.00000	0.00003	-0.00110	0.00116	0.00019	-0.00424	0.00154

TABLE IV

The Filter Coefficients of the Cosine Modulated Five Band System with 55-tap filters and 54 samples of delay ($n_0 = 5$)

$h_0(n)$	$g_0(n)$
0.0002	-0.0011
0.0007	-0.0011
-0.0003	-0.0012
0.0006	-0.0016
0.0012	-0.0017
0.0012	-0.0011
0.0013	0.0004
0.0032	0.0029
0.0026	0.0066
0.0007	0.0115
-0.0010	0.0175
-0.0034	0.0242
-0.0084	0.0310
-0.0118	0.0365
-0.0149	0.0398
-0.0156	0.0396
-0.0132	0.0344
-0.0082	0.0239
0.0002	0.0070
0.0111	-0.0157
0.0285	-0.0439
0.0468	-0.0760
0.0652	-0.1101
0.0827	-0.1437
0.0970	-0.1743
0.1075	-0.1991
0.1123	-0.2162
0.1114	-0.2241
0.1056	-0.2219
0.0943	-0.2099
0.0789	-0.1896
0.0615	-0.1629
0.0438	-0.1320
0.0264	-0.1002
0.0114	-0.0697
-0.0001	-0.0426
-0.0077	-0.0209
-0.0122	-0.0051
-0.0138	0.0047
-0.0117	0.0092
-0.0099	0.0093
-0.0066	0.0064
-0.0028	0.0020
-0.0008	-0.0027
0.0012	-0.0069
0.0020	-0.0093
0.0023	-0.0104
0.0011	-0.0100
0.0009	-0.0086
0.0008	-0.0068
0.0005	-0.0049
-0.0001	-0.0031
0.0005	-0.0016
0.0002	-0.0005
0.0004	-0.0005

TABLE V

The Filter Coefficients of The Baseband Analysis and Synthesis of the 16-Band Cosine Modulated System with 96-Tap filters. ($n_0 = 1$)

$h_0(n)$		$g_0(n)$	
0.00020	-0.03234	0.00010	0.06316
0.00034	-0.03363	0.00025	0.05892
0.00051	-0.03473	0.00032	0.05445
0.00071	-0.03563	0.00050	0.04951
0.00094	-0.03632	0.00073	0.04462
0.00121	-0.03680	0.00107	0.03949
0.00151	-0.03706	0.00135	0.03438
0.00185	-0.03710	0.00178	0.02911
0.00221	-0.03693	0.00226	0.02404
0.00260	-0.03655	0.00282	0.01901
0.00301	-0.03597	0.00364	0.01435
0.00344	-0.03520	0.00456	0.00977
0.00388	-0.03425	0.00569	0.00556
0.00432	-0.03313	0.00681	0.00152
0.00475	-0.03187	0.00835	-0.00209
0.00516	-0.03048	0.00992	-0.00524
0.00554	-0.02899	0.01190	-0.00792
0.00587	-0.02740	0.01405	-0.01031
0.00615	-0.02574	0.01637	-0.01229
0.00636	-0.02403	0.01893	-0.01387
0.00649	-0.02230	0.02176	-0.01496
0.00652	-0.02055	0.02479	-0.01573
0.00645	-0.01881	0.02795	-0.01612
0.00626	-0.01710	0.03123	-0.01624
0.00594	-0.01543	0.03480	-0.01608
0.00549	-0.01381	0.03858	-0.01576
0.00490	-0.01226	0.04232	-0.01504
0.00415	-0.01079	0.04611	-0.01428
0.00326	-0.00941	0.05009	-0.01337
0.00221	-0.00812	0.05385	-0.01235
0.00102	-0.00694	0.05762	-0.01116
-0.00032	-0.00585	0.06136	-0.01005
-0.00181	-0.00488	0.06480	-0.00888
-0.00343	-0.00400	0.06809	-0.00777
-0.00517	-0.00323	0.07102	-0.00662
-0.00703	-0.00255	0.07358	-0.00566
-0.00897	-0.00197	0.07580	-0.00471
-0.01100	-0.00148	0.07753	-0.00380
-0.01309	-0.00107	0.07891	-0.00319
-0.01521	-0.00074	0.07976	-0.00255
-0.01735	-0.00047	0.08005	-0.00198
-0.01949	-0.00026	0.07973	-0.00153
-0.02159	-0.00011	0.07892	-0.00108
-0.02364	-0.00000	0.07758	-0.00070
-0.02562	0.00007	0.07574	-0.00045
-0.02750	0.00011	0.07327	-0.00024
-0.02925	0.00013	0.07032	-0.00000
-0.03087	0.00013	0.06690	0.00012

Computing Maximum Entropy Densities: A Hybrid Approach

Badong Chen

chenbd04@mails.tsinghua.edu.cn

*Department of Precision Instruments and Mechanology
Tsinghua University
Beijing, 100084, P. R. China*

Jinchun Hu

hujinchun@tsinghua.edu.cn

*Department of Precision Instruments and Mechanology
Tsinghua University
Beijing, 100084, P. R. China*

Yu Zhu

zhuyu@tsinghua.edu.cn

*Department of Precision Instruments and Mechanology
Tsinghua University
Beijing, 100084, P. R. China*

Abstract

This paper proposes a hybrid method to calculate the maximum entropy (MaxEnt) density subject to known moment constraints, which combines the linear equation (LE) method and Newton's method together. The new approach is more computationally efficient than ordinary Newton's method as it usually takes fewer Newton iterations to reach the final solution. Compared with the simple LE method, the hybrid algorithm will produce a more accurate solution. Numerical examples confirm the excellent performance of the proposed method.

Keywords: Maximum entropy principle (MEP), maximum entropy density, Lagrange multiplier, Newton's method, hybrid algorithm.

1. INTRODUCTION

The maximum entropy (MaxEnt) density is obtained by maximizing an entropy measure subject to known moment constraints. The underlying theoretical basis of the MaxEnt density is Jaynes' Maximum Entropy Principle (MEP), which states that among all the distributions that satisfy certain constraints (say the moment constraints), one should choose the distribution that maximizes the entropy [1, 2, 3]. The distribution determined by MEP fits the known data without committing extensively to unseen data.

The MaxEnt density provides flexible and powerful tool for density approximation and estimation since it nests a wide range of statistical distributions as special cases, yet, according to the MEP, it yields the most uniform (unbiased) density estimation conditioned on the available a priori knowledge. In fact, most known distributions can be regarded as the MaxEnt distribution with certain moment constraints [2]. The MaxEnt density has found applications in many areas (see [2] for typical examples).

The computation of the MaxEnt density, however, is not an easy task. This is in part, because that the maximization of the entropy is usually achieved through the use of Lagrange multipliers

whose numerical solution requires involved nonlinear optimization. Most existing approaches adopt the iterative Newton's method [4-7]. The Newton's method is too computationally demanding and is sensitive to the choice of the initial values. To reduce the computational complexity, Erdogmus et al. [8] have proposed a simple method to compute the Lagrange multipliers by solving a set of linear equations (LE). The main drawback of Erdogmus' LE method is its poor accuracy. In [9], an efficient numerical approximation of the MaxEnt density has been proposed by Balestrino et al. This method, however, does not compute the exact maximum entropy density (i.e. generalized exponential family).

In this work, we propose a hybrid approach to compute the MaxEnt density, which combines together LE and Newton's methods. The new approach is more computationally efficient than standard Newton's method while produces more accurate solution than LE method. The organization of the paper is as follows. In section II, the MaxEnt densities and some theoretical background are briefly described. In section III some existing algorithms for computing the MaxEnt density are reviewed, and a hybrid method is proposed. In section IV, numerical examples are presented to demonstrate the efficiency of the new approach. Finally, section V gives the conclusion.

2. MAXIMUM ENTROPY DENSITIES

This section gives some theoretical background about the maximum entropy (MaxEnt) densities. The entropy definition in this work is the Shannon's information entropy, which is given by [1]

$$H_s(p) = - \int_{\square} p(x) \log p(x) dx \tag{1}$$

where $p(x)$ is the probability density function (PDF) of a random variable X . Shannon's entropy measures the uncertainty (or dispersion) contained in $p(x)$.

In general, the MaxEnt density is obtained by maximizing the entropy (1) subject to certain moment constraints. Specifically, we have to solve the constrained non-linear optimization problem:

$$\begin{cases} \max_p H_s(p) = - \int_{\square} p(x) \log p(x) dx \\ \text{s.t.} \begin{cases} \int_{\square} p(x) dx = 1 \\ \int_{\square} g_k(x) p(x) dx = \mu_k, \quad k = 1, 2, \dots, K \end{cases} \end{cases} \tag{2}$$

where $\int_{\square} p(x) dx = 1$ is the normalization constraint, $\int_{\square} g_k(x) p(x) dx = \mu_k$ ($k = 1, 2, \dots, K$) are the K moment constraints, with known functions $g_k(x)$ and known real constants μ_k . Usually the moment constraints take the form ($g_k(x) = x^k$)

$$\int_{\square} x^k p(x) dx = \mu_k, \quad k = 1, 2, \dots, K \tag{3}$$

which are the so called arithmetic moment (or power moment) constraints.

By Lagrange's method and the calculus of variation, we can easily derive the analytical solution of the optimization (2), which is expressed as [2]

$$p_{MaxEnt}(x) = \exp \left(-\lambda_0 - \sum_{k=1}^K \lambda_k g_k(x) \right) \tag{4}$$

where $\lambda_0, \lambda_1, \dots, \lambda_K$ are the Lagrange multipliers that satisfy

$$\left\{ \begin{array}{l} \int_{\square} \exp\left(-\sum_{k=1}^K \lambda_k g_k(x)\right) dx = \exp(\lambda_0) \\ \frac{\int_{\square} g_i(x) \exp\left(-\sum_{k=1}^K \lambda_k g_k(x)\right) dx}{\exp(\lambda_0)} = \mu_i, \quad i = 1, 2, \dots, K \end{array} \right. \quad (5)$$

The existence and uniqueness of the MaxEnt density is not guaranteed when arbitrary combinations of moments are used as the side conditions. For the Hausdorff moment problem in which the PDF is defined over $[0,1]$, and the moment constraints are restricted to the arithmetic moments, a necessary and sufficient condition for the existence and uniqueness of the MaxEnt density is as follows [10]

$$\sum_{k=0}^m (-1)^k \binom{m}{k} \mu_k > 0, \quad m = 0, 1, 2, \dots \quad (6)$$

The above condition is not restrictive as it is satisfied by almost all the PDF defined over $[0,1]$. In [6], it is shown that the arithmetic sample moments for any finite sample always satisfy this condition.

Another important problem involved in MaxEnt density is the convergence problem. Let $p_0(x)$ be a nonnegative function integrable in $[0,1]$ whose arithmetic moments are μ_0, μ_1, \dots , and let $p_K(x)$, $K = 1, 2, \dots$ be the MaxEnt density sequence associated with the same moments, then [10]

$$\lim_{K \rightarrow \infty} \int_0^1 F(x) p_K(x) dx = \int_0^1 F(x) p_0(x) dx \quad (7)$$

where $F(x)$ is some continuous function in $[0,1]$. This convergence result suggests that for any finite sample, the MaxEnt density can be used to approximate the underlying distribution arbitrarily well provided that the sample size is large enough to allow precise estimates of the moments.

3. A HYBRID ALGORITHM TO COMPUTING THE MAXIMUM ENTROPY DENSITIES

To compute a MaxEnt density p_{MaxEnt} , we have to determine the Lagrange multipliers $\lambda_0, \lambda_1, \dots, \lambda_K$ by solving the non-linear system of $K + 1$ equations (5). One may use the familiar Newton's method which solves the Lagrange multipliers by iteratively updating [4-6]

$$\lambda_{t+1} = \lambda_t - \mathbf{H}^{-1} \partial\Gamma/\partial\lambda \quad (8)$$

where $\lambda = [\lambda_1, \dots, \lambda_K]^T$ denotes the Lagrange multipliers vector, $\Gamma = \lambda_0 + \left(\sum_{k=1}^K \lambda_k \mu_k\right)$ is the dual objective function, $\partial\Gamma/\partial\lambda$ and \mathbf{H} are the gradient and Hessian that take the form $(i, j = 1, 2, \dots, K)$

$$\begin{cases} \frac{\partial \Gamma}{\partial \lambda_i} = \mu_i - \mu_{g_i}(\boldsymbol{\lambda}) \\ \mathbf{H}_{ij} = \frac{\partial^2 \Gamma}{\partial \lambda_i \partial \lambda_j} = \mu_{g_i g_j}(\boldsymbol{\lambda}) - \mu_{g_i}(\boldsymbol{\lambda}) \mu_{g_j}(\boldsymbol{\lambda}) \end{cases} \quad (9)$$

where

$$\begin{cases} \mu_{g_i}(\boldsymbol{\lambda}) = \frac{\int_{\square} g_i(x) \exp\left(-\sum_{k=1}^K \lambda_k g_k(x)\right) dx}{\int_{\square} \exp\left(-\sum_{k=1}^K \lambda_k g_k(x)\right) dx} \\ \mu_{g_i g_j}(\boldsymbol{\lambda}) = \frac{\int_{\square} g_i(x) g_j(x) \exp\left(-\sum_{k=1}^K \lambda_k g_k(x)\right) dx}{\int_{\square} \exp\left(-\sum_{k=1}^K \lambda_k g_k(x)\right) dx} \end{cases} \quad (10)$$

The Newton's method described above is straightforward but has at least two disadvantages: (1) it is computationally expensive due to a lot of numerical integrals involved, (2) it is sensitive to the choice of the initial values ($\boldsymbol{\lambda}_0$) and only works for a limited set of moment constraints¹. Wu proposed in [6] a sequential updating method (sequential Newton's method) to calculate the MaxEnt density, which increases the chance of converging to the optimum solution but is still computationally costly.

In order to reduce the computational burden for computing the MaxEnt density, Erdogmus et al. [8] proposed an approximate approach to calculate the Lagrange multipliers by solving a linear system of equations. Specifically, let $\partial \Gamma / \partial \lambda_i = 0$, we have

$$\mu_i = \int_{\square} g_i(x) \exp\left(-\lambda_0 - \sum_{k=1}^K \lambda_k g_k(x)\right) dx \quad (11)$$

Applying the integrating by parts method and assuming the function $G_k(x) \square \int g_k(x) dx$ satisfies $G_k(x) p(x) \Big|_{-\infty}^{\infty} = 0$, it follows that

$$\mu_i = \sum_{j=1}^K \lambda_j \mathbf{E}_p \left[G_i(x) g_j'(x) \right] = \sum_{j=1}^K \lambda_j \beta_{ij} \quad (12)$$

where $\beta_{ij} = \mathbf{E}_p \left[G_i(x) g_j'(x) \right]$, \mathbf{E}_p denotes the expectation operator over $p(x)$. Thus the Lagrange multipliers $\boldsymbol{\lambda}$ can be expressed as the solution of a linear system of equations, that is

$$\boldsymbol{\lambda} = \boldsymbol{\beta}^{-1} \boldsymbol{\mu} \quad (13)$$

where $\boldsymbol{\mu} = [\mu_1, \dots, \mu_K]^T$, $\boldsymbol{\beta} = [\beta_{ij}]$.

In this work we refer to (13) as the linear equations (LE) method for solving the Lagrange multipliers of MaxEnt density. It should be noted that in practical applications, one may obtain only approximate solution of (13). In fact, as the expectation in β_{ij} is over the maximum entropy

¹ For this disadvantage, Ormonet and White [5] suggested two possible reasons: (a) numerical errors may build up during the updating process; (b) near-singularity of the Hessian may occur for a large range of $\boldsymbol{\lambda}$ space.

distribution which is unknown (to be solved), we have to approximate it using the sample mean from actual data distribution:

$$\hat{\beta}_{ij} = \frac{1}{L} \sum_{l=1}^L G_i(x_l) g'_j(x_l) \quad (14)$$

Therefore, the LE method may produce a solution with less accuracy although it is very computationally simple.

Now we propose a more efficient hybrid method for computing the MaxEnt density, which combines the previous two methods (Newton's and the LE). Specifically, the hybrid method consists of two steps:

Step 1: use the simple LE method to calculate an approximate solution $\tilde{\lambda}$ ($\tilde{\lambda} = \hat{\beta}^{-1} \mu$) for the Lagrange multipliers λ .

Step 2: apply Newton's method to search a more accurate solution, with the estimated Lagrange multipliers $\tilde{\lambda}$ as the initial values for iteration.

The obvious advantages of the proposed approach over previous methods are as follows:

- (i) *More computationally efficient than the standard Newton's method:* As the estimated Lagrange multipliers are close to the optimum values, it takes only few (usually one or two) Newton iterations to reach the final solution.
- (ii) *No choice of the initial values:* In the hybrid method, the initial values for Newton's iteration are not chosen randomly but instead, are calculated by the LE method. Then there is no problem such as sensitivity to the choice of the initial values and not converging to the optimum solution.
- (iii) *More accurate than the LE method:* Due to the refinements by Newton's method, the new approach will produce more accurate solution than the simple LE method.

The hybrid algorithm can be interpreted as a Newton's method for computing the minimum cross-entropy² (MinxEnt) density [2]. The MinxEnt density is obtained by minimizing the cross-entropy between $p(x)$ and an a priori density $q(x)$, subject to the same moment constraints on $p(x)$.

This yields the following optimization:

$$\begin{cases} \min_p D_{KL}(p||q) = \int_{\square} p(x) \log \left(\frac{p(x)}{q(x)} \right) dx \\ \text{s.t.} \begin{cases} \int_{\square} p(x) dx = 1 \\ \int_{\square} g_k(x) p(x) dx = \mu_k, \quad k = 1, 2, \dots, K \end{cases} \end{cases} \quad (15)$$

where $D_{KL}(p||q)$ denotes the cross-entropy (or Kullback-Leibler information divergence, KLID).

For the case in which the a priori distribution is a uniform distribution, the MinxEnt density will reduce to the MaxEnt density. The analytical solution for optimization (15) takes the form [2]

$$p_{MinxEnt}(x) = q(x) \exp \left(-\bar{\lambda}_0 - \sum_{k=1}^K \bar{\lambda}_k g_k(x) \right) \quad (16)$$

If the a priori density $q(x)$ is chosen as the MaxEnt density produced by the LE method, we have

$$q(x) = \exp \left(-\tilde{\lambda}_0 - \sum_{k=1}^K \tilde{\lambda}_k g_k(x) \right) \quad (17)$$

² The cross-entropy is also named the Kullback entropy, relative entropy, discrimination information, directed divergence, or the Kullback-Leibler information divergence (KLID).

where $\tilde{\lambda} = \hat{\beta}^{-1} \mu$. And hence

$$p_{MinxEnt}(x) = \exp\left(-\gamma_0 - \sum_{k=1}^K \gamma_k g_k(x)\right) \quad (18)$$

where $\gamma_i = \bar{\lambda}_i + \tilde{\lambda}_i$, $i = 0, 1, \dots, K$. In this case, the parameters $\{\gamma_i\}$ can be solved by Newton's method with initial values $\gamma_0 = \tilde{\lambda}$, that is

$$\gamma_{t+1} = \gamma_t - \mathbf{H}^{-1} \partial \Gamma' / \partial \gamma, \quad \gamma_0 = \hat{\beta}^{-1} \mu \quad (19)$$

where $\Gamma' = \gamma_0 + \left(\sum_{k=1}^K \gamma_k \mu_k\right)$ is the dual objective function. This is actually the proposed hybrid algorithm (i.e. Newton's method with initial values calculated by the LE method).

4. NUMERICAL EXAMPLES

This section presents numerical examples to demonstrate the efficiency of the hybrid algorithm for computing the MaxEnt density estimates. Consider the case in which the sample data is generated from a mixed-Gaussian distribution with two peaks located at ± 1 . Fig. 1 plots the empirical density (histogram) of 5000 samples generated.

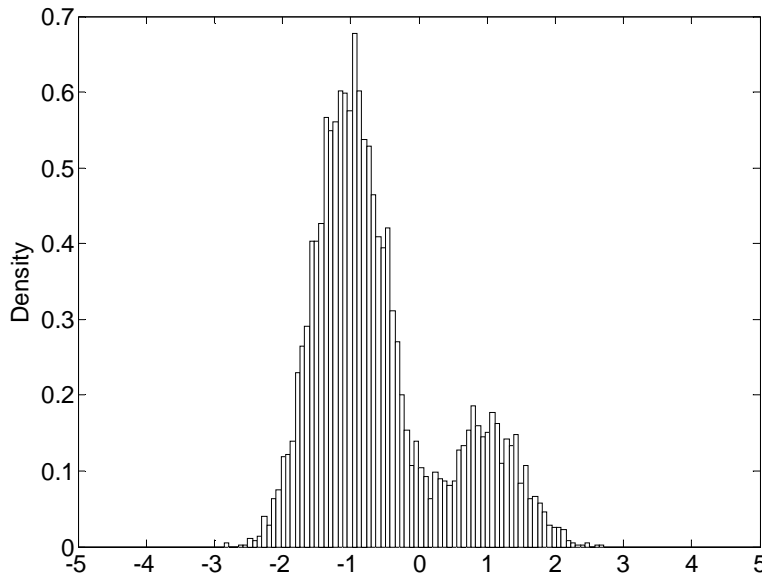


FIGURE 1: Empirical density of data sample obtained from a mixed-Gaussian distribution with peaks located at ± 1 .

From the sample, the first eight empirical power moments ($g_k(x) = x^k, k = 1, 2, \dots, 8$) have been calculated, and used as the known constants, μ_k , in computing the MaxEnt density. Fig. 2 illustrates a comparison among LE, Newton and hybrid (LE+Newton) algorithms. In Fig. 2, the number N stands for the total number of Newton iterations. The initial values of Newton's method are set as parameters of the standard Gaussian distribution ($\lambda_0 = \log \sqrt{2\pi}$, $\lambda_2 = 0.5$, $\lambda_1 = \lambda_3 = \lambda_4 = \dots = \lambda_8 = 0$). From Fig. 2, it is evident that the hybrid algorithm converges much faster than ordinary Newton's method and achieves better accuracy than LE method in density

estimation. Note that the hybrid algorithm takes just one Newton iteration to approach the final solution. To further compare the convergence performance between Newton's and hybrid methods, we plot in Fig. 3 the Kullback-Leibler information divergence (KLID) between the estimated and final MaxEnt density.

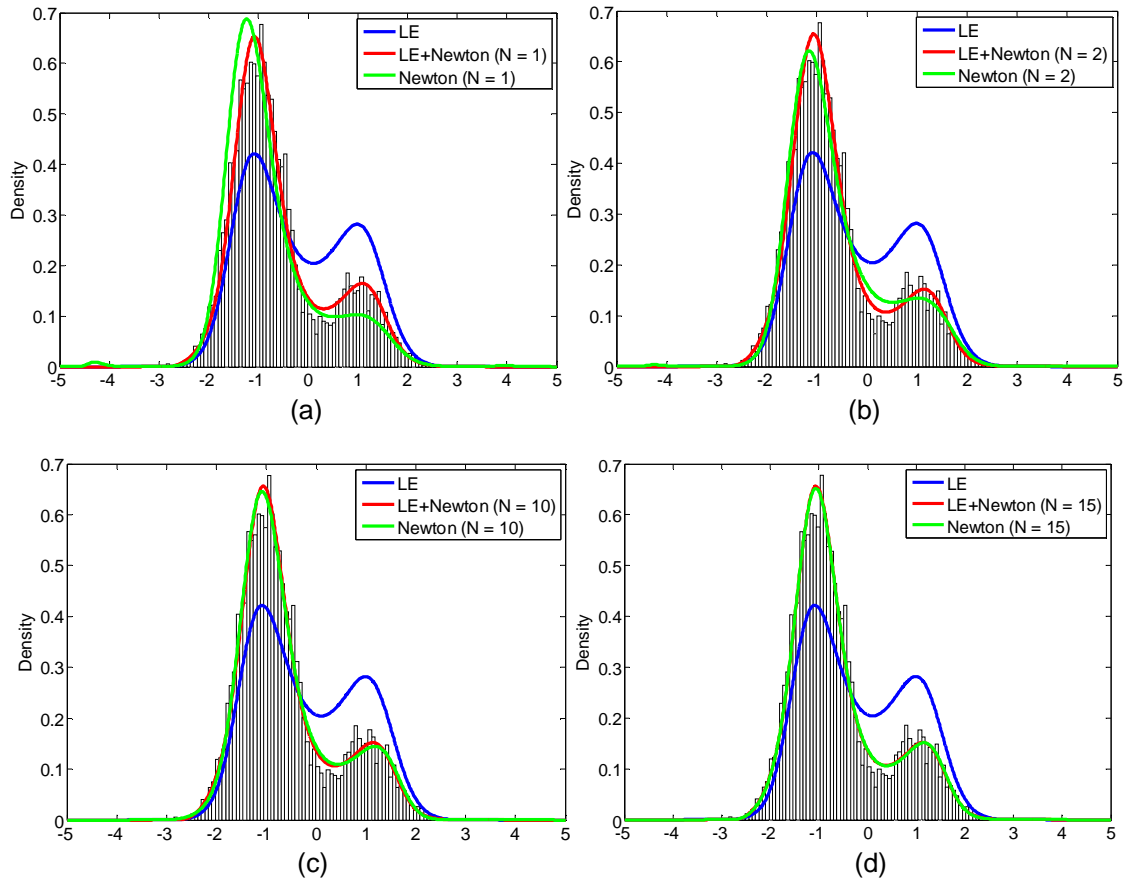


FIGURE 2: MaxEnt density estimates from the data reported in Fig.1.

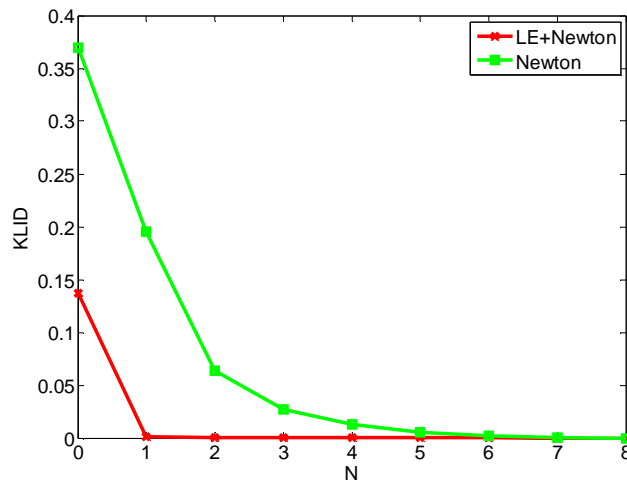


FIGURE 3: Convergence performance of LE+Newton and standard Newton's method.

Consider another set of sample data which are generated from mixed-Gaussian distribution with peaks located at ± 2 (see Fig. 4 for the empirical density). In this case, Newton's method fails to

converge. However, the LE and hybrid methods still work. As shown in Fig. 5, the hybrid algorithm takes only one Newton iteration to reach the final solution and again, achieves better results than LE method.

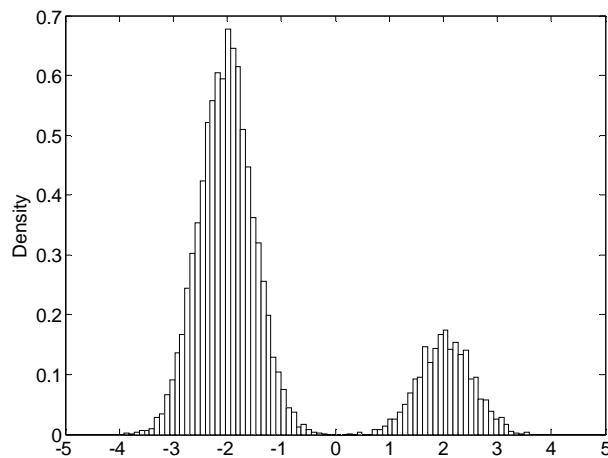


FIGURE 4: Empirical density of data sample obtained from a mixed-Gaussian distribution with peaks located at ± 2 .

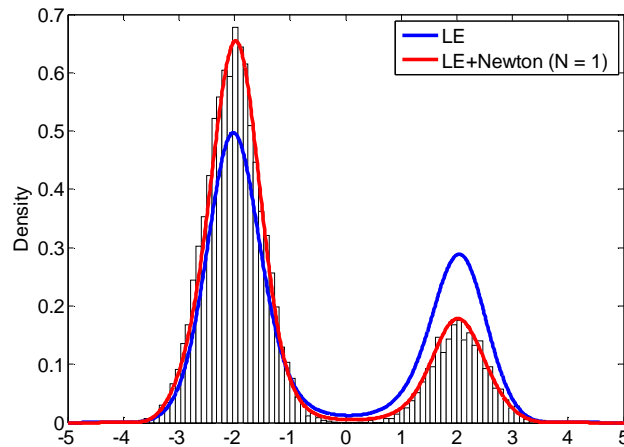


FIGURE 5: MaxEnt density estimates from the data reported in Fig.4.

5. CONCLUSION

A hybrid approach has been proposed to compute the MaxEnt density, which combines the linear equation (LE) method and Newton's method together. First, a rough solution is calculated by the simple LE method. Afterward, a more precise solution is obtained by Newton's method with the rough solution as starting values. The advantages of the proposed approach over standard Newton's method are: (i) increased computational efficiency (faster convergence), (ii) no need for the choice of initial values, (iii) higher numerical stability (converging to the optimum solution). The efficiency of the hybrid algorithm has been confirmed by numerical examples.

6. ACKNOWLEDGEMENTS

This work was supported by the National Natural Science Foundation of China (No. 60904054), National Key Basic Research and Development Program (973) of China (No. 2009CB724205), and China Postdoctoral Science Foundation Funded Project (20080440384).

7. REFERENCES

1. T. M. Cover and J. A. Thomas, *"Element of Information Theory"*, Chichester: Wiley & Son, Inc., 1991
2. J. N. Kapur, H. K. Kesavan, *"Entropy Optimization Principles with Applications"*, Academic Press, Inc., 1992
3. E. T. Jaynes, *"Information theory and statistical mechanics"*, Phys. Rev., 106: 620-630, 1957
4. A. Zellner, R. A. Highfield, *"Calculation of maximum entropy distributions and approximation of marginal posterior distributions"*, Journal of Econometrics, 37: 195-209, 1988
5. D. Ormoneit, H. White, *"An efficient algorithm to compute maximum entropy densities"*, Econometrics Reviews, 18(2): 127-140, 1999
6. X. Wu, *"Calculation of maximum entropy densities with application to income distribution"*, Journal of Econometrics, 115(2): 347-354, 2003
7. X. Wu, T. Stengos, *"Partially adaptive estimation via the maximum entropy densities"*, Econometrics Journal, 8: 352-366, 2005
8. D. Erdogmus, K. E. Hild II, Y. N. Rao, J. C. Principe, *"Minimax mutual information approach for independent component analysis"*, Neural Computation, 16: 1235-1252, 2004
9. A. Balestrino, A. Caiti, E. Crisostomi, *"Efficient numerical approximation of maximum entropy estimates"*, International Journal of Control, 79(9): 1145-1155, 2006
10. L. R. Mead, N. Papanicolaou, *"Maximum entropy in the problem of moments"*, Journal of Mathematical Physics, 25(8): 2404-2417, 1984

Symbol Based Modulation Classification using Combination of Fuzzy Clustering and Hierarchical Clustering

Negar Ahmadi

*Department of Computer Engineering
Iran University of Science and Technology
Narmak, Tehran, Post Code: 1684613114, Iran*

negar.ahmadi670@gmail.com

Reza Berangi

*Department of Computer Engineering
Iran University of Science and Technology
Narmak, Tehran, Post Code: 1684613114, Iran*

rberangi@iust.ac.ir

Abstract

Most of approaches for recognition and classification of modulation have been founded on modulated signal's components. In this paper, we develop an algorithm using fuzzy clustering and consequently hierarchical clustering algorithms considering the constellation of the received signal to identify the modulation types of the communication signals automatically. The simulation that has been conducted shows high capability of this method for recognition of modulation levels in the presence of noise and also, this method is applicable to digital modulations of arbitrary size and dimensionality. In addition this classification finds the decision boundary of the signal which is critical information for bit detection.

Keywords: Fuzzy C-means, AMR, Modulation Classification, Hierarchical Clustering.

1. INTRODUCTION

Modulation classification (MC) is an important subject in both military and commercial communication applications. This is a challenging problem, especially in non-cooperative environments, where no prior knowledge on the incoming signal is available. The aim of modulation classification (MC) [1-5] is to identify the modulation type [6] of a Communication signal. It plays an important role in many communication applications such as software radio, intelligent modem, and electronic surveillance system [7].

In many military communication situations such as reconnaissance, surveillance and electronic warfare, an indispensable step is to classify automatically the modulation types of the received signals. Automatic modulation recognition plays an important role in civil fields such as interference identification and spectrum management.

Modulation recognition is an intermediate step on the path to full message recovery. As such, it lies somewhere between low level energy detection and a full fledged demodulation. Therefore, correct recovery of the message per se is not an objective, or even a requirement [8, 9]. The existing methods for modulation classification span four main approaches. Statistical pattern recognition, decision theoretic (Maximum Likelihood), M-th law non-linearity and filtering and ad hoc [10, 11].

Early on it was recognized that modulation classification is, first and foremost, a classification problem well suited to pattern recognition algorithms. A successful statistical classification requires the right set of features extracted from the unknown signal. There have been many attempts to extract such optimal feature. Histograms derived from functions like amplitude, instantaneous phase, frequency or combinations of the above have been used as feature vectors for classification, Jondral [12], Dominguez et al. [13], Liedtke [14]. Also of interest is the work of Aisbett [15] which considers cases with very poor SNR.

The current state of the art in modulation classification is the decision theoretic approach using appropriate likelihood functional or approximations thereof. Polydoros and Kim [16] derive a quasi-log-likelihood functional for classification between BPSK and QPSK modulations. In a later publication, Huang and Polydoros [17] introduce a more general likelihood functional to classify among arbitrary MPSK signals. They point out that the S -classifier of Liedtke, based on an ad hoc phase-difference histogram, can be realized as a noncoherent, synchronous version of their qLLR. Statistical Moment-Based Classifier (SMBC) of Solimon and Hsue [18] are also identified as special coherent version of qLLR. Wei and Mendel [19] formulate another likelihood-based approach to modulation classification that is not limited to any particular modulation class. Their approach is the closest to a constellation-based modulation classification advocated here although they have not made it the central thesis of their work. Carrier phase and clock recovery issues are also not addressed. Chugg et al [20] use an approximation of log-ALF to handle more than two modulations and apply it to classification between OQPSK/BPSK/QPSK. Lin and Kuo [21] propose a sequential probability ratio test in the context of hypothesis testing to classify among several QAM signals. Their approach is novel in the sense that new data continuously updates the evidence.

Past work on modulation recognition has primarily used signal properties in time and/or frequency domain to identify the underlying modulation. One of the typical analysis methods for the modulated signal is the extraction of In-Phase (I) and Quad-Phase (Q) components. According to these components, we can see the signal as a vector in the $I-Q$ plane which is referred to as the constellation diagram. With the use of modulated signal constellation, modulation classification can be investigated as pattern recognition problem and well known pattern recognition algorithms can be used. For example in a recent publication Ahmadi and Berangi [22] introduce a method to classify modulation by using Genetic Algorithm and template matching Based on constellation diagram.

2. CLASSIFICATION OF QAM AND PSK MODULATIONS USING FUZZY CLUSTERING

As mentioned, constellation diagram, which consists of In-phase and Quad-phase components, can be used for modulation classification. Since the constellation is symmetric with respect to its axes, in order to reduce complexity, we can map all the received symbols into the first quadrant in the constellation diagram. After obtaining number and location of clusters in the first quadrant, centroids of the clusters could be extended to the whole constellation, symmetrically.

The proposed technique has been designed so that it would be capable of recognizing the types: 4-PSK, 8-PSK, 16-PSK, 4-QAM, 16-QAM and 64-QAM. So the initial number of clusters has been set to 16 in the first quadrant. This technique consists of two stages of FCM (Fuzzy C-means) clustering and post processing. Therefore the initial clusters can be defined as a vector of 16 elements in which, each element is a point in the first constellation quadrant. Initial value of centroids of the clusters is used for obtaining initial elements of the membership matrix. In order to reduce processing, calculation is done in the first quadrant, absolute value of signal's $I-Q$ components is calculated and stored in a 2D matrix and used in the future processing.

2.1. An Overview of Fuzzy C-mans Algorithm

Fuzzy C-means algorithm executed as follows [23, 24, and 25]:

Initial membership matrix constructed according to equation (1).

$$u_{ij} = \frac{1}{\sum_{k=1}^C \left(\frac{\|x_i - c_j\|}{\|x_i - c_k\|} \right)^{\frac{2}{m-1}}} \quad (1)$$

where m is the Fuzzy exponent, x_i are the input symbols and c_j denote the centroids.

2. New centroids shall be calculated using membership function as equation (2).

$$c_j = \frac{\sum_{i=1}^N u_{ij}^m \times x_i}{\sum_{i=1}^N u_{ij}^m} \quad (2)$$

Values of the old membership matrix are stored for the future comparisons.

3. New membership matrix is calculated using equation (1) and the objective function is calculated using equation (3).

$$J_m = \sum_{i=1}^N J_i = \sum_{i=1}^N \left(\sum_{j=1}^C u_{ij}^m \|x_i - c_j\|^2 \right) \quad 1 \leq m \leq \infty \quad (3)$$

In fact the aim of clustering is assigning symbols to clusters so that the value of the objective function is minimized. The algorithm convergence and termination condition are evaluated as equation (4).

$$\max_{ij} \left\{ \left| u_{ij}^{(k+1)} - u_{ij}^{(k)} \right| \right\} < \varepsilon \quad (4)$$

If the above condition is satisfied or the number of iterations reaches its end, then the algorithm is terminated, otherwise it returns to the step 2. Through this stage the number of centroids is constant. Hence to reduce the number of centroids, a post-processing step is necessary.

2.2. Post-Processing Stage

In this stage the centroids resulted from fuzzy clustering have been merged such that they result in the actual number and the location of centroids. The number of clusters in one quadrant could be 1, 2, 4, 8 or 16. The foundation of this step is based on hierarchical clustering [26]. Therefore, upon the completion of the fuzzy algorithm when centroids are obtained naturally, we use hierarchical clustering. To do this, first we calculate the Euclidean distance of the clusters pairwise and construct the hierarchical tree. After constructing the tree, all the possibilities of the merged centroids are calculated based on the number of the centroids. For each possibility the fitness value of the merged centroids with signal's symbols is calculated. This fitness value is calculated using hard C-means clustering [26]. Since clustering is performed to assign symbols to clusters, in a sense that the objective function (fitness value) is minimized. The number of optimum clusters corresponds to the objective function that is minimum between all possibilities.

It must be mentioned that, since the value of the objective function increases naturally as the number of clusters increases, which in turn causes an error in recognition of the actual number of cluster, the value of the objective function is multiplied by a weight proportional to the number of clusters to prevent producing error.

After multiplication of the weights, the number of clusters corresponding to the objective function with minimum value is chosen as the final number of cluster. After the final clusters on the first quadrant are obtained, these clusters are extended to the whole constellation diagram. For example, consider Figure (1) which corresponds to post processing of 16-QAM. It can be seen that the value of the objective function for 4 clusters in one quadrant is minimum with respect to the function's value for other possibilities; therefore 4 clusters are chosen for the first quadrant, and for the whole constellation diagram, 16 clusters are chosen (equal to the number of points of the 16-QAM constellation).

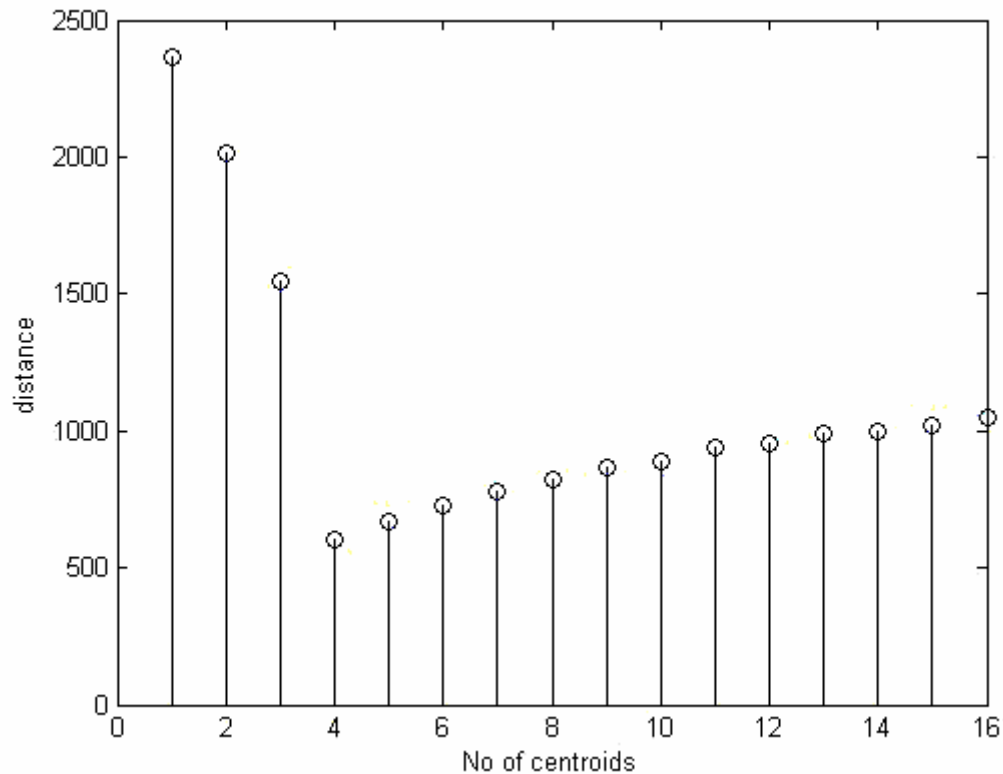


Figure 1: Values of the objective functions for possible clusters in the first quadrant (16-QAM).

Also in Figure (2) which corresponds to 8-PSK modulation, objective function for two clusters in the first quadrant has the minimum value, so the modulation levels in the whole constellation diagram are equal to 8, which is equal to points of 8-PSK constellation. In this way, for all modulations of QAM and PSK families, the post-processing step can lead to finding the actual number of clusters from the 16 clusters resulted by the fuzzy algorithm.

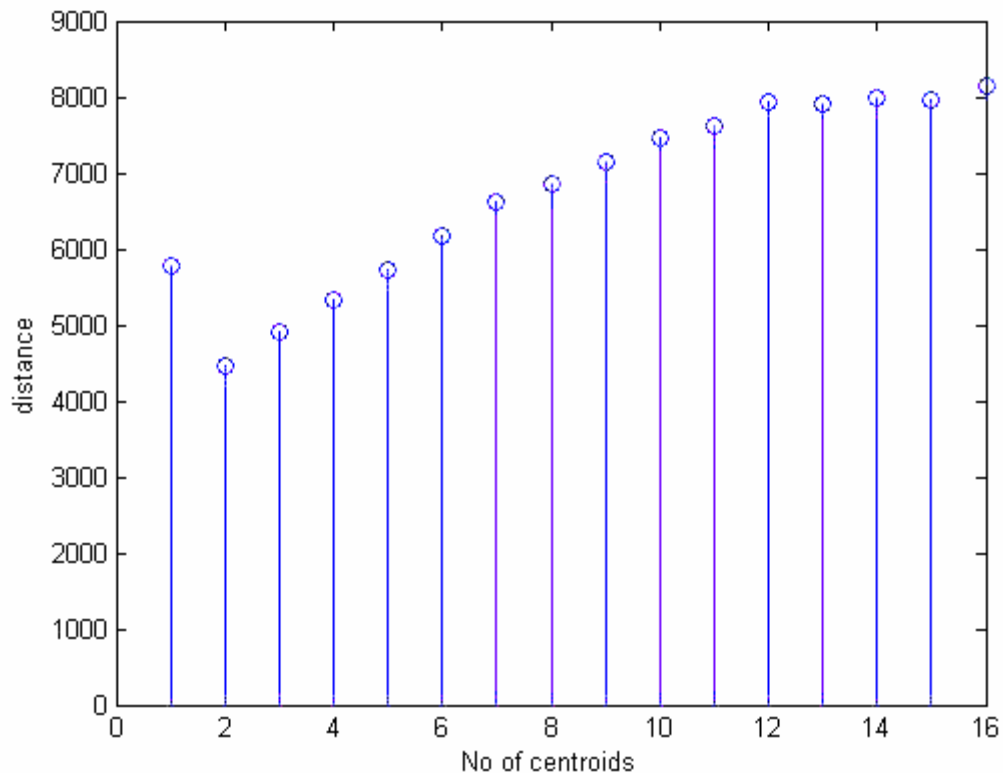


Figure 2: Values of the objective functions for possible clusters in the first quadrant (8-PSK).

3. EVALUATION AND SIMULATION RESULTS

In order to evaluate the performance of the proposed method, simulation has been performed for various SNR values and various types of QAM and PSK modulations. Channel model, applied in this work, has been assumed to be an AWGN channel, and it is also assumed that there is no time and/or frequency synchronization error. Simulation results show that this method has an efficient performance and high accuracy for the recognition of modulation. The performances of this method for 16-QAM and 16-PSK have been investigated. Figure (3) and Figure (4) show the centroids in the first quadrant obtained from fuzzy algorithm.

After completion of fuzzy algorithm, post-processing is performed to achieve the actual number of clusters in the first quadrant and consequently modulation type is recognized. For both 16-QAM and 16-PSK modulations, the value of objective function for 4 clusters in one quadrant will be minimum. Therefore closest clusters are combined so that 4 clusters are obtained in the first quadrant. Figure (5) and Figure (6) show extended clusters and signal symbols together, for 16-QAM and 16-PSK modulations, respectively.

Accuracy of this method for different modulations and different values of SNR is evaluated. The accuracy percentages have been obtained by executing the algorithm enough number of times and by calculating the ratio between correct recognition and total number of execution. Figure (7) shows the accuracy of recognition versus SNR ratio for different modulation types of QAM family; Also, this figure shows the results for the PSK family. As it can be seen in Figure (7) and (8), as modulation level increases, higher SNR is needed for the correct recognition of modulation type.

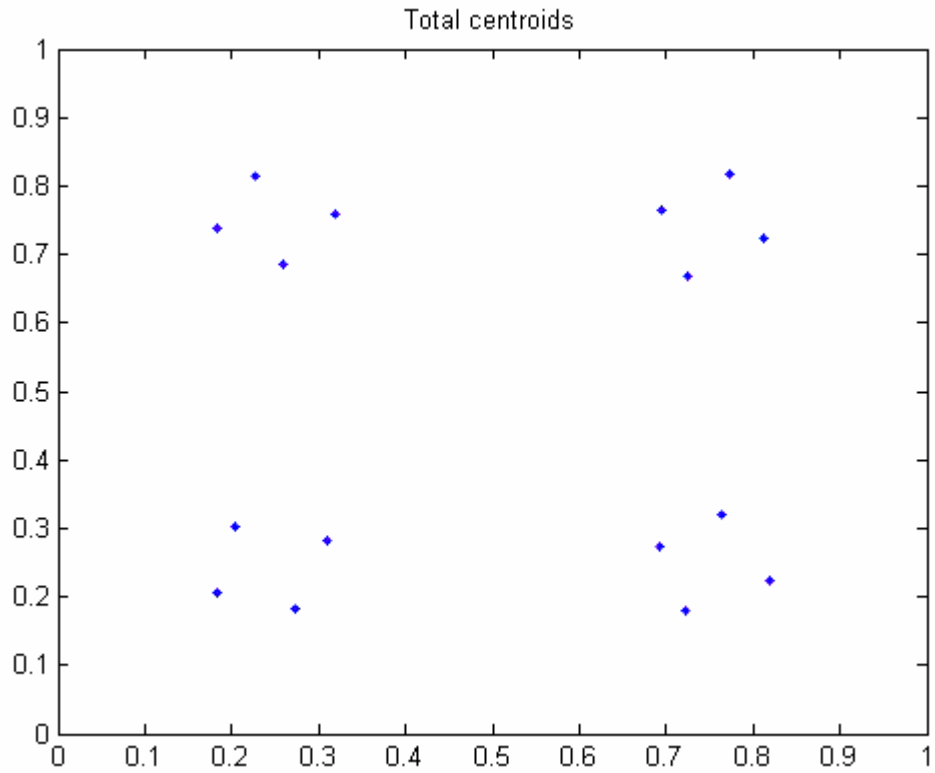


Figure 3: Centroids in the first quadrant obtained from fuzzy clustering (16-QAM).

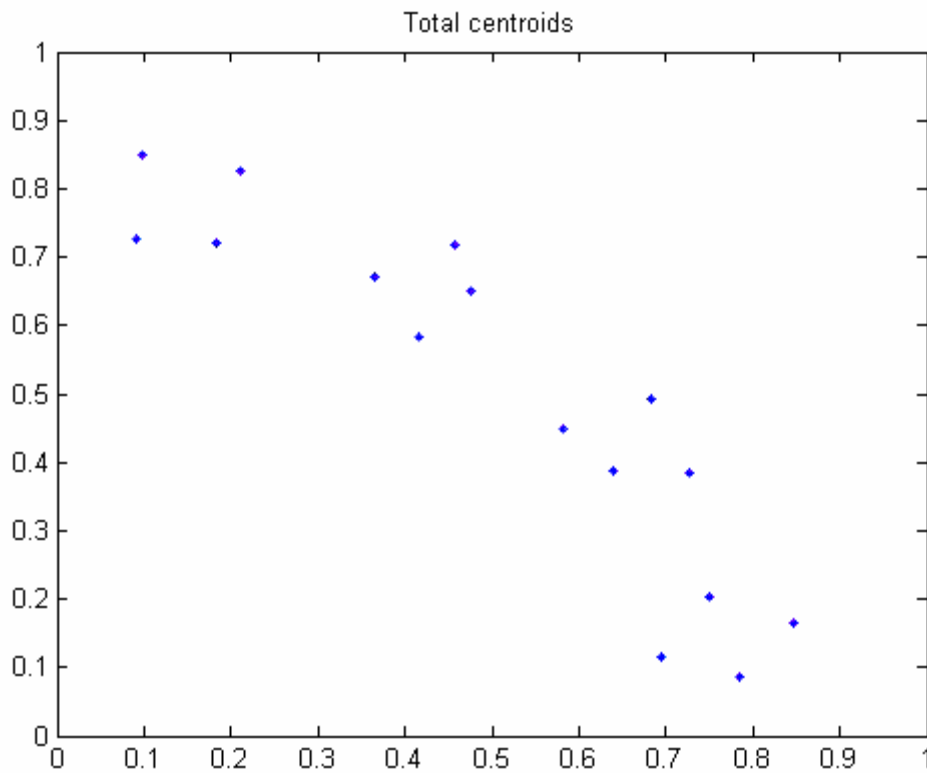


Figure 4: Centroids in the first quadrant obtained from fuzzy clustering (16-PSK).

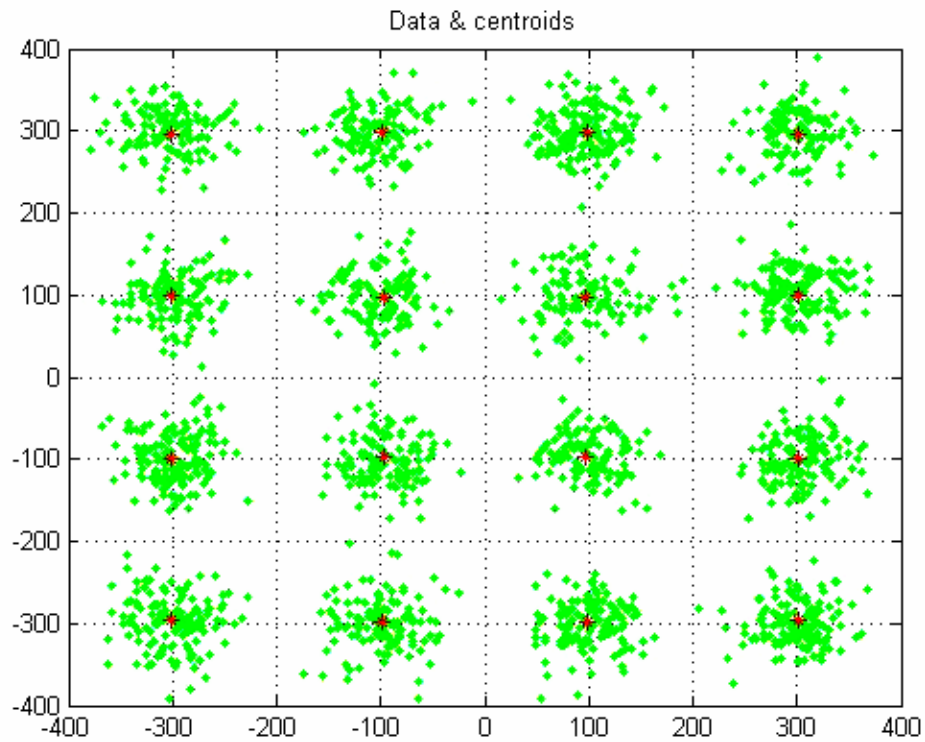


Figure 5: Extended clusters and their centroids in whole constellation diagram after post-processing step (16-QAM).

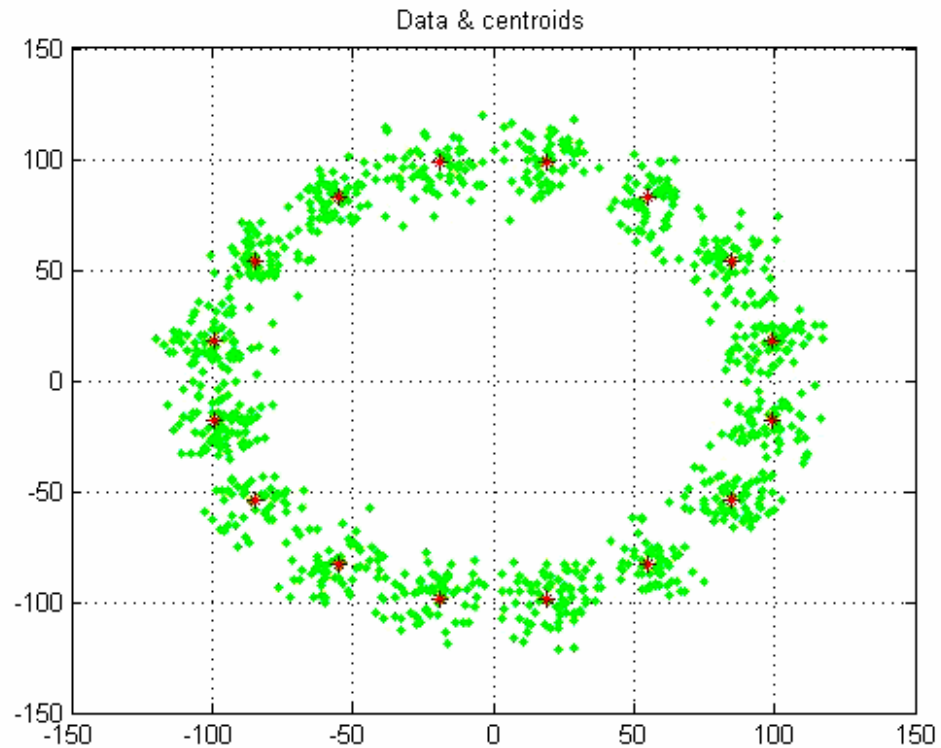


Figure 6: Extended clusters and their centroids in whole constellation diagram after post-processing step (16-PSK).

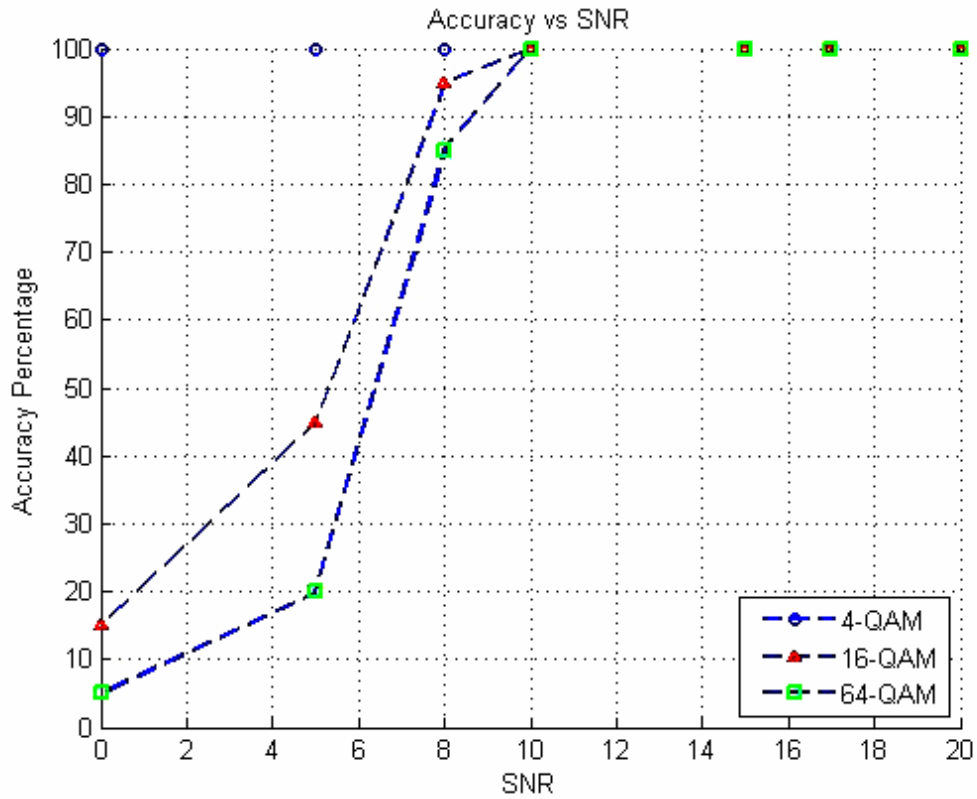


Figure 7: Accuracy of QAM modulation recognition versus SNR.

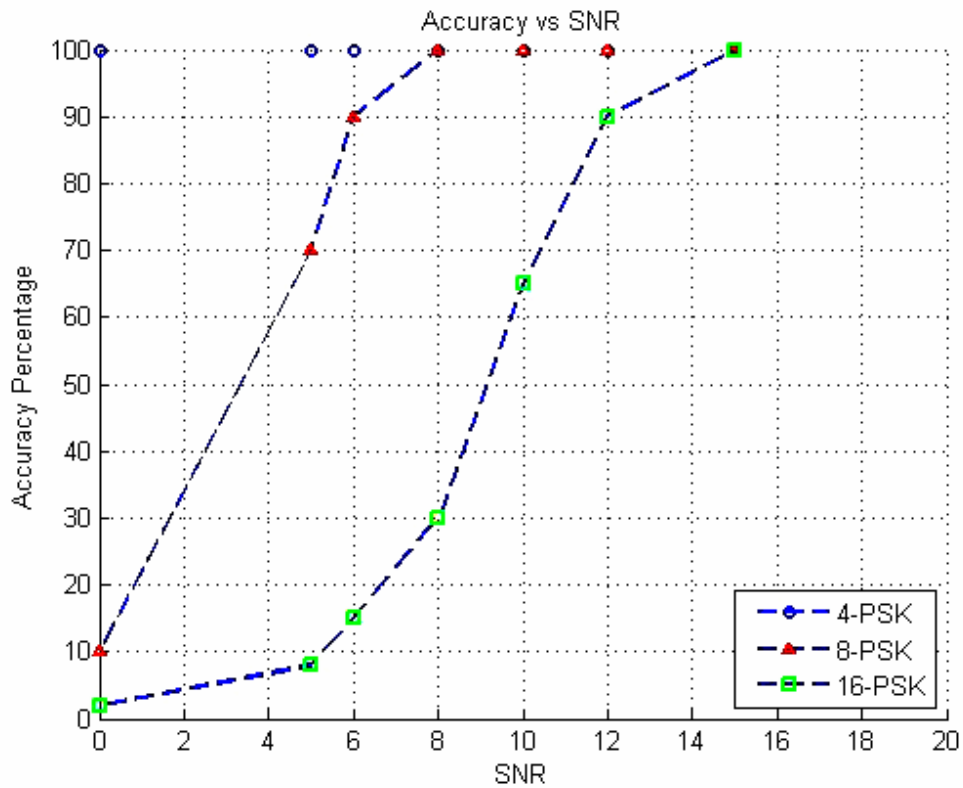


Figure 8: Accuracy of PSK modulation recognition versus SNR.

Having analyzed the obtained results from the fuzzy clustering method, we can imply the following cases:

- This method can recognize all the 4-QAM modulations with 100% accuracy and its recognition truth does not depend on the signal to the noise, and it can also identify this modulation type with SNR=0.
- This method can identify all the 16-QAM modulations with SNR=8 with a 95% accuracy, whereas it can also recognize the signal to the noise ratio lower than 8 with a less exactness and higher than 8 with a more exactness; it is noteworthy to say that in lower SNR, the more the sample is increased, the more efficient is the recognition of the modulation type.
- Accuracy of recognition of 64-QAM for the signal of the noise 10 and higher than that is 100% and for a level lower than it is less. Here, for the lower SNR, as the number of specimens increases, the accuracy would also increase.
- This research aims to recognize the modulation of QAM modulation family, but can be applied practically to recognize and separate the PSK modulation family. The proposed method to recognize PSK modulation can recognize all the QPSK modulations with 100% accuracy. Exactitude of this method to recognize the 8-PSK modulation with the signal to noise 8 and higher is 100% and for the lower level it is less; moreover, this method is able to identify 16PSK modulation with SNR=15 and higher than that with 100% accuracy and for a level lower than this it is less.

In this method fuzzy clustering and hierarchical clustering was used to classify different modulation types of QAM and PSK families, using the constellation diagram of the received signal, which is the noisy version of transmitted signal.

As can be seen in the simulation section, the proposed method shows a good performance for recognition even in low SNR condition, of course it must be mentioned that the performance could be increased with a higher number of data symbols. Another advantage of this method is calculating final centroids of clusters and determining the location of these centroids in constellation diagram. Also this approach could be extended and modified to recognize other types of digital modulation. Figures (9), (10), (11), (12) show some more simulation results of this method.

4. CONCLUSION

In this paper fuzzy clustering and hierarchical clustering were used to classify different modulation types of QAM and PSK families, using the constellation diagram of the received signal, which is the noisy version of the transmitted signal. By using fuzzy clustering algorithm, the clustering of input samples in the $I-Q$ plane is done with a high accuracy, and then in the post-processing stage, by using hierarchical clustering the number of real clusters that are representative of levels of modulation is recognized. As can be seen in simulation section, the proposed method shows a good recognition performance even in low SNR condition, and adapt to engineering applications.

of course, it must be mentioned that the performance could be improved with higher number of data symbols. Another advantage of this method is calculating final centroids of the clusters and determining the location of these centroids in constellation diagram. In addition this approach could be extended and modified to recognize other types of digital modulations.

The method that has been used can be expanded and uses them for modulation recognition of any PAM signals. These signals have one-dimensional constellation while in this research we study the signals with two-dimensional constellations, which are more complicated. Thus with a little change we can use them for recognition of PAM signals. From these signals the MFSK and MASK modulations can be referred.

With little changes in the proposed method it can be used in the recognition of modulations that have non-standard one dimensional or two-dimensional constellation. By rotating the

constellation diagram of PAM signals for 45° in the $I-Q$ plane, without any change in the proposed method, it can recognize modulations.

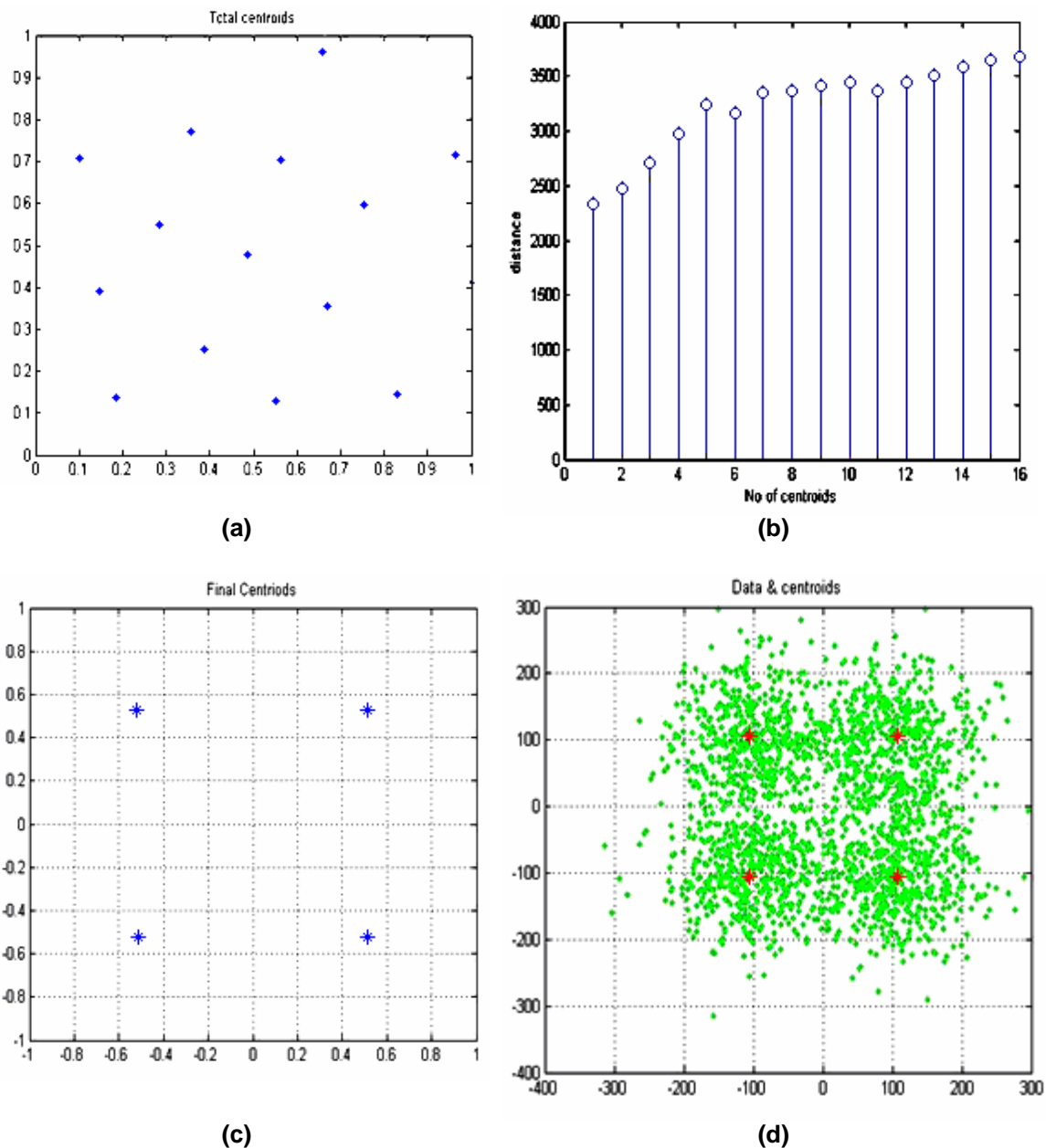


Figure 9: Recognition of 4-QAM with SNR=0dB and 1000 samples.

- a) Centroids in the first quadrant obtained from fuzzy clustering,
- b) values of the objective functions for possible clusters in first quadrant,
- c) centroids of the clusters in whole constellation diagram after post-processing step and
- d) extended clusters and their centroids in whole constellation diagram after post processing step.

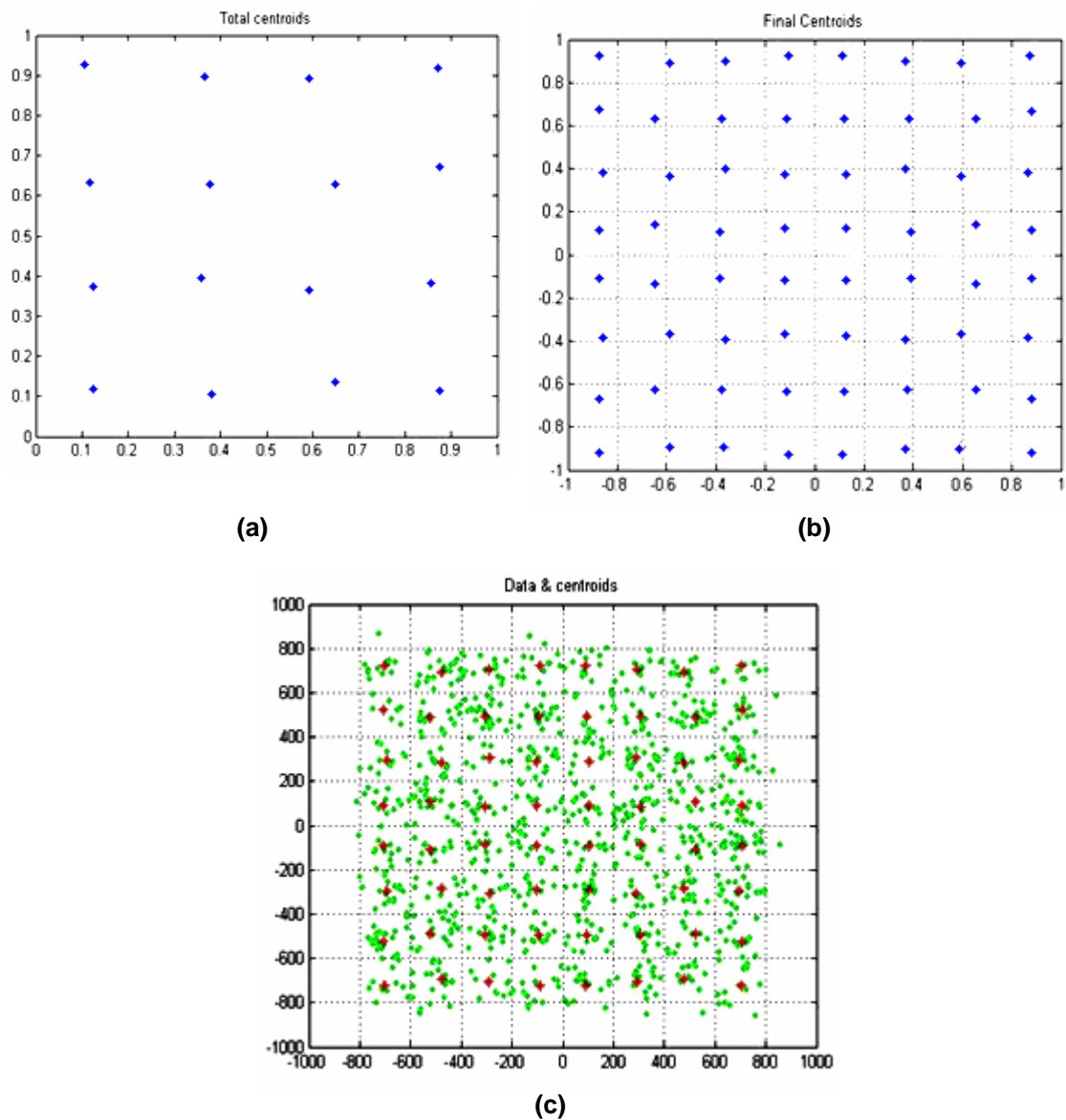


Figure 10: Recognition of 64-QAM with SNR=13dB and 1000 samples.

- a) centroids in the first quadrant obtained from fuzzy clustering,
- b) centroids of the clusters in whole constellation diagram after post processing-step and
- c) extended clusters and their centroids in whole constellation diagram after post processing step.

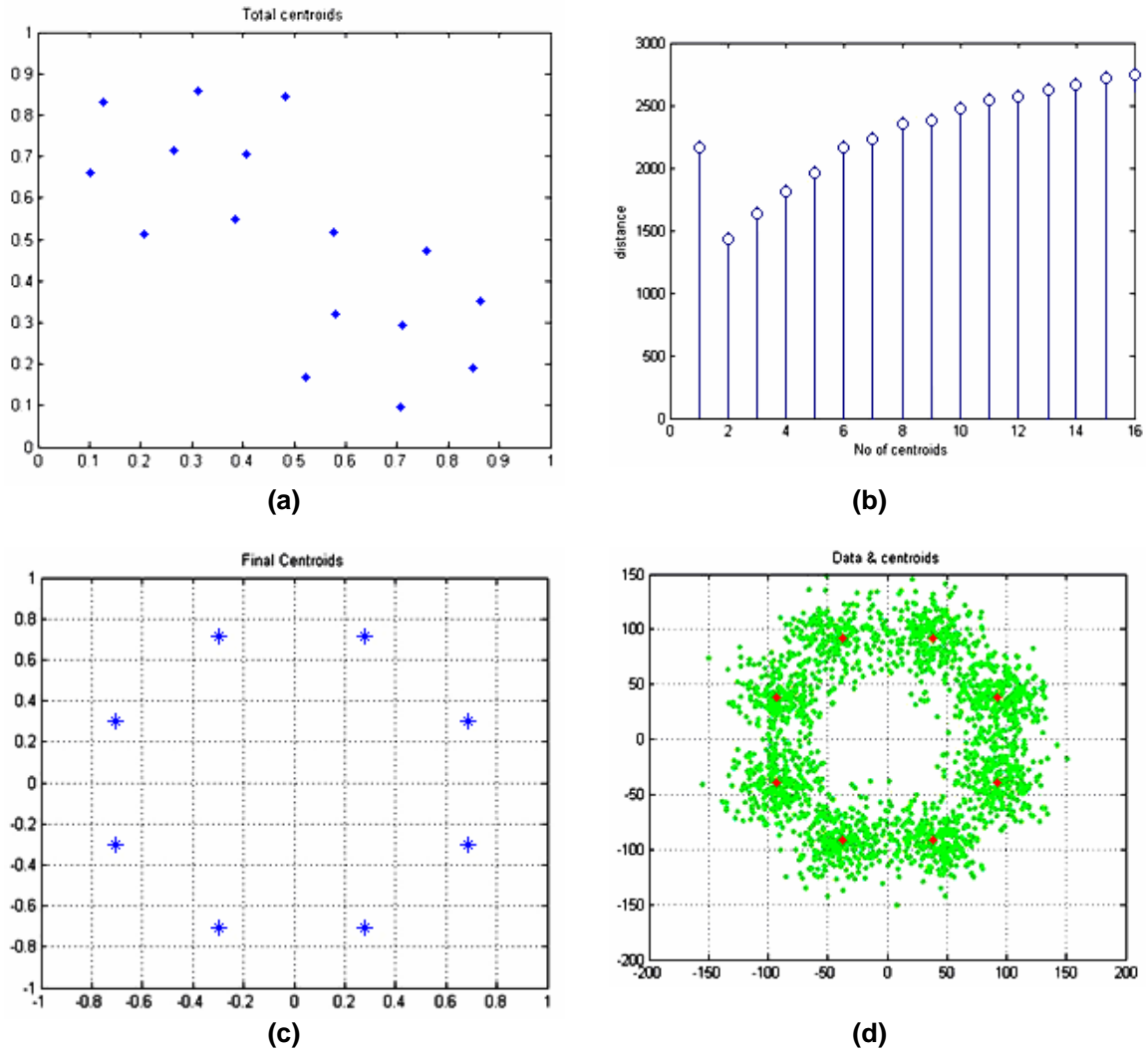


Figure 11: Recognition of 8-PSK with SNR=7dB and 2000 samples.
 a) centroids in the first quadrant obtained from Fuzzy clustering,
 b) values of the objective functions for possible clusters in first quadrant,
 c) centroids of the clusters in whole constellation diagram after post processing-step and
 d) extended clusters and their centroids in whole constellation diagram after post processing-step.

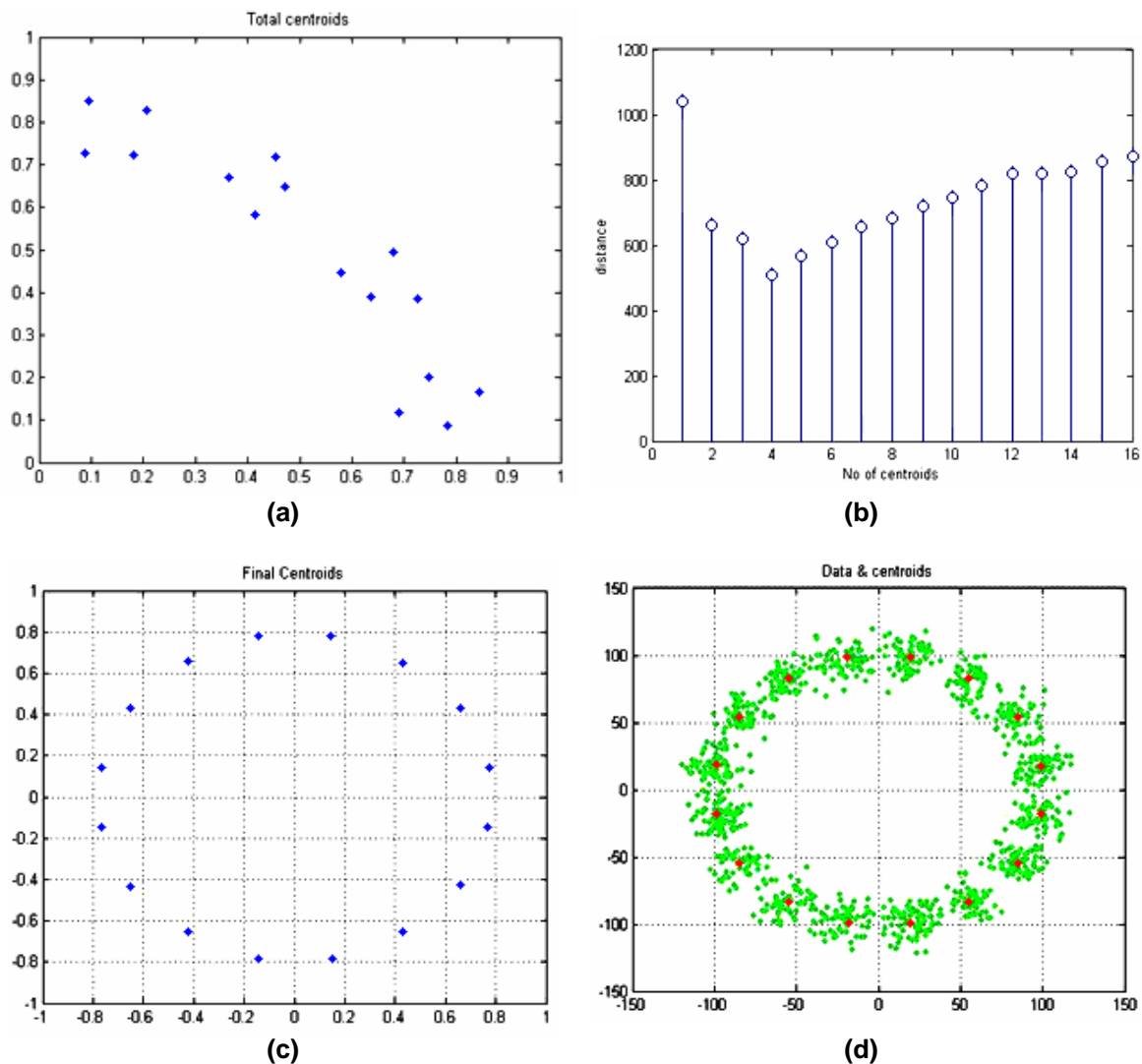


Figure 12: Recognition of 16-PSK with SNR=13dB and 1000 samples.

- a) centroids in the first quadrant obtained from fuzzy clustering,
- b) values of the objective functions for possible clusters in first quadrant,
- c) centroids of the clusters in whole constellation diagram after post processing-step and
- d) extended clusters and their centroids in whole constellation diagram after post processing step.

REFERENCES

- [1] A. Swami, B. M. Sadler, "Hierarchical Digital Modulation Classification Using Cumulants", *IEEE Trans. Communications*, Vol. 48(3), pp.416-429, 2000
- [2] A.K. Nandi, E.E. Azzouz, "Algorithms for Automatic Modulation Recognition of Communication Signals", *IEEE Trans. Communications*, Vol. 46(4), pp. 431-436, April 1998
- [3] E.E. Azzouz, A.K.Nandi., "Automatic Modulation Recognition of Communication Signals", *Kluwer Academic Publisher*, Norwell, MA, 1996

- [4] Wen Wei, Jerry M. Mendel, "A Fuzzy Logic Method for Modulation Classification in Nonideal Environments", *IEEE Trans. Fuzzy Systems*, Vol.7 (3), pp.333-344, June 1999
- [5] J. Lopatka, M. Pedzisz, "Automatic Modulation Classification Using Statistical Moments and a Fuzzy Classifier", in *Proceedings of ICSP2000*, pp 1500-1506, 2000
- [6] S. G. Wilson, "Digital Modulation and Coding", New York, *Prentice-Hall, Inc.*, Ch.3, (1996)
- [7] Daniel Boudreau, Christian Dubuc, Francois Patenaude et al., "A Fast Automatic Modulation Recognition Algorithm and Its Implementation in a Spectrum Monitoring Application", *MILCOM2000*, Los Angeles, California, Oct. 22-25, 2000
- [8] J. Reichert, "Automatic Classification of Communication Signals using Higher Order Statistics", *ICASSP 92*, pp.221-224, 1992
- [9] R. Schalkoff, "Pattern Recognition: Statistical, Structural and Neural Approach" , *John Wiley*, (1992)
- [10] Bijan G. Mobaseri, "Constellation shape as a robust signature for digital modulation recognition", Military Communications Conference Proceedings, *MILCOM IEEE*, Volume 1, Issue, pp. 442-446, 1999
- [11] Bijan G. Mobasseri, "Digital Modulation Classification using Constellation Shape", *Signal Processing*, Vol. 80, No. 2, pp.251-277, 2000
- [12] F. Jondral, "Automatic Classification of High Frequency Signals", *Signal Processing*, Vol. 9, No. 3, pp.177-190, 1985
- [13] L. Dominguez, J. Borrallo, J. Garcia, "A General Approach to the Automatic Classification of Radiocommunication Signals", *Signal Processing*, Vol. 22, No. 3, pp.239-250, 1991
- [14] F.F. Liedtke, "Computer Simulation of an Automatic Classification Procedure for Digitally Modulated Communication Signals with Unknown Parameters", *Signal Processing*, Vol. 6, pp.311-323, 1984
- [15] J. Aisbett, "Automatic Modulation Recognition using Time-Domain Parameters", *Signal Processing*, Vol.13, No. 3, pp.323-329, 1987
- [16] A. Polydoros, K. Kim, "On the Detection and Classification of Quadrature Digital Modulation in Broad-Band Noise", *IEEE Transactions on Communications*, Vol. 38, No. 8, pp. 1199-121, 1990
- [17] C. Huang, A. Polydoros, "Likelihood Method for MPSK Modulation Classification", *IEEE Transaction on Communications*, Vol. 43, No. 2/3/4, pp.1493-1503, 1995
- [18] S. Soliman, S. Hsue, "Signal classification using statistical moments", *IEEE Transactions on Communications*, Vol. 40, No. 5, pp. 908-915, 1992
- [19] W. Wei, J. Mendel, "A New Maximum Likelihood for Modulation Classification," *Asilomar-29*, pp. 1132-1138, 1996
- [20] K. Chugg, et al, "Combined Likelihood Power Estimation and Multiple Hypothesis Modulation Classification", *Asilomar-29*, pp. 1137-114, 1996

[21] Y.Lin, C.C. Kuo, "Classification of Quadrature Amplitude Modulated (QAM) Signals via Sequential Probability Ratio Test (SPRT)", *Report of CRASP*, University of Southern California, July 15, 1996

[22] Negar Ahmadi, Reza Berangi, "A Template Matching Approach to Classification of QAM Modulation using Genetic Algorithm", *Signal Processing: An International Journal*, Vol.3, Issue 5, pp: 95-109, 2009

[23] Krishna K. Chintalapudi and Moshe Kam, "A Noise-Resistant Fuzzy C Means Algorithm for Clustering", *Fuzzy systems proceedings, IEEE international Conference*, Vol. 2, pp. 1458-1463, 1998

[24] Sadaaki Miyamoto, "An Overview and New Methods in Fuzzy Clustering", *Knowledge-Based Intelligent Electronic Systems, Second International Conference*, Vol. 1, , pp. 33-40, 1998.

[25] Frank Chung-Hoon Rhee and Cheul Hwang, "A Type-2 Fuzzy C-Means Clustering Algorithm", *20 th NAFIPS international conference*, Vol. 4, pp. 1926-1929, 2001

[26] E. Gose, R. Johnsonbaugh, S. Jost, "Pattern Recognition and Image Analysis", *Prentice Hall PTR*, (1996)

CALL FOR PAPERS

Journal: Signal Processing: An International Journal (SPIJ)

Volume: 4 **Issue:** 2

ISSN: 1985-2339

URL: <http://www.cscjournals.org/csc/description.php?JCode=SPIJ>

About SPIJ

The International Journal of Signal Processing (SPIJ) lays emphasis on all aspects of the theory and practice of signal processing (analogue and digital) in new and emerging technologies. It features original research work, review articles, and accounts of practical developments. It is intended for a rapid dissemination of knowledge and experience to engineers and scientists working in the research, development, practical application or design and analysis of signal processing, algorithms and architecture performance analysis (including measurement, modeling, and simulation) of signal processing systems.

As SPIJ is directed as much at the practicing engineer as at the academic researcher, we encourage practicing electronic, electrical, mechanical, systems, sensor, instrumentation, chemical engineers, researchers in advanced control systems and signal processing, applied mathematicians, computer scientists among others, to express their views and ideas on the current trends, challenges, implementation problems and state of the art technologies.

To build its International reputation, we are disseminating the publication information through Google Books, Google Scholar, Directory of Open Access Journals (DOAJ), Open J Gate, ScientificCommons, Docstoc and many more. Our International Editors are working on establishing ISI listing and a good impact factor for SPIJ.

SPIJ List of Topics

The realm of International Journal of Signal Processing (SPIJ) extends, but not limited, to the following:

- Biomedical Signal Processing
- Communication Signal Processing
- Detection and Estimation
- Earth Resources Signal Processing
- Industrial Applications
- Optical Signal Processing
- Acoustic and Vibration Signal Processing
- Data Processing
- Digital Signal Processing
- Geophysical and Astrophysical Signal Processing
- Multi-dimensional Signal Processing
- Pattern Recognition

- Radar Signal Processing
- Signal Filtering
- Signal Processing Technology
- Software Developments
- Spectral Analysis
- Stochastic Processes
- Remote Sensing
- Signal Processing Systems
- Signal Theory
- Sonar Signal Processing
- Speech Processing

CFP SCHEDULE

Volume: 4

Issue: 3

Paper Submission: May 2010

Author Notification: June 30 2010

Issue Publication: July 2010

CALL FOR EDITORS/REVIEWERS

CSC Journals is in process of appointing Editorial Board Members for ***Signal Processing: An International Journal (SPIJ)***. CSC Journals would like to invite interested candidates to join **SPIJ** network of professionals/researchers for the positions of Editor-in-Chief, Associate Editor-in-Chief, Editorial Board Members and Reviewers.

The invitation encourages interested professionals to contribute into CSC research network by joining as a part of editorial board members and reviewers for scientific peer-reviewed journals. All journals use an online, electronic submission process. The Editor is responsible for the timely and substantive output of the journal, including the solicitation of manuscripts, supervision of the peer review process and the final selection of articles for publication. Responsibilities also include implementing the journal's editorial policies, maintaining high professional standards for published content, ensuring the integrity of the journal, guiding manuscripts through the review process, overseeing revisions, and planning special issues along with the editorial team.

A complete list of journals can be found at <http://www.cscjournals.org/csc/byjournal.php>. Interested candidates may apply for the following positions through <http://www.cscjournals.org/csc/login.php>.

Please remember that it is through the effort of volunteers such as yourself that CSC Journals continues to grow and flourish. Your help with reviewing the issues written by prospective authors would be very much appreciated.

Feel free to contact us at coordinator@cscjournals.org if you have any queries.

Contact Information

Computer Science Journals Sdn Bhd

M-3-19, Plaza Damas Sri Hartamas
50480, Kuala Lumpur MALAYSIA

Phone: +603 6207 1607

+603 2782 6991

Fax: +603 6207 1697

BRANCH OFFICE 1

Suite 5.04 Level 5, 365 Little Collins Street,
MELBOURNE 3000, Victoria, AUSTRALIA

Fax: +613 8677 1132

BRANCH OFFICE 2

Office no. 8, Saad Arcad, DHA Main Bulevard
Lahore, PAKISTAN

EMAIL SUPPORT

Head CSC Press: coordinator@cscjournals.org

CSC Press: cscpress@cscjournals.org

Info: info@cscjournals.org

COMPUTER SCIENCE JOURNALS SDN BHD
M-3-19, PLAZA DAMAS
SRI HARTAMAS
50480, KUALA LUMPUR
MALAYSIA